Contributions

from the Museum of Paleontology, University of Michigan

VOL. 32, NO. 11, PP. 189–243 APRIL 10, 2017

MOABOSAURUS UTAHENSIS, N. GEN., N. SP., A NEW SAUROPOD FROM THE EARLY CRETACEOUS (APTIAN) OF NORTH AMERICA

BY

BROOKS B. BRITT[1], RODNEY D. SCHEETZ[1], MICHAEL F. WHITING[2], AND D. RAY WILHITE[3]

Abstract — The Early Cretaceous was a time of dramatic change for sauropod dinosaurs in North America. Between the Late Jurassic-aged Morrison Formation and overlying Early Cretaceous strata, there was a dramatic decline in sauropod diversity. Here, we describe a new sauropod that adds to the diversity of the Early Cretaceous, from strata that can be no older than the early Aptian, (125 Ma) some 25 million years younger than the Morrison Formation.

Moabosaurus utahensis, n. gen., n. sp., is diagnosed in part by the following suite of characters: axially thin ventral basioccipital with posteriorly sweeping basal tubera; low-spined cervical vertebrae with neural spines that range from shallowly notched on anterior cervical vertebrae to shallow, but widely notched on middle and some posterior cervical vertebrae; posterior cervical and anterior dorsal neural spines with extremely low, axially thin, laterally wide ridges at the level of the zygapophyses; some cervical ribs with bifid posterior shafts; anterior and posterior caudal vertebrae with strongly procoelous centra, middle caudal vertebrae with mildly procoelous centra, and distal caudal vertebrae with moderately-to-strongly procoelous centra.

To determine the phylogenetic position of *Moabosaurus* we utilized three different datasets and performed four analyses. All results are in agreement that *Moabosaurus* is a neosauropod. The two most resolved trees indicate it is a macronarian, specifically a basal titanosauriform. The thick-walled, camerate presacral vertebrae and other characters, however, preclude a more highly nested position of *Moabosaurus* within either Titanosauriformes, which is characterized by moderately camellate presacral vertebrae, or Somphospondyli, which is characterized by fully camellate presacral vertebrae, including the neural arches. Incorporation of these and other characters, particularly those shared with *Turiasaurus* and *Tendaguria*, into phylogenetic analyses will help resolve the interrelationships of *Moabosaurus* with other neosauropods.

[1]Museum of Paleontology, Department of Geological Sciences, S389 ESC, Brigham Young University, Provo, Utah 84602, U.S.A. (brooks_britt@byu.edu; rod_scheetz@byu.edu)

[2]Department of Biology, 4142 LSB and M. L. Bean Museum, Brigham Young University, Provo, Utah 84602, U.S. A. (michael_whiting@byu.edu)

[3]College of Veterinary Medicine, 1130 Wire Road, Auburn University, Auburn, Alabama 36849, U.S.A. (ultrasauros@hotmail.com)

INTRODUCTION

The Early Cretaceous of North America was a time of transition for sauropods, representing the interval between the Late Jurassic, as best represented by the highly diverse sauropod fauna of the Morrison Formation, and the Late Cretaceous, when sauropods were represented by a single titanosaurian taxon, *Alamosaurus*. A gap of 25 million years separates the Morrison and Cedar Mountain formations (Eberth et al., 2006), spanning from the Tithonian to the earliest Aptian, during which there was a dramatic drop in the diversity of sauropods (Bakker, 1978; Hunt et al., 1994). In North America, there are only two sauropod occurrences from that gap: tracks and possible gastroliths from the latest Jurassic or the earliest Cretaceous of southeastern British Columbia (McCrea et al., 2014) and two bones of a *Camarasaurus*-like neosauropod from Berriasian–Valanginian-aged strata from South Dakota (D'Emic and Foster, 2016). The discovery of *Moabosaurus utahensis*., n. gen., n. sp., adds to the Cretaceous sauropod diversity of North America. Here we describe known elements of the skull, vertebrae, and appendicular skeleton and test its phylogenetic position.

Locality, Horizon and Age

The holotype and all referred specimens of *Moabosaurus utahensis*, n. gen., n. sp., are from the Dalton Wells Quarry, which lies circa 20 km north-northwest of Moab, Utah (Fig. 1). The bone-bearing lithosome lies unconformably on the Brushy Basin Member of the Morrison Formation at the base of the Yellow Cat Member of the Cedar Mountain Formation (Eberth et al., 2006). The bones are preserved in four superimposed diamictites, consisting of unsorted angular mudstone clasts and small siliceous pebbles in a mudstone matrix, all derived from the underlying Morrison Formation. The fluvial units of the quarry interfinger with clean sandstones representing the final channel fill overlying the basal diamictites. These fluvial units interfinger with lacustrine units (Eberth et al., 2006). The Cedar Mountain Formation spans some 24 million years and consists of three terrestrial sequence stratigraphic packages (Greenhalgh and Britt, 2007). The quarry resides at the base of the lowermost of these three sequences. Detrital zircons from the quarry and adjacent, lateral equivalents provide a maximum depositional age of 125 Ma, indicating the horizon is no older than early Albian (Eberth et al., 2006).

Taphonomy

Some 5,500 bones, most of them incomplete, were collected from the Dalton Wells Quarry between 1975 and 2005 (Fig. 2). A summary of the history of the quarry was provided in Eberth et al. (2006). A taphonomic analysis of the quarry (Britt et al., 2009) revealed that a majority (97%) of the bones at the quarry were broken in two episodes of trampling, one at the site of death and the other following deposition after minor transport in a fluvial system. The same study indicated that at least 20% of the bones suffered severe damage by osteophagous

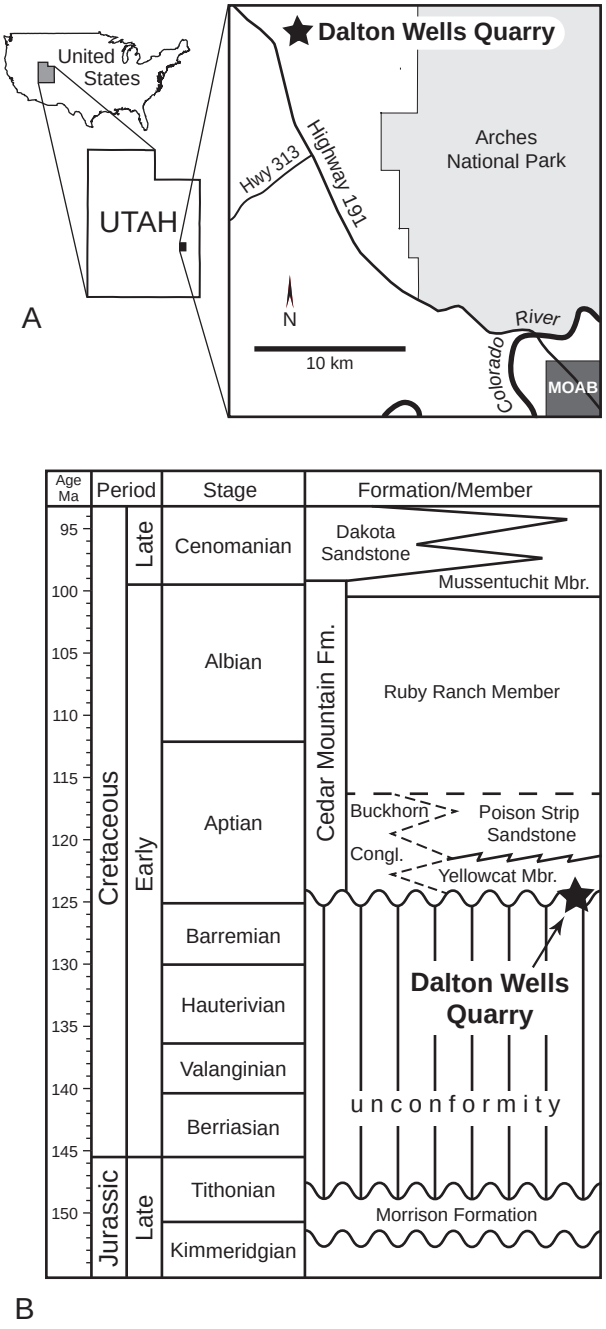

FIGURE 1 — Locality, stratigraphy, and age. **A**, all specimens described in this paper are from the Dalton Wells Quarry (BYU locality 7510). The quarry is about 20 km northwest of Moab, Utah. Specific locality information is on file at Brigham Young University's Museum of Paleontology. **B**, the quarry is at the base of the Yellow Cat Member, which is the lowest member of the Cedar Mountain Formation. Detrital zircons provide a maximum depositional age of 125 Ma for the Yellow Cat Member, indicating the specimens can be no older than early Aptian (Eberth et al., 2006). The stratigraphic column is modified from Britt et al. (2009). Ages follow Cohen et al. (2013).

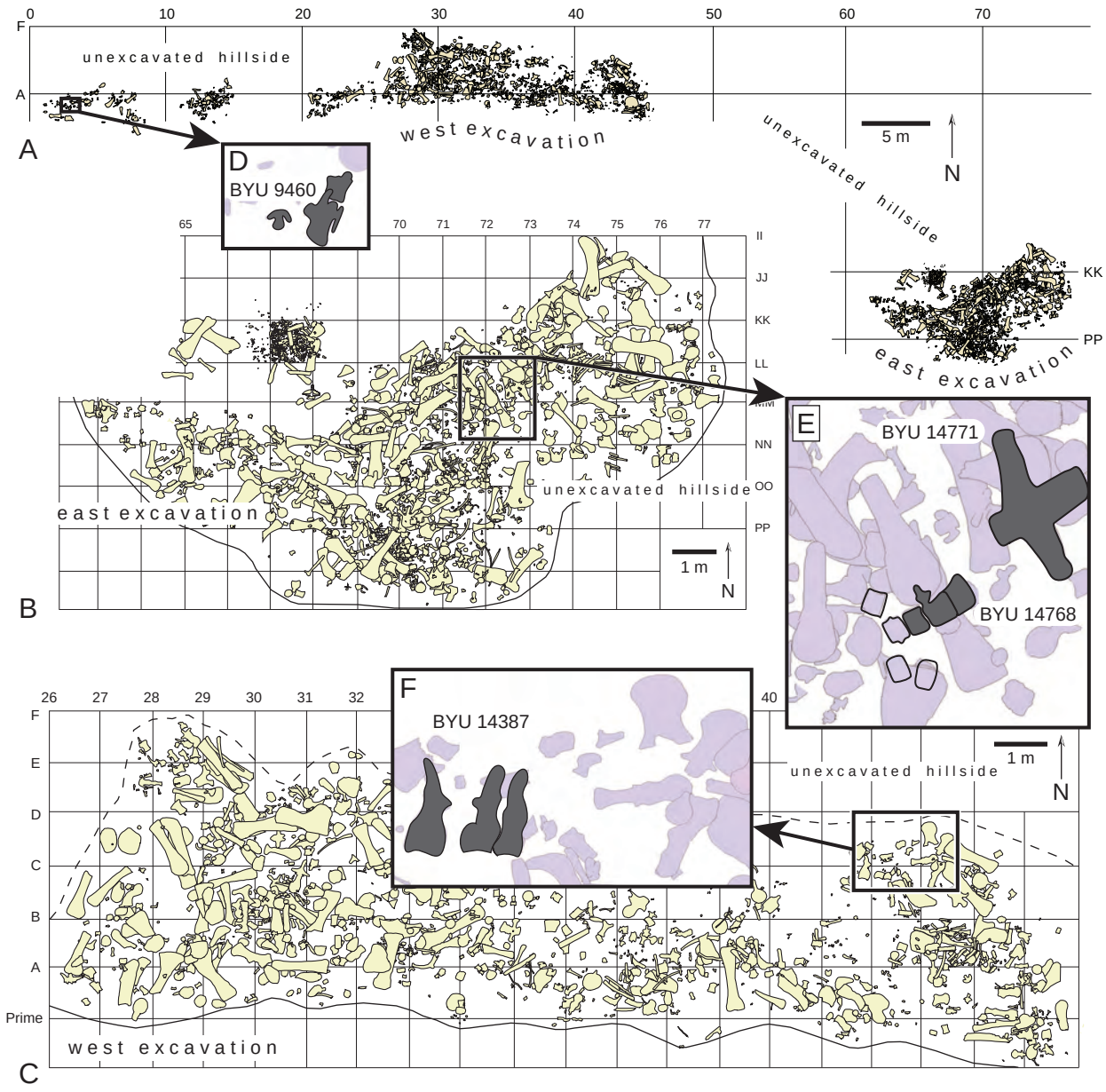

FIGURE 2 — Quarry map showing the locations and relationships of select articulated bones. **A**, overall quarry map. **B**, enlargement of east end of quarry. **C**, enlargement of west end of quarry. **D**, BYU 9460 highlighted in dark gray. Preparation yielded a braincase and cervical vertebrae 1–4 with a cervical rib. **E**, BYU 14771, a sacrum articulated with the last dorsal and caudal vertebrae 1 and 2, and BYU 14768, caudal vertebrae 3–5 from the same individual. The caudal vertebrae with black outlines have not been prepared. **F**, BYU 14387, the holotype of *Moabosaurus utahensis*, two articulated, and one closely associated, anterior dorsal vertebrae.

insects. Following that report, it became clear that insect damage is far more common than was originally reported, a pattern that remains to be quantified. The insects, likely beetle larvae, created burrows on the surface of the bone, often consumed articular surfaces, and fed on the undersurfaces of the bones giving them a planed-off appearance (Britt et al., 2009). For example, the undersurface of sauropod vertebrae resting on the paleo substrate were often consumed from below by the insects (Britt et al., 2009: fig. 14F). The damage is most common on articular faces or other non-laminar bone surfaces, such as occipital condyles, the ends of centra, prezygapophyses and postzygapophyses, and the apices of neural spines. The assemblage is also biased in that small bones and block-shaped and flat bones were substantially

winnowed as a consequence of fluvial hydraulics (Britt et al., 2009). The result of this winnowing is that the majority of bones represent a lag deposit, favoring the preservation of irregularly-shaped vertebrae and dense elements such as limb bones and braincases. Because transport distance of these bones was minimal, portions of some individuals can be associated. A consequence of the overall, harsh taphonomic conditions of the assemblage, however, is that the bones are often incomplete, broken and shattered and articular surfaces are frequently bioeroded by insects as will be noted in the descriptions of some of the bones of *Moabosaurus utahensis*, n. gen., n. sp. These taphonomic conditions, including the impact of osteophagous insects, are common in basal units of the Cedar Mountain Formation (Britt et al., 2009).

Fauna

The biota recovered from the Dalton Wells Quarry is biased in favor of large vertebrates, specifically dinosaurs. Plants are represented by a single fossil, the short-shoot of a coniferous tree. Non-dinosaurian taxa are rare, consisting of isolated, fragmentary bones of a pterosaur, crocodilian, and turtle (Britt et al., 2009) and the partial femur of a neochoristodere (Britt et al., 2006). The dinosaur fauna is moderately diverse, consisting of six taxa: the thyreophoran *Gastonia bergei*, a tall-spined iguanodontian-grade ornithopod (Galton and Jensen, 1979; Scheetz et al., 2010), the theropods *Nedcolbertia justinhofmanni* and *Utahraptor ostrommaysorum*, and two sauropods – a brachiosaurid, tentatively identified as *Venenosaurus dicrocei*, and *Moabosaurus utahensis*, n. gen., n. sp.

It has been reported previously (e.g., Britt et al., 1997a,b, 2009) that the Dalton Wells Quarry fauna included a *Camarasaurus*-like taxon, based on the presence of lightly built, camerate anterior cervical and posterior dorsal vertebrae. The cervical vertebrae bore short, slightly notched neural spines, and the dorsal vertebrae had moderately high neural arch peduncles and short neural spines. All of these features were generally similar to *Camarasaurus*, except they were of a lighter build. Specimens interpreted as *Camarasaurus*-like included BYU 9460, a small braincase closely associated with a string of small, anterior cervical vertebrae. The braincase shares derived characters with *Moabosaurus utahensis*, n. gen., n. sp., and our current study indicates they belong to that species. The morphology of the cervical vertebrae associated with the braincase also matches that of the new species. The light construction is attributed to their small size and immaturity of the individual. The other lightly built vertebrae formerly considered *Camarasaurus*-like by Britt et al. (2009) were limited to posterior dorsal vertebrae.

Several abstracts (e.g., Britt et al. 1996, 1997a,b, 1998) reported a titanosaur sauropod in Dalton Wells Quarry. The titanosaur assignment was based on five characters detailed in a letter from John S. McIntosh dated October 1998 to BBB. These characters are as follows. First, strongly procoelous proximal and distal caudal vertebrae—a condition considered at that time to be diagnostic of titanosaurians (McIntosh, 1990), but which is now known to occur convergently in a range of sauropods, including several non-neosauropods (as summarized in Mannion et al., 2013). Second, a biconvex caudal, BYU 10956, that Britt et al. (1998) cited as evidence of titanosaurian affinity. The anterior cotyle of BYU 10956 may be a developmental anomaly, as it is the only one that was found in the quarry. Third, extremely low neural spines on the posterior cervical vertebrae and anterior dorsal vertebrae. At the time, the sample size was small and it was not clear whether the spines were single or slightly bifid. Fourth, a robust ulna with a prominent olecranon process and prominent proximolateral process. Fifth, sternal plates resembling those of *Alamosaurus* and a relatively straight scapula blade with minimal distal expansion.

Tidwell and Carpenter (2007) also identified a titanosaurian from the basal Cedar Mountain Formation sequence based on an articulated series of four vertebrae: the last three cervical vertebrae, with low undivided neural spines, and the first dorsal vertebra with a laterally wide, anteroposteriorly thin spine that rises little above the prezygapophyses. These vertebrae match those assigned to *Moabosaurus utahensis*, n. gen., n. sp.

Two genera, both brachiosaurid titanosauriforms, have been established on specimens from the basal sequence (Buckhorn Conglomerate + Yellow Cat + Poison Strip members, sensu Greenhalgh and Britt, 2007) of the Cedar Mountain Formation: *Venenosaurus dicrocei* (Tidwell et al., 2001) and *Cedarosaurus weiskopfae* (Tidwell et al., 1999). Both are usually recovered as brachiosaurid titanosauriforms (e.g., Royo-Torres and Upchurch, 2012; Carballido and Sander, 2014). Britt et al. (2009) noted that the brachiosaurid *Venenosaurus* occurs in the Dalton Wells quarry without justifying the assignment. The brachiosaurid identification was based on elongate humeri (BYU 14734, BYU 18045) with robustness indices (maximum length/least breadth) of 0.13 and 0.12, respectively, which are nearly identical to the robustness index of *Brachiosaurus altithorax* (Wilhite, 2005). This confirms that a brachiosaurid occurs in the quarry but is insufficient to determine if the Dalton Wells brachiosaurid pertains to *Venenosaurus* or *Cedarosaurus*. The *Venenosaurus* identification was based on the similarity between the ischium of *Venenosaurus* and an ischium from Dalton Wells Quarry, BYU 14072 (Britt et al., 2009). This generic assignment remains tenuous. There are three or four brachiosaurid individuals in the quarry located in three clusters (Britt et al., 2009). All individuals are diminutive, with the largest element being an 889 mm long humerus. Additional brachiosaurid elements are limited to gracile ulnae with distinctive, L-shaped proximal ends and amphicoelous caudal vertebral centra that are slightly wider than tall with strongly backswept ribs (transverse processes) and anterior-leaning neural arch peduncles located anteriorly on the centrum. Neither the elongate arm elements nor the amphicoelous caudal vertebrae could be confused with those of *Moabosaurus*. There is, however, the potential for confusion in the hind limb elements so, except for the femur (for which there is a large sample size), we do not figure nor score hind limb elements in this study. No brachiosaurid precaudal vertebrae have been

recognized in the assemblage. Their absence is attributed their delicate nature combined with two phases of trampling and other destructive taphonomic conditions (Britt et al., 2009). Should they be present, the morphological differences make it unlikely they would be confused with *Moabosaurus* vertebrae.

METHODOLOGY

For anatomical terms, we follow Romer's conventions (Wilson, 2006), for example "anterior centrum" as opposed to "cranial corpus." We use the nomenclature for vertebral laminae of Wilson (1999) and the nomenclature for vertebral fossae of Wilson et al. (2011). For the general pneumatic structures of centra interiors we follow Britt (1993, 1997). That is, we use "camerate" to indicate large pneumatic chambers/camerae with thick outer walls and "camellate" to indicate pneumatic structures consisting of numerous small pneumatic spaces (camellae) separated by thin inner walls and thin outer walls.

All specimens are in the Museum of Paleontology at Brigham Young University, Provo, Utah, U.S.A. Bones were mechanically prepared by standard techniques.

Prior to photographic imaging, most bones were coated to eliminate the visually distracting, often strongly mottled colors typical on bones from the Dalton Wells Quarry. The resultant photographs better show a bone's relief. Small bones were coated with clay sprayed on using the solvent-based aerosol Spotcheck™ SKD-S2 developer made by Magnaflux. The larger bones were sprayed with fine, aerosol drywall texture clay. Teeth were coated with ammonium chloride condensate (Teichert, 1948). All coatings wash off with water. Bones were illuminated by multiple incandescent light sources to best show morphology.

INSTITUTIONAL ABBREVIATIONS

BYU — Brigham Young University, Museum of Paleontology, Provo, Utah, U.S.A.

MB — Museum für Naturkunde, Humboldt University of Berlin, Germany.

USNM — United States National Museum, Smithsonian Institution, Washington, D.C., U.S.A.

SYSTEMATIC PALEONTOLOGY

DINOSAURIA Owen 1842
SAUROPODA Marsh 1878
NEOSAUROPODA Bonaparte 1986
MACRONARIA Wilson and Sereno 1998

Moabosaurus gen. nov.

Etymology.— The generic name refers to the city of Moab, which is near the holotypic locality.

Type species.— *Moabosaurus utahensis* sp. nov.

Diagnosis.— As for the species.

Moabosaurus utahensis sp. nov.
Figs. 3–32

Etymology.— The specific name honors the state of Utah.

Holotype.— BYU 14387, three closely associated dorsal vertebrae, two of which were found in articulation, with the other separated by 20 cm.

Referred specimens.— See Table 1.

Type Locality.— Dalton Wells Quarry, about 20 km northwest of Moab, Utah. Detailed locality information is on file with the Museum of Paleontology at Brigham Young University, Provo, Utah.

Diagnosis.— *Moabosaurus utahensis* is a ca. 10 m long sauropod diagnosed by: anterior margin of conjoined frontals convex in dorsal view; frontals (individual bones) axially elongated with axial dimension almost equal to lateral dimension; ventral portion of basioccipital anteroposteriorly thin, with ventral apron spanning the gap between basal tubera and their weak vertical pillars; basal tubera reduced with posterior projecting wedges and extending posteriorly in same vertical plane as occipital condyle; postaxial cervical vertebrae (except for last cervical vertebrae) with bifid spines characterized by a shallow notch bounded laterally by low metapophyses (the notch is a small slit on cervical 3), increasing in width to the posterior cervical vertebrae which are shallowly bifid - the notch is almost twice as wide laterally as axially long and flat-bottomed and thereafter the notch narrows on subsequent vertebrae; neural spines of the last cervical vertebrae through dorsal vertebrae 3 or 4 low, consisting of a low, laterally wide lip between and/or on the anterior portions of the spinopostzygapophyseal laminae; bifid rib blades on mid to posterior cervical vertebrae; first neural spine with cruciate cross-section on dorsal 4 or 5; a combination of procoelous proximal and distal caudal centra with middle caudal centra that vary from amphiplatyan to weakly procoelous.

Referred Specimens.— Building the taxon from multiple articulated or associated specimens (Fig. 2) that can be linked by either autapomorphies (or diagnostic characters shared by serial homologues) and relative abundance (Longrich, 2008), we refer selected specimens (Table 1) to *Moabosaurus utahensis*. The number of cervical, dorsal, and caudal vertebrae is unknown in the absence of an articulated vertebral column. However, we confidently link the cervical vertebrae through caudal vertebrae using autapomorphies and serial homologues working anteriorly and posteriorly from the holotypic anterior dorsal vertebrae, BYU 14387 (Figs. 3, 4). For the anterior to mid-cervical vertebrae, and the anterior six dorsal vertebrae we also use overlapping sets of elements. A string of 12 articulated vertebrae (BYU 14771; Fig. 6) including the last two dorsal vertebrae, sacrum, caudal vertebrae 1 and 2, and three closely associated caudal vertebrae provide crucial linkage between the dorsal and caudal series. A braincase, atlas and axis found adjacent to articulated cervical vertebrae 3 and 4 pertaining to a single individual, BYU 9460 (Fig. 5), is referred to *Moabosaurus utahensis* because the cervical vertebrae can be linked to the holotypic dorsal vertebrae via serial homologs.

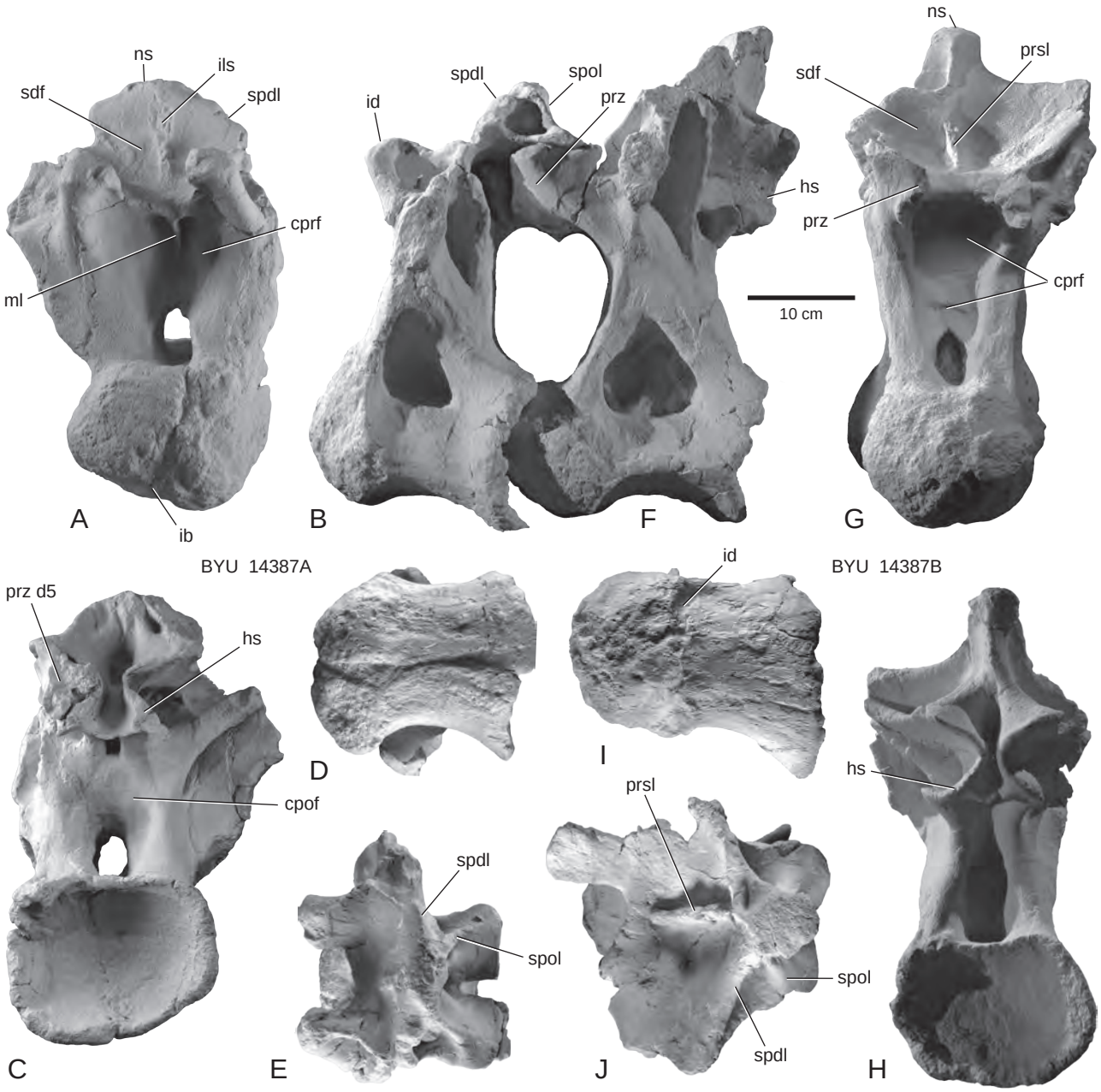

FIGURE 3 — *Moabosaurus utahensis*, holotypic dorsal vertebrae 4–5, BYU 14387A and 14387B. **A–E**, dorsal 4, BYU 14387A, in anterior, left lateral, posterior, ventral, and dorsal views. **F–J**, dorsal 5, BYU 14387B, in left lateral, anterior, posterior, ventral, and dorsal views. Dorsal vertebrae 4 and 5 were found articulated in the field; dorsal 6 (Fig. 4) was closely associated (Fig. 2F). Abbreviations: *cpof*, centropostzygapophyseal fossa; *cprf*, centroprezygapophyseal fossa; *d5*, dorsal vertebra 5; *hs*, hyposphene; *ib*, insect burrow; *id*, insect damage; *ils*, intervertebral ligament scar; *ml*, median lamina; *ns*, neural spine; *prsl*, prespinal lamina; *prz*, prezygapophysis; *sdf*, spinodiapophyseal fossa; *spdl*, spinodiapophyseal lamina; *spol*, spinopostzygapophyseal lamina.

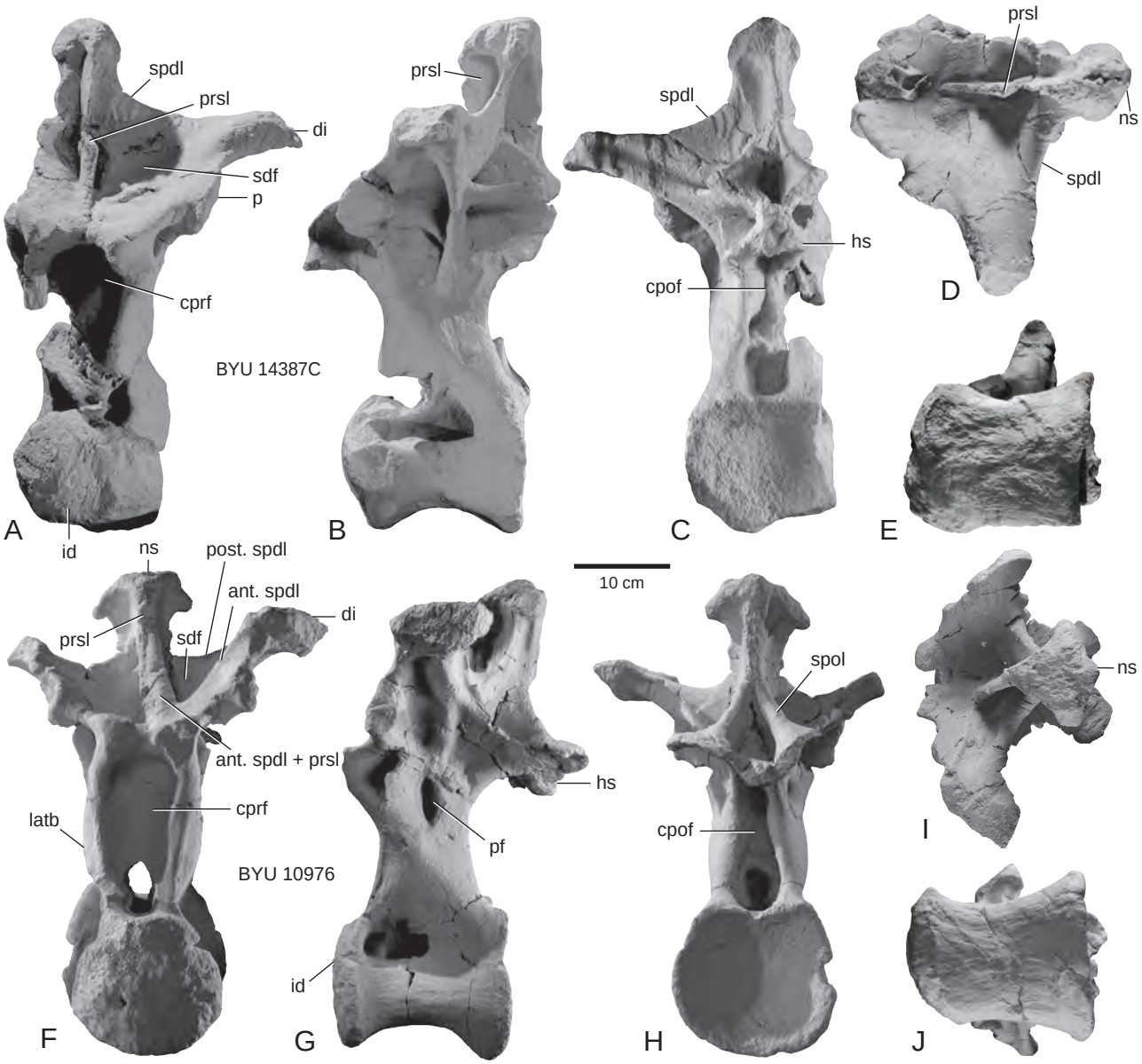

FIGURE 4 — *Moabosaurus utahensis*, holotypic dorsal vertebra 6, BYU 14387C, and referred mid-series dorsal, BYU 10976. **A–E**, dorsal 6, BYU 14387C, in anterior, left lateral, posterior, dorsal, and ventral views. **F–J**, anterior mid-series dorsal, BYU 10976 in anterior, left lateral, posterior, dorsal, and ventral views. Most of the hyposphene is missing. The spinodiapophyseal + prespinal lamina is developed only on the right side **(F)**. The centroprezygapophyseal and centropostzygapophyseal fossae attain maximal development in this portion of the dorsal series. There is an accessory pneumatic foramen (*pf*) that pneumatizes the hollow peduncles of BYU 10976 **(G)**. Abbreviations: *ant*, anterior; *cpof*, centropostzygapophyseal fossa; *cprf*, centroprezygapophyseal fossa; *di*, diapophysis; *hs*, hyposphene; *id*, insect damage; *latb*, lateral bulge; *ns*, neural spine; *p*, parapophysis; *pf*, pneumatic foramen; *post*, posterior; *prsl*, prespinal lamina; *sdf*, spinodiapophyseal fossa; *spdl*, spinodiapophyseal lamina; *spol*, spinopostzygapophyseal lamina.

The referral of a limited number of non-axial elements is based on relative abundance, and absence of features diagnostic of brachiosaurids (e.g., gracile arm elements). All 18 braincases share autapomorphies and/or characters considered by to be diagnostic of basal macronarians, indicating they pertain to the same taxon, a conclusion supported by the domination of the quarry's sauropod fauna by *Moabosaurus utahensis* with a MNI (minimum number of individuals) of 18 compared to an MNI of 3 for *Venenosaurus*. Given there are only two sauropod taxa in the quarry, and that most elements of brachiosaurids and *Moabosaurus* in the quarry can be differentiated, we feel confident in the referral of the elements to *Moabosaurus* given in Table 1. Casts of the holotypic dorsal vertebrae (BYU 14387A–C) of *Moabosaurus utahensis* as well as several key referred specimens (BYU 10815, 10976, 14063A, 14122, 11241, 14777) have been accessioned to the University of Michigan Museum of Paleontology.

DESCRIPTION

In this contribution, we focus on a description of the cranial and axial elements along with a few, select appendicular elements.

Skull and Teeth

Premaxilla.— A single, right premaxilla (BYU 14055; Fig. 7) is known, consisting of the main body, which is broken horizontally just under the premaxillary shelf. Both articular surfaces, the anterior median symphysis and the posterior maxillary contact, are broken and incomplete. The premaxilla preserves four large alveoli, and only the anterior-most, unerupted tooth is exposed (Fig. 7B). The premaxilla has a similar robustness to that of *Camarasaurus*. It was closely associated with a dentary given the same catalog number, BYU 14055, described below.

Maxilla.— Two partial maxillae were recovered from the quarry. One right maxilla (BYU 14178) consists of nearly the entire tooth-bearing portion, but broken pre-burial posterior to the last alveolus. The articular surface for the premaxilla is damaged and the ascending nasal process is missing. It bears nine alveoli, with unerupted teeth embedded in the posteriormost two alveoli. The other specimen (BYU 14143) is a thick, blocky fragment of the central portion of another right maxilla. Broken through at mid-section horizontally, it bears the central five alveoli, each filled with cross-sections of teeth and replacement teeth. This section shows teeth replacing posterior to anterior. In *Moabosaurus* the distal edge of one tooth overlaps the mesial edge of the succeeding tooth labially. This *en echelon* pattern is shared with *Camarasaurus* but is lost in *Giraffatitan* (Wilson and Sereno, 1998; Wiersma and Sander, 2016).

Frontal-Parietal.—Frontals and parietals are preserved in articulation with six of the braincases, two of them are figured here (BYU 14360, Fig. 8; BYU 14494, Fig. 9). In each case, suture lines with adjoining elements are not evident (Figs. 8, 9). Along the midline, just anterior to the supraoccipital, the parietals are thin, because this area of the skull roof covers the diencephalon, the highest portion of the cranial cavity. In four cases (BYU 15187, 11614, 14360, 14592), there is a large, central opening (Fig. 8A, E, F). We interpret this to be the result of breaking the thin bone, but we cannot rule out that it is a natural feauture that may imply individual variation. Similar variation can be seen in the *Camarasaurus* braincases illustrated in Madsen et al (1995), but this feature was not discussed. A postparietal foramen occurs in *Dicraeosaurus*, *Amargasaurus*, and *Tornieria* in the same position (Upchurch et al., 2004). Posteriorly, the parietals are expanded laterally and are fused to the supraoccipital and otoccipitals. In dorsal view, the parietals form the entire margin of the concave, medial margin of the preserved portion of the supratemporal fenestra. The full configuration of the supratemporal fenestra is unknown because the postorbital has not been found in articulation with the skull and no squamosal is known (Figs. 8, 9).

Where preserved, the frontals are fused to each other and to adjoining braincase elements (Figs. 8, 9). They form the anterior roof of the cranial cavity centrally, and the posterior roof of the orbit laterally. The frontals are dorsally flat and are fused to the parietals posteriorly and to the laterosphenoid-orbitosphenoid below. They are at their widest point above the lateral wing of the laterosphenoid, where they would articulate with the postorbital, although this articular facet is lost or biocorroded in all specimens. In dorsal view, each side is nearly as long as it is wide, ending anteriorly in a convex arc (Fig. 9F). A short, anteriorly directed prong extends from near the anterolateral corner of each frontal (Fig. 9F). The prefrontal articulated lateral to this prong, and the nasals anterior and medial to the prong.

Postorbital.— Three incomplete postorbitals have been recovered from the quarry, with BYU 11229 being the best preserved. *Moabosaurus* postorbitals are robust and T-shaped, making them more similar to those of *Camarasaurus* than those of *Giraffatitan*. In addition, like *Camarasaurus*, the posterodorsal rim of the orbit is laterally rugose. They differ from postorbitals described and illustrated for *Camarasaurus* (Madsen et al., 1995), in that the squamosal (posterior) process is tabular instead of tapering, the deep fossa within the concave orbital wall is absent, and the entire element is mediolaterally deeper, especially the ventral process.

Quadrate.—The quadrate is represented by seven specimens (five left, two right), although four of these specimens consist only of the distal condyles. The quadrates show considerable variation, as do the quadrates in *Camarasaurus*, although Madsen et al (1995) described it as one of the most conservative bones in the sauropod skull. The best-preserved quadrate, BYU 14375 (Fig. 7D–I), lacks only the pterygoid wing. The quadrate is similar that of *Camarasaurus* and falls within the range of morphological variation of that taxon (Madsen et al., 1995). All the quadrates exhibit a distinctive step on the distal articular condyle (Fig. 7G–H). Carpenter and Tidwell (1998) considered this one of the characters that set *Brachiosaurus* apart from *Camarasaurus*. However, the distal condyles in *Camarasaurus* vary considerably. Three of

TABLE 1 — Specimens referred to *Moabosaurus utahensis*. All are from the Dalton Wells Quarry, near Moab, Utah (Fig. 1). The bone-bearing horizon is at base of the Yellow Cat Member of the Cedar Mountain Formation which is no older than early Albian. Measurements for braincases are the maximum lateral dimension, as preserved. Measurements for other cranial elements are for the longest dimension as preserved. Measurements for teeth and appendicular elements are for the longest dimension. Measurements for vertebrae are the centrum length. The tilde (~) prefix indicates the measurement is approximate due to incomplete preservation or overlapping elements.

	Specimen #	Element	Dimension mm
1	BYU 14387A-C	holotypic dorsal vertebrae	210, 225, 210
2	BYU 15187	braincase	119
3	BYU 11614	braincase	138
4	BYU 14360	braincase	165
5	BYU 14592	braincase	120
6	BYU 14359	braincase	220
7	BYU 14114	braincase	168
8	BYU 14760	braincase	130
9	BYU 15186	braincase	92
10	BYU 9460	braincase+cervicals 1-4+rib	140
11	BYU 14544	braincase	129
12	BYU 14877	braincase	152
13	BYU 14759	braincase	138
14	BYU 15185	braincase	124
15	BYU 11294	braincase	148
16	BYU 14322	braincase	47
17	BYU 14494	braincase	184
18	BYU 20816	braincase	225
19	BYU 20817	braincase	149
20	BYU 14375	quadrate	204
21	BYU 11229	postorbital	120
22	BYU 14055	premaxilla	145
23	BYU 14178	maxilla	156
24	BYU 14143	maxilla	87
25	BYU 14055	dentary	97
26	BYU 20818	tooth, anterior dentary	70
27	BYU 14327	tooth, left premaxilla	72
28	BYU 18172	tooth, anterior maxilla	67
29	BYU 18120	atlas intercentrum	60
30	BYU 10815	axis	217
31	BYU 14790	cervical vertebra 3	142
32	BYU 18143	cervical vertebra ~4	160
33	BYU 14063A, B	cervical vertebrae ~5&6, rib	216, 260
34	BYU 14388	cervical vertebra, mid series	360
35	BYU 10794	cervical vertebra, mid series	350
36	BYU 15151	cervical vertebra, posterior	250
37	BYU 14346	cervical vertebra, posterior	295
38	BYU 14373	cervical vertebra, posterior	170
39	BYU 14758	cervical vertebra, posterior	283
40	BYU 10945	cervical rib	355
41	BYU 10946	cervical rib	500
42	BYU 14051	dorsal vertebra 1	160
43	BYU 10492	dorsal vertebra 1	210
44	BYU 14557	dorsal vertebra 2	180
45	BYU 10950	dorsal vertebra 2	120
46	BYU 15249B, C	dorsal vertebrae 2 & 3	240, ~220
47	BYU 14122	dorsal vertebra 3	~190
48	BYU 14905A, B	dorsal vertebrae 3 & 4	~140, 160
49	BYU 15248	dorsal vertebra, mid series	180
50	BYU 10976	dorsal vertebra, mid series	200
51	BYU 14502	dorsal vertebra, posterior	170
52	BYU 14771	sacrum+caudals 1&2dorsal	802
53	BYU 14785	caudal vertebra 1	190
54	BYU 10911	caudal vertebra, ~2	180
55	BYU 14768	caudal vertebrae 3-5	140, ~135, 135
56	BYU 11275	caudal vertebra, ~4	175
57	BYU 10883	caudal vertebra ~9	125
58	BYU 11687	caudal vertebra, mid series	113
59	BYU 10957	caudal vertebra, mid series	152
60	BYU 10837	caudal vertebra, mid series	132
61	BYU 9449	caudal vertebra, mid series	135
62	BYU 11634	caudal vertebra, distal	130
63	BYU 11313	caudal vertebra, distal	89
64	BYU 11657	caudal vertebra, distal	102
65	BYU 11657	caudal vertebra, distal	96
66	BYU 14386	caudal vertebra, distal	83
67	BYU 11241	left sternal plate	640
68	BYU 10798	left humerus	1070
69	BYU 14777	right ulna	815
70	BYU 14783	left femur	1210

the four *Camarasaurus* quadrates illustrated by Madsen et al. (1995) from the Cleveland Lloyd Quarry show some degree of a step.

Braincase.— Eighteen sauropod braincases (Table 1), some with the skull roof, were recovered from the Dalton Wells Quarry (Figs. 5A–D, 8–10). Reflecting the complex taphonomic history of the Dalton Wells deposit, the crania exhibit a wide range of preservation. Many specimens lack processes and ridges due to combinations of trampling and insect damage, but all are completely fused ventrally with elements of the lateral walls and occiput. In nearly every case, the sutural contacts between elements are indiscernible, but individual elements can sometimes be identified based on differences in direction of the bone grain.

All braincases are similar to those of *Camarasaurus*, by virtue of their robust, posteroventrally directed occipital

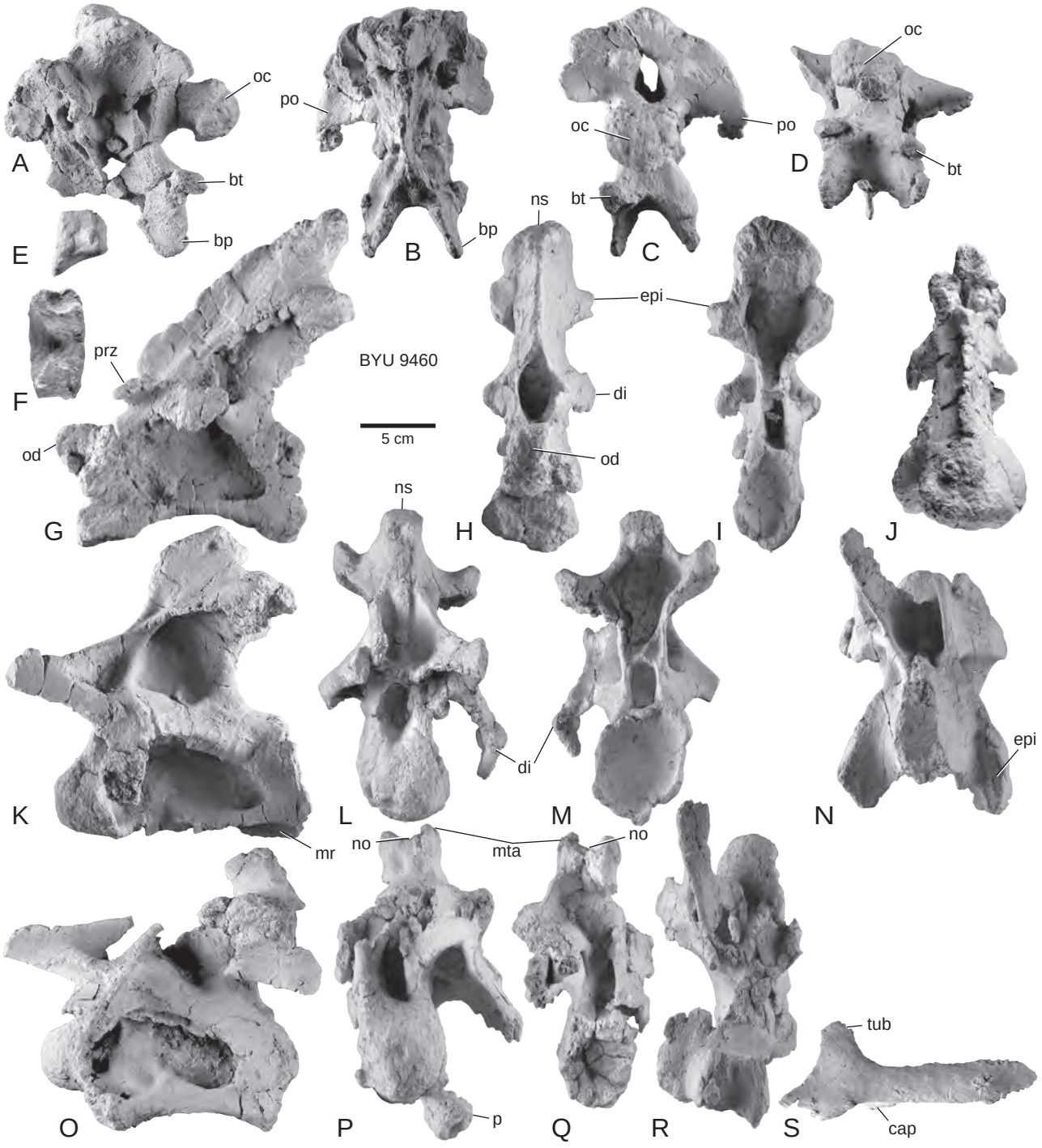

FIGURE 5 — *Moabosaurus utahensis*, referred braincase and closely associated and articulated cervical vertebrae, BYU 9460. **A–D**, braincase in left lateral, anterior, posterior, and ventral views. **E–F**, atlas in left lateral and dorsal views. **G–J**, axis in left lateral, anterior, posterior, and dorsal views. **K–N**, cervical 3 in left lateral, anterior, posterior, and dorsal views. **O–R**, cervical 4 in left lateral, anterior, posterior, and dorsal views. **S**, left cervical rib found closely associated with cervical vertebrae 3 and 4, in left lateral view. Abbreviations: *bp*, basipterygoid process; *bt*, basal tubera of basioccipital; *cap*, capitulum of rib; *di*, diapophysis; *epi*, epipophysis; *mr*, median ridge; *mta*, metapophysis; *no*, notch; *ns*, neural spine; *oc*, occipital condyle; *od*, odontoid process; *p*, parapophysis; *po*, paraoccipital process; *prz*, prezygapophysis; *tub*, tuberculum of rib.

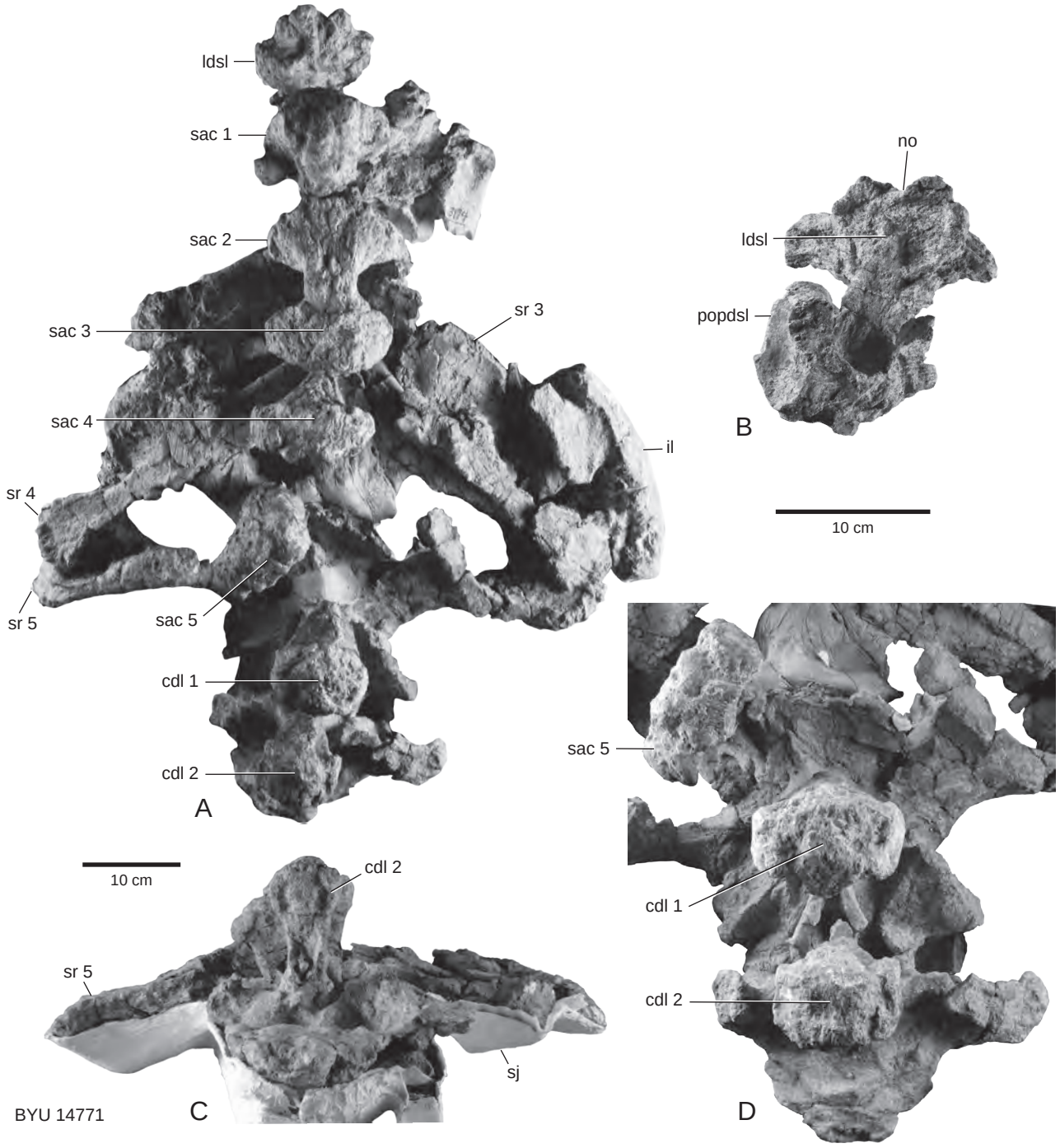

FIGURE 6 — *Moabosaurus utahensis*, referred sacrum, BYU 14771, articulated with the last dorsal (and prezygapophysis of penultimate dorsal) and caudal vertebrae 1–2. **A**, articulated vertebral series consisting of the last dorsal spine, sacral vertebrae 1–5 and caudal vertebrae 1–2 in dorsal view. **B**, neural spine of last dorsal vertebra in anterior view with the vertically displaced right postzygapophysis of the penultimate dorsal. **C**, sacrum with caudal vertebrae 1 and 2 in posterior view. **D**, Detail of neural spines of sacral vertebra 5 and caudal vertebrae 1 and 2 in posterodorsal view. A and C share same scale; B and D share same scale. Abbreviations: *cdl*, caudal vertebra; *il*, ilium; *ldsl*, last dorsal vertebra; *no*, notch; *popdsl*, postzygapophysis of penultimate dorsal vertebra; *sac*, sacral vertebra; *sj*, supporting jacket; *sr*, sacral rib.

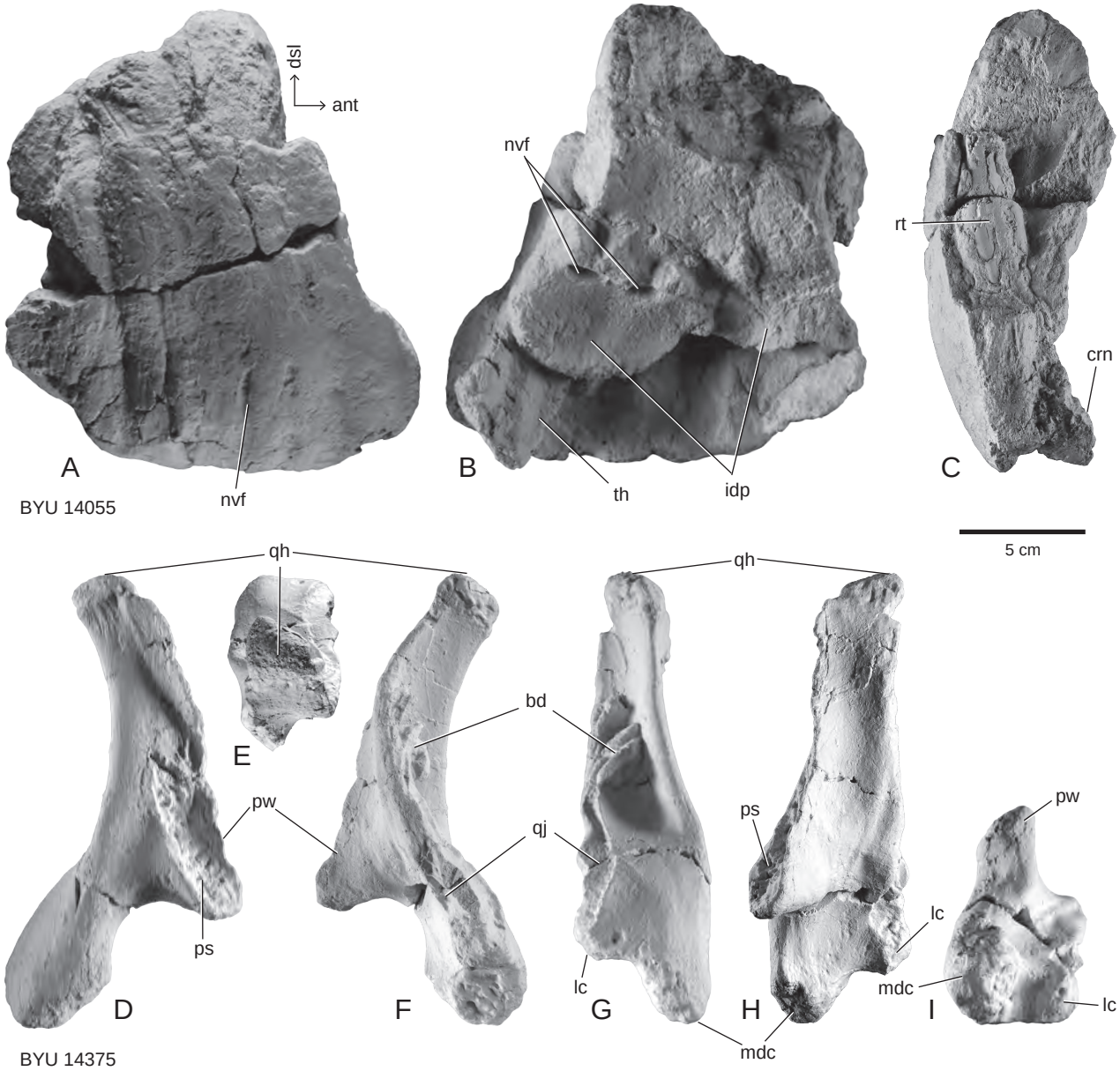

FIGURE 7 — *Moabosaurus utahensis*, referred right premaxilla (BYU 14055) and left quadrate (BYU 14375). **A–C**, right premaxilla (BYU 14055) in lateral, medial, and anterior views. **D—I**, quadrate (BYU 14375) in medial, dorsal, lateral, posterior, anterior and ventral views. Abbreviations: *ant*, anterior; *bd*, bone debris; *crn*, crown; *dsl*, dorsal; *idp*, interdental plate; *lc*, lateral condyle; *mdc*, medial distal condyle of quadrate; *nvf*, neurovascular foramen; *ps*, articular surface for pterygoid; *pw*, pterygoid wing of quadrate; *qh*, quadrate head; *qj*, quadrojugal contact; *rt*, root; *th*, tooth.

condyle, ventrally directed basipterygoid processes that are somewhat ventral to the occipital condyle, and anteriorly directed olfactory tracts (Figs. 5A–D, 8–10). The basicrania exhibit a considerable range of variation, from the size and shape of the processes, foramina and fossae, to the relative dimensions. Despite this variation, they differ from all other sauropods in having a basioccipital with a thin ventral apron adpressed against the basisphenoid, as can be seen in lateral view (Figs. 8B, 9B). The basal tubera are posteriorly projecting (Figs. 5A, 8B, 9B, 10B) at the end of weak stalks that tend to fade into the bony apron (Figs. 5C, 8A, 9A, 10A). In posterior view, the broadly flattened bone bridges the gap between the basal tubera (Figs. 5C, 8A, 9A, 10A). In contrast, both *Camarasaurus* and *Giraffatitan* bear broad, robust basal tubera that are supported above by stout ridges separated by a deep groove.

The otoccipitals, or paired exoccipital-opisthotic complexes, form much of the occiput. They sit firmly on the basioccipital, comprise the lateral walls of the foramen magnum, separated dorsally by the supraoccipital. Two bulging proatlantal facets occur on either side of the foramen magnum, just lateral to the contact with the supraoccipital. The prootic is firmly fused to the anterior side of the otoccipital. The wing-like paraoccipital processes extend outward but are incomplete on all the preserved crania, lacking their terminus. As in *Camarasaurus*, *Brachiosaurus*, and *Giraffatitan*, the paraoccipital processes extend laterally and slightly posteroventrally (Figs. 5C, 8C, 10A).

At the anterior base of the otoccipital, a relatively deep metotic foramen is present for passage of cranial nerves IX–XI and probably the jugular vein (Madsen et al., 1995). The size and complexity of this foramen varies among specimens, but in all, the metotic foramen opens ventrolaterally and somewhat posteriorly (Figs. 8A, B, 9A, B). A small foramen for cranial nerve XII enters the otoccipital-basioccipital contact just inside the ventrolateral corners of the foramen magnum and exiting just posterodorsal to the large metotic foramen.

The crista tubularis is the posteriormost of two ridges that extend ventrally along the braincase from near the base of the paraoccipital process (Figs. 8C, 9C). Unlike what is described for *Camarasaurus* (Madsen et al., 1995), *Turiasaurus* (Royo-Torres and Upchurch, 2012), and an Early Cretaceous sauropod from Texas (Tidwell and Carpenter, 2003), the crista tubularis borders the posterior part of the metotic foramen and then converges anteriorly to abut against the crista prootica for some distance, running down the lateral side of the basioccipital-basisphenoid contact. The two ridges then diverge, the crista tubularis ending at the basal tubera, and the crista prootica sweeping posteriorly, ending at the basipterygoid process.

The supraoccipital is a pentagon-shaped bone, roughly as tall as it is wide, that roofs the foramen magnum (Figs. 8A, 9A, 10E). This robust, blocky bone is bound firmly on either side by the exoccipital-opisthotic complex (otoccipital) and the prootics. Some specimens bear a broad but faint nuchal crest. The supraoccipital articulates with the parietals along its dorsal edges by a thick, digitate suture. Dorsolaterally, at the supraoccipital-otoccipital-parietal juncture, there is a relatively narrow post-temporal fenestra.

The lateral and anterior wall of the braincase is a fused unit consisting of the prootic, laterosphenoid and the orbitosphenoid. The contacts are indistinct in lateral view, and only on the exposed sutural contact with the skull roof in BYU 14877, and in BYU 14760 is the upper contact for the prootic and laterosphenoid apparent. Here, it occurs along the anterior wall of the supratemporal fenestra, along the posterior side of the crista antotica of the laterosphenoid. For the most part, the prootic is a smooth, concave expansive bone that extends posteriorly onto the anterior face of the paraoccipital processes of the otoccipital complex, occupying the portion between two vertically running ridges, the crista prootica and crista antotica. Ventrally, the prootic is fused to the basisphenoid, but it is not certain whether it contacts the basioccipital. A large foramen for the trigeminal nerve (V) occurs in the anteroventral corner of the lateral wall of the prootic, just under the ventral terminus of the crista antotica (Figs. 8B, 9B, 10B). The trigeminal foramen is bordered anteriorly by the laterosphenoid.

The laterosphenoid and orbitosphenoid together form the anterolateral walls of the brain cavity, measuring about the width of the prootic. There exists no hint to their individual identities in the preserved braincases, because no sutural lines are evident. Dorsally they contact the frontals in a thick digitate suture, being higher here at the posterior edge of the laterosphenoid wing (Fig. 10F). The laterosphenoid-orbitosphenoid complex is pierced in lateral view by three foramina (Figs. 8B, 9B, 10B). The moderately sized foramen for cranial nerve III occurs just anterior to the prominent trigeminal foramen. A smaller foramen for cranial nerve IV occurs just posterodorsal to number III, situated just anterior to the crista antotica. The foramen for cranial nerve II is anterior to III, just posterior to where the lower portions of the right and left orbitosphenoids converge along the sagittal midline (Figs. 8B, 9B, 10B). In anterior view, the upper anterior edges of the orbitosphenoids diverge to create a large opening for the olfactory tracts (cranial nerve I) just below the frontals. In most of the preserved sauropod braincases from Dalton Wells Quarry, this cavity is very similar to that of *Camarasaurus* and *Giraffatitan*. However, in BYU 14494 (Fig. 9) there is a septum which thickens dorsally to the underside of the frontals, dividing the cavity into left and right portions (Fig. 9D). This is either a feature that is rarely ossified/preserved, a function of individual variation, or it may occur in larger individuals of *Moabosaurus* (BYU 14494 is the largest known braincase).

The basisphenoid is the anteroventral element of the braincase and forms the forward half of the floor of the cranial cavity. Centered within the top of the basisphenoid and the floor of the cranial cavity, is a large foramen for the pituitary body. This foramen expands ventrally, occupying much of the internal chamber of the basisphenoid. The sides are marked by one or more deep vertical fossae. Posteriorly, the basisphenoid is firmly fused to the basioccipital and is marked by the crista prootica, which runs down its posterolateral edge (Figs. 8A–C, 9C, 10A). Its anterior margin forms a sharp sagittal edge that slopes anterodorsally, in line with the orbitosphenoid above. Because of the delicate nature of the thin anteriorly-directed parasphenoid process, it is missing in all braincases, save for a small remnant preserved in BYU 9460 (Fig. 5). Here, its base is high on the basisphenoid, at the level of the occipital condyle. Ventrally, in posterior view, the basisphenoid diverges into two basipterygoid processes that extend 30–45 degrees out from midline. The processes vary in shape, but all extend only moderately below the basal tubera, much like in *Camarasaurus*. The basipterygoid processes are separated by a V- to U-shaped notch, posterior to which occurs a deep pit, just anterior to the ventral apron of the basioccipital (Figs. 5C,

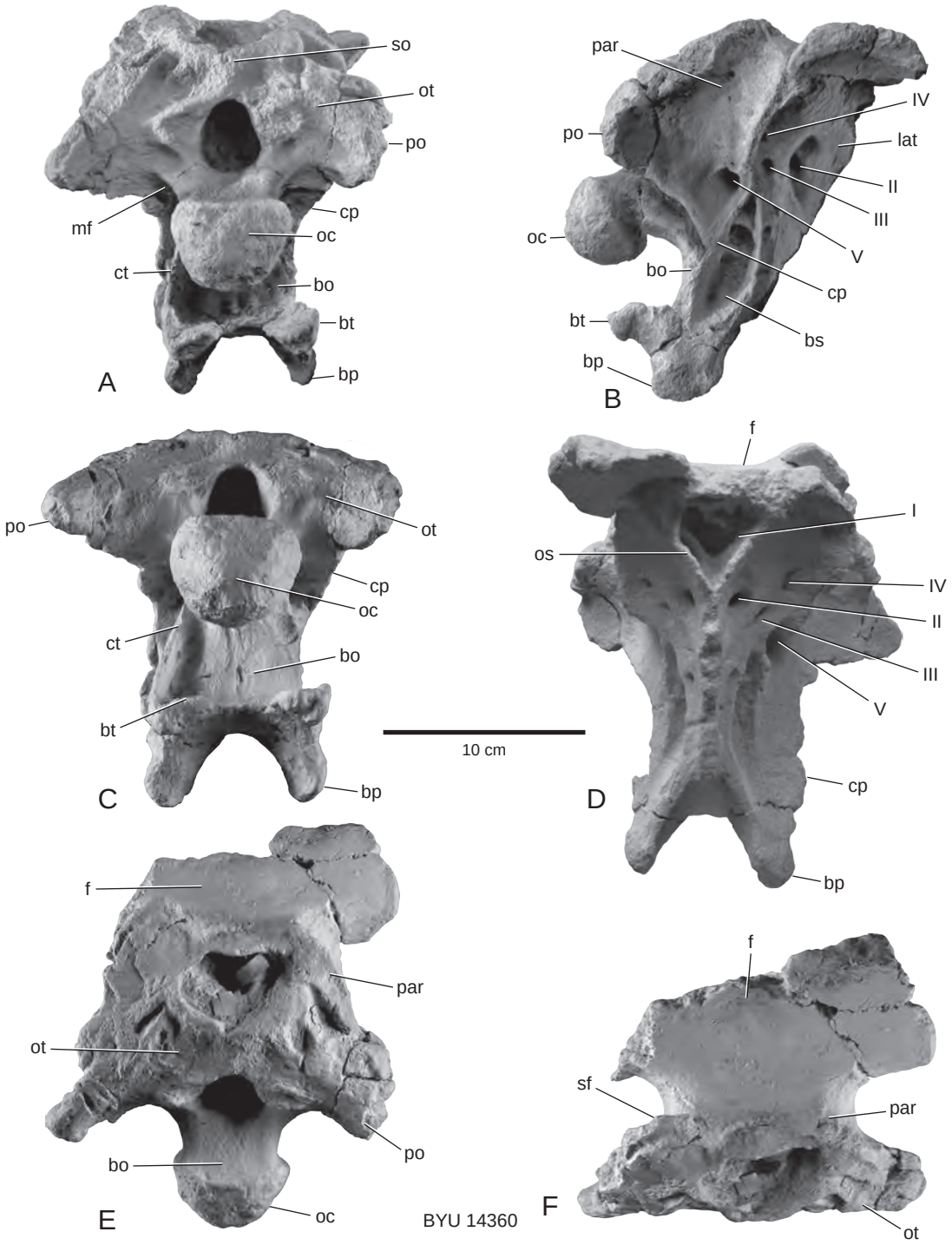

FIGURE 8 — *Moabosaurus utahensis*, referred braincase BYU 14360. Braincase BYU 14360 in posterior (**A**), right lateral (**B**), posteroventral (**C**), anterior (**D**), posterodorsal (**E**), and dorsal (**F**) views. Abbreviations: I–V, cranial nerve foramina; *bo*, basioccipital; *bp*, basipterygoid process; *bs*, basisphenoid; *bt*, basal tubera; *cp*, crista prootica; *ct*, crista tabularis; *f*, frontal; *lat*, laterosphenoid; *mf*, metotic foramen; *oc*, occipital condyle; *os*, orbitosphenoid; *ot*, otoccipital (exoccipitals & opisthotic); *par*, parietal; *po*, paraoccipital process; *sf*, supratemporal fenestra; *so*, supraoccipital.

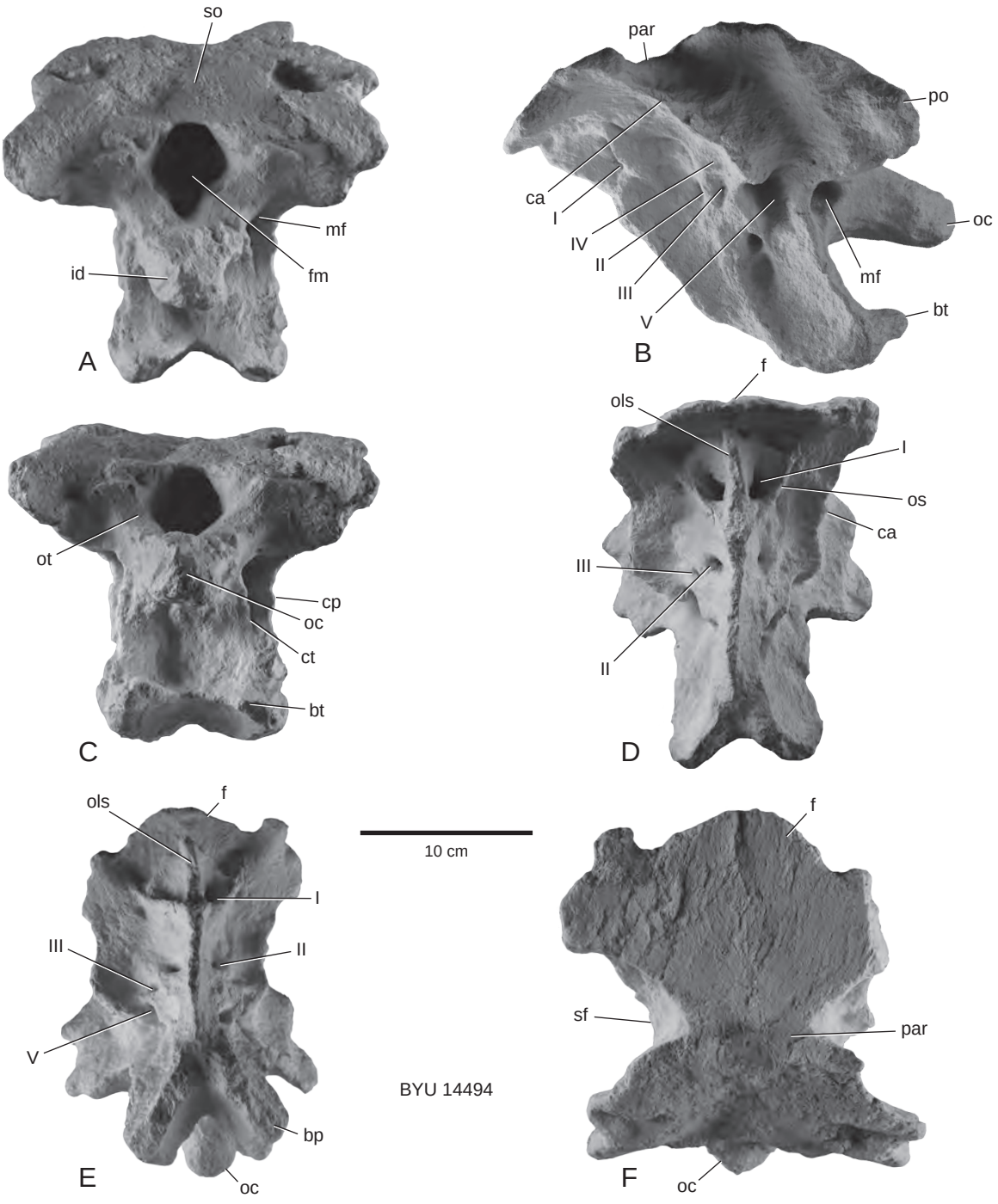

FIGURE 9 — Moabosaurus utahensis, referred braincase BYU 14494. Braincase, BYU 14494, in posterior (**A**), left lateral (**B**), posteroventral (**C**), anterior (**D**), anteroventral (**E**), and dorsal (**F**) views. Abbreviations: I–V, cranial nerve foramina; *bp*, basipterygoid process; *bt*, basal tubera; *ca*, crista antotica; *cp*, crista prootica; *ct*, crista tabularis; *f*, frontal; *fm*, foramen magnum; *id*, insect damage; *mf*, metotic foramen; *oc*, occipital condyle; *ols*, olfactory lobe septum; *os*, orbitosphenoid; *ot*, otoccipital (exoccipitals & opisthotic); *par*, parietal; *po*, paraoccipital process; *sf*, supratemporal fenestra; *so*, supraoccipital.

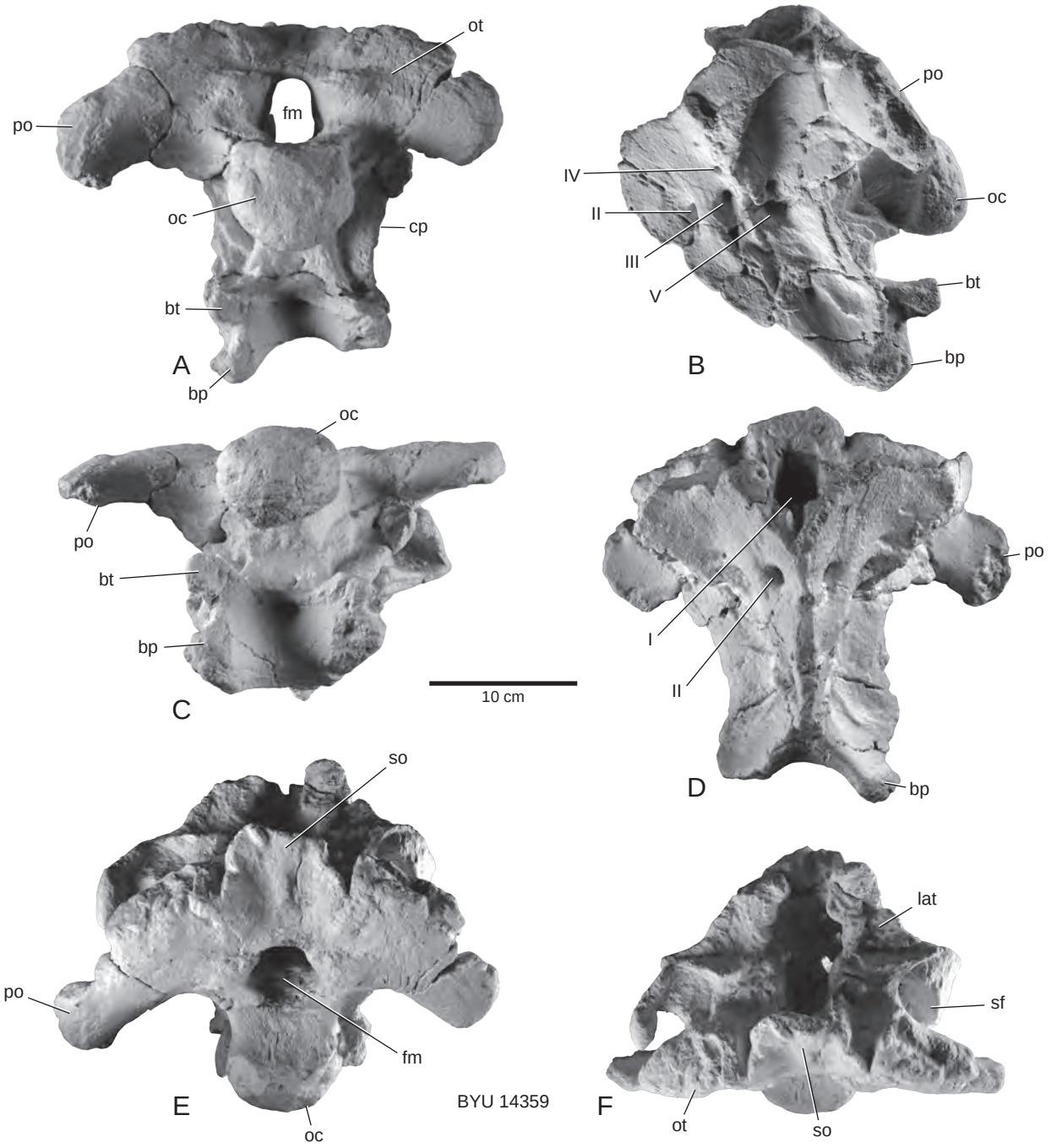

FIGURE 10 — *Moabosaurus utahensis*, referred braincase BYU 14359. Braincase BYU 14359 in posterior (**A**), left lateral (**B**), ventral (**C**), anterior (**D**), posterodorsal (**E**), and dorsal (**F**) views. Abbreviations: *I–V*, cranial nerve foramina; *bp*, basipterygoid process; *bt*, basal tubera; *cp*, crista prootica; *fm*, foramen magnum; *lat*, laterosphenoid; *oc*, occipital condyle; *ot*, otoccipital (exoccipitals & opisthotic); *po*, paraoccipital process; *sf*, supratemporal fenestra; *so*, supraoccipital.

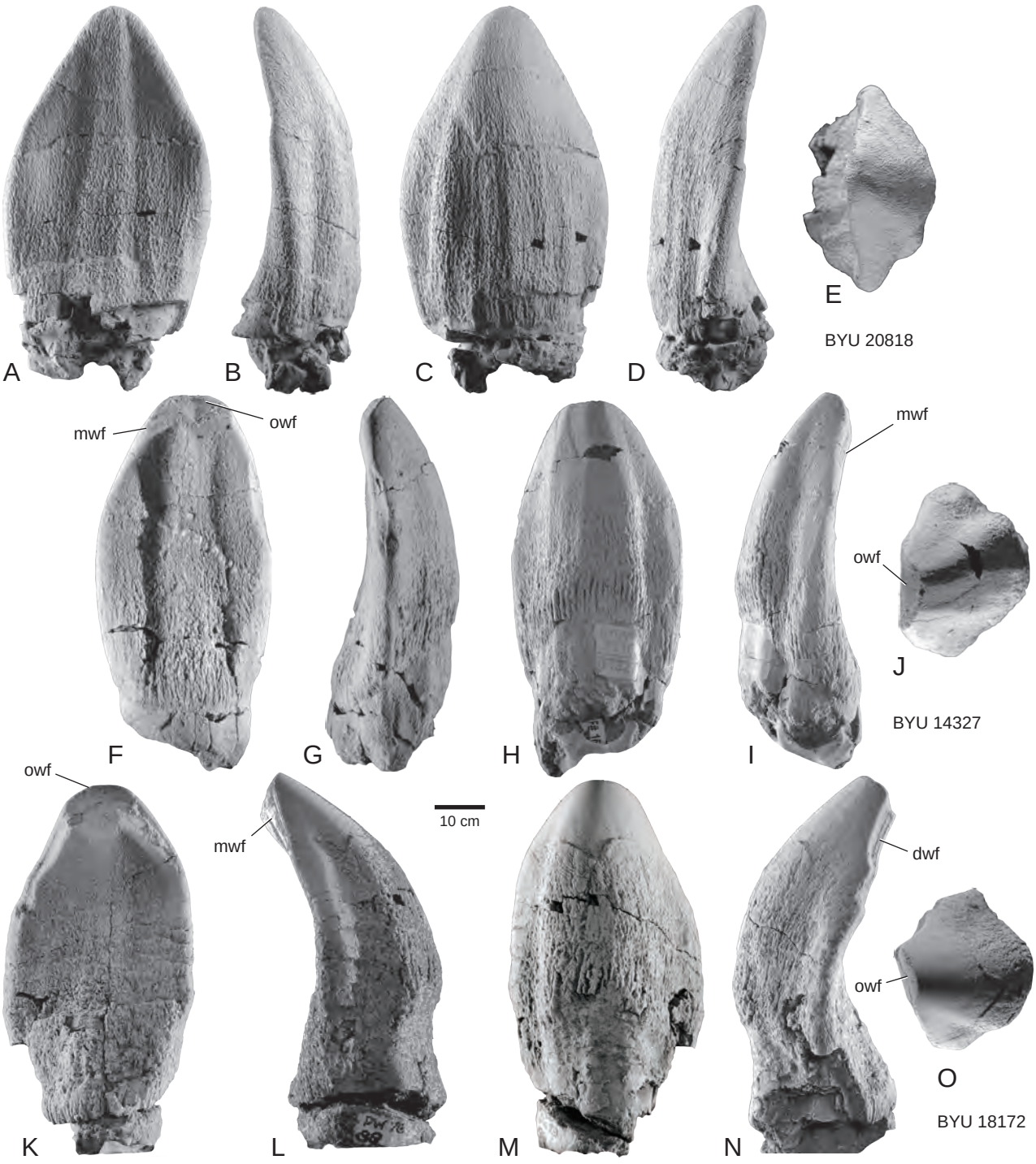

FIGURE 11 — *Moabosaurus utahensis*, referred teeth. **A–E**, unworn left, anterior dentary tooth BYU 20818 in lingual, mesial, labial, distal, and occlusal views. **F–J**, left premaxillary tooth BYU 14327 in lingual, mesial, labial, distal, and occlusal views. **K–O**, right, anterior maxillary tooth BYU 18172 in lingual, mesial, labial, distal, and occlusal views. Abbreviations: *dwf*, distal wear facet; *mwf*, medial wear facet; *owf*, occlusal wear facet.

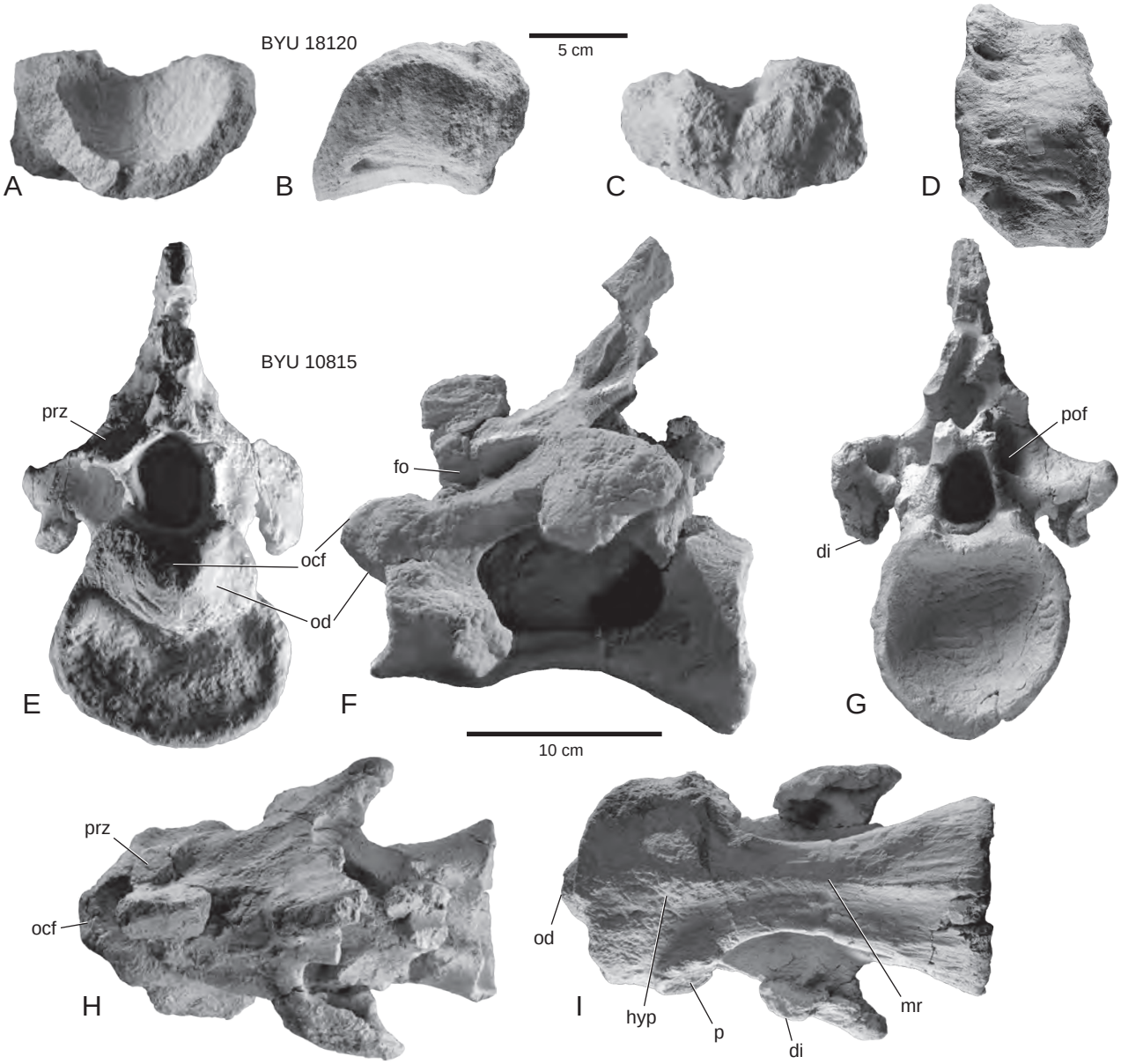

FIGURE 12 — *Moabosaurus utahensis*, referred atlas, BYU 18120, and axis, BYU 10815. **A–D**, atlas, BYU 18120, in anterior, left lateral, posterior, and ventral views. **E–I**, axis, BYU 10815, in anterior, left lateral, posterior, dorsal, and ventral views. Abbreviations: *di*, diapophysis; *fo*, fossa; *hyp*, hypophysis; *mr*, median ridge; *ocf*, occipital condyle facet; *od*, odontoid; *p*, parapophysis; *pof*, postzygapophyseal fossa; *prz*, prezygapophysis.

8A, C, 9A, C, 10A, C). Unlike *Camarasaurus* (Madsen et al., 1995), the basisphenoid does not contribute to the basal tubera in *Moabosaurus*.

The basioccipital comprises the posteroventral portion of the braincase and occipital condyle. The robust occipital condyle is similar to *Camarasaurus* and *Giraffatitan*, being directed posteroventrally and being wider than high, with a well-defined constricted neck, especially ventrolaterally and ventrally. A deep fossa houses the metotic foramen at its upper end, near the uppermost anterior corner of the bone (Figs. 8A, C, 9A, C, 10A). The crista tabularis borders the posterior side of this fossa, running ventrally and then swinging forward to run adjacent to the crista prootica for most of its length before turning again posteriorly down the side of the basal tubera. As in *Turiasaurus* (Royo-Torres and Upchurch, 2012) the body of the basisphenoid, ventral to the neck of the occipital condyle, is antero-posteriorly thin, being adpressed to the basisphenoid. The basal tubera are modest in size, supported from above by

modest to weak struts that are contiguous with the apron of the basioccipital. The area between the occipital condyle and basal tubera is moderately to deeply concave vertically, but tends to be weakly concave to nearly flat horizontally. Unlike *Camarasaurus* and *Giraffatitan*, the basal tubera are for the most part connected by the thin apron of bone between them (Figs. 8C, 9C, 10A) and the tubera often extend posteriorly (Figs. 5A, 8B, 9B, 10B).

Dentary.— A single fragment of a dentary is known, BYU 14055, which was found closely associated with the right premaxilla described above. It consists of the anterior portion of a large left dentary, and all edges were broken pre-burial. It preserves eight alveoli, the anterior two of which contain un-erupted teeth. As in *Camarasaurus*, the 'chin' is ventrally expanded to house large teeth.

Teeth.— The dentigerous *Moabosaurus* elements preserve few unerupted teeth, so the bulk of the dental information comes from the more than one hundred isolated *Moabosaurus* teeth recovered from the Dalton Wells Quarry. All possess wrinkled enamel on a stout, broadly spatulate crown (Fig. 11). Wrinkled enamel is a synapomorphy of Eusauropoda (Wilson and Sereno, 1998). Tooth enamel thickness is uniform lingually-labially. All teeth closely resemble those of *Camarasaurus* described in a thorough study by Wiersma and Sander (2016). Consistent within individuals of both *Camarasaurus* (Carey and Madsen, 1972; Madsen et al., 1995), and *Giraffatitan* (Janensch 1935-1936) tooth morphology and size vary widely. The dentary teeth (Fig. 11A–E) bear large, lingually-directed mesial wear facets that occluded with apical facets on maxillary teeth (Fig. 11J, K, N, O). Distal facets are common but not as pronounced (Fig. 11K, N). In contrast, the wear facets in *Brachiosaurus* tend to be more apical. Like *Camarasaurus*, and unlike *Giraffatitan* and *Europasaurus*, *Moabosaurus* teeth lack denticles (Wiersma and Sander, 2016).

The Slenderness Index (SI) of Barrett and Upchurch (2005), or ratio of crown height to width, was calculated for *Moabosaurus* based on eighteen fairly complete crowns. The resultant slenderness index ranges between 1.7 to 1.9, which falls within the upper range of variability (from 1.0 to 2.0) for *Camarasaurus* (Wiersma and Sander, 2016). In comparison to *Camarasaurus*, *Moabosaurus* teeth tend to be in the narrower range, but still significantly broader than brachiosaurids (Chure et al., 2010) and *Europasaurus* (Régent, 2011) which vary with an SI of between 2.5 and 3.0.

Although the teeth are not in place, the dentition pattern described by Wiersma and Sander (2016) for *Camarasaurus* is reflected among the teeth of *Moabosaurus*. Anterior teeth are large and spatulate, and tend to be more symmetrical mesiodistally (Fig. 11A–I). Their widest mesiodistal point is at mid-height (Fig. 11A, F, K). Lingual faces are modestly concave both vertically and horizontally, with a centrally placed faint apicobasal ridge (Fig. 11A, F, K). Labially, the anteriormost crowns are convex vertically and horizontally, with a wide central vertical ridge flanked by a faint distal groove and a distinctive mesial groove (Fig. 11C, H, M). Enamel extends further below the crown on the lingual side than on the labial side (Fig. 11H). The roots of anterior teeth are equal in length to the crown and are oval in cross-section with their long axis oriented lingual-labially.

The size and shape of teeth progressively change in the lower and upper jaws posteriorly. The teeth decrease in crown height and width, and their grooves and ridges become more pronounced. The teeth increase in degree of asymmetry posteriorly. The apices, supported by their main lingual and labial ridges, are more distally oriented, and progressively turn in more lingually. A deeper lingual concavity rises higher on the tooth, as does the widest point mesiodistally. Tooth roots are still as long as their crown but the long axis of their oval cross-section is oriented mesiodistally with the crown.

Overall, the teeth of *Moabosaurus* are similar to those of *Camarasaurus*, although in several features they are not as extreme, tooth position for tooth position. The crown width, lingual concavity and lingual in-turning of the apex, labial convexity, and the prominence in ridges and grooves are generally less pronounced. Unlike *Camarasaurus*, the maxillary tooth roots are straight.

Vertebrae

Vertebrae are some of the most diagnostic elements of *Moabosaurus* (see "Diagnosis," above). Although the number of cervical, dorsal, and caudal vertebrae is unknown, the sacrum is complete. We know with precision the positions of the first four cervical vertebrae from specimen BYU 9460, which includes a braincase closely associated with cervical vertebrae 1–4. The positions of the first six dorsal vertebrae was deciphered using several overlapping sets of vertebrae, including the holotype (BYU 14387), which consists of dorsal vertebrae 4–6. A sacrum articulated with the last dorsal vertebra (and the prezygapophyses of the penultimate dorsal vertebra) and the first two caudal vertebrae (BYU 14771) and three associated caudal vertebrae (BYU 14768) allows us to link the dorsal series and the caudal series. Positions of the remaining vertebrae were approximated using serial changes and comparisons to other animals, such as *Camarasaurus*.

Cervical Vertebrae.— The cervical vertebrae from the anterior and middle portions of the neck are well-represented, some by short articulated series. The posterior cervical vertebrae, due to their more delicate construction, are less well represented.

The atlas is represented by nearly complete intercentra BYU 9460 (Fig. 5E–F) and BYU 18120 (Fig. 12A–D). They are unremarkable except for a notable change in robustness from the juvenile (BYU 9460) to the subadult (BYU 18120). The ventral surface bears a series of large neurovascular foramina set in fossae immediately posterior to the anterior edge, and the posterolateral edge of the intercentrum bears a robust parapophysis (Fig. 12D).

We describe two axes, BYU 9460 (part of the juvenile articulated skull/cervical vertebra series) and BYU 10815, which pertains to a subadult individual. They differ primarily in robustness, with the juvenile being more thinly built for its size. BYU 9460 (Fig. 5G–J) has a nearly a complete neural

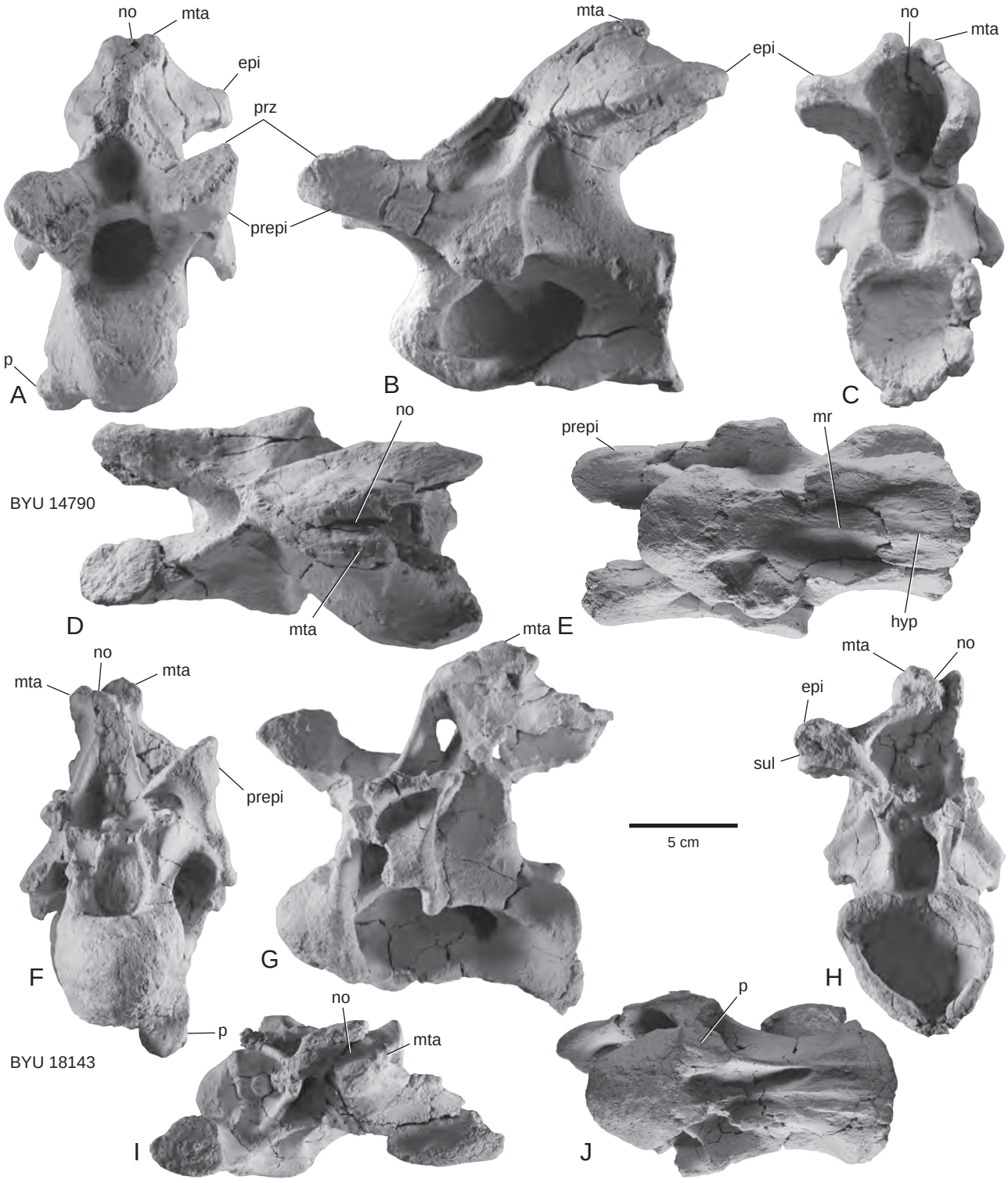

FIGURE 13 — *Moabosaurus utahensis*, referred anterior cervical vertebrae, approximately cervical vertebrae 3 and 4. **A–E**, cervical 3 BYU 14790 in anterior, left lateral, posterior, dorsal, and ventral views. **F–J**, cervical ?4, BYU 18143, in anterior, right lateral (reversed), posterior, dorsal, and ventral views. Abbreviations: *epi*, epipophysis; *hyp*, hypopophysis; *mr*, median ridge; *mta*, metapophysis; *no*, notch; *p*, parapophysis; *prepi*, pre-epipophysis; *prz*, prezygapophyses; *sul*, sulcus.

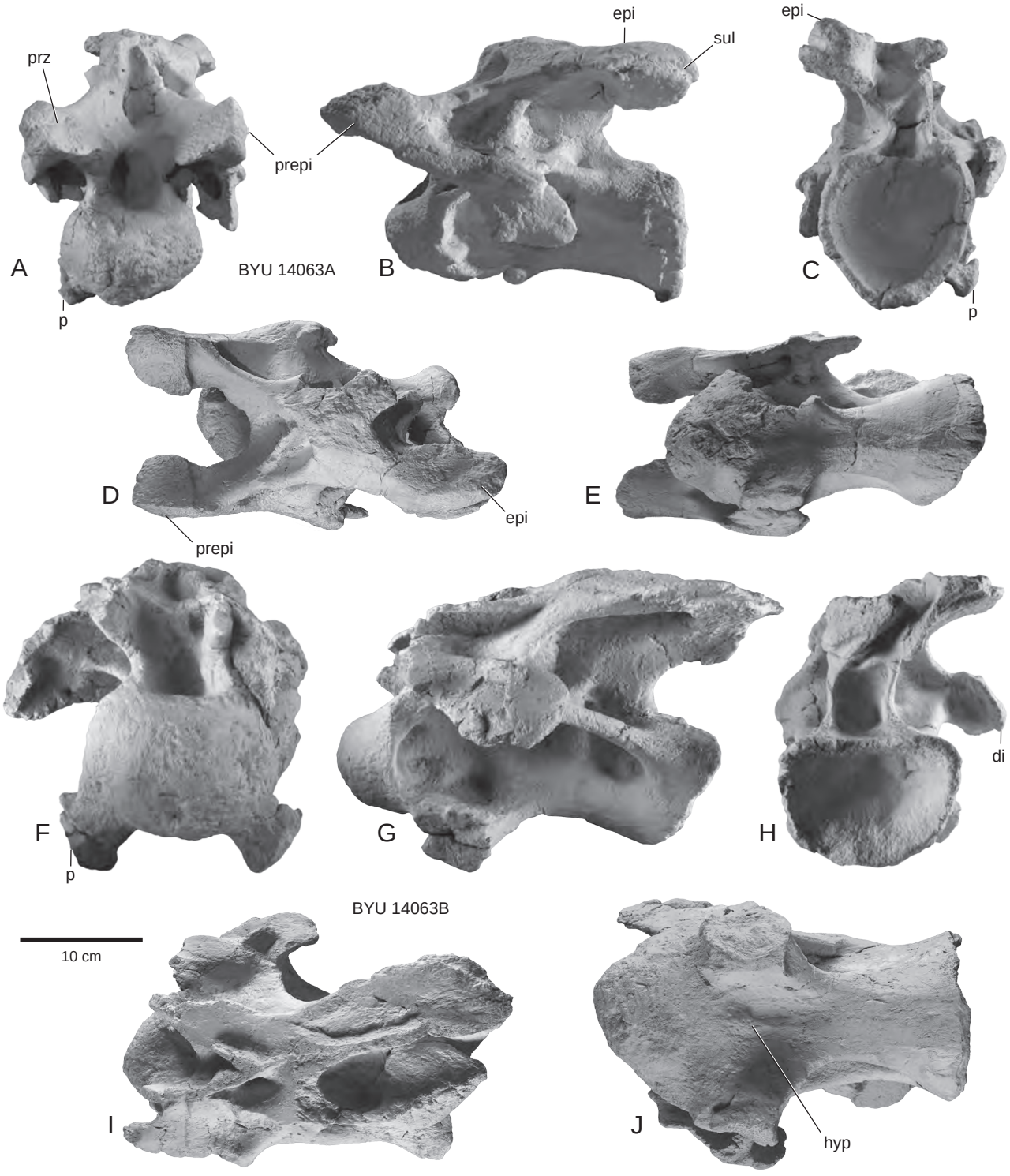

FIGURE 14 — *Moabosaurus utahensis*, referred cervical vertebrae 5 and 6, BYU 14063A and B. **A–E**, cervical 4, and **F–J**, cervical 5, in anterior, left lateral, posterior, dorsal, and ventral views. These vertebrae were articulated in the field and cervical 5 was closely associated with cervical rib BYU 14063. Abbreviations: *di*, diapophysis; *epi*, epipophysis; *hyp*, hypopophysis; *p*, parapophysis; *prepi*, pre-epipophysis; *prz*, prezygapophysis; *sul*, sulcus.

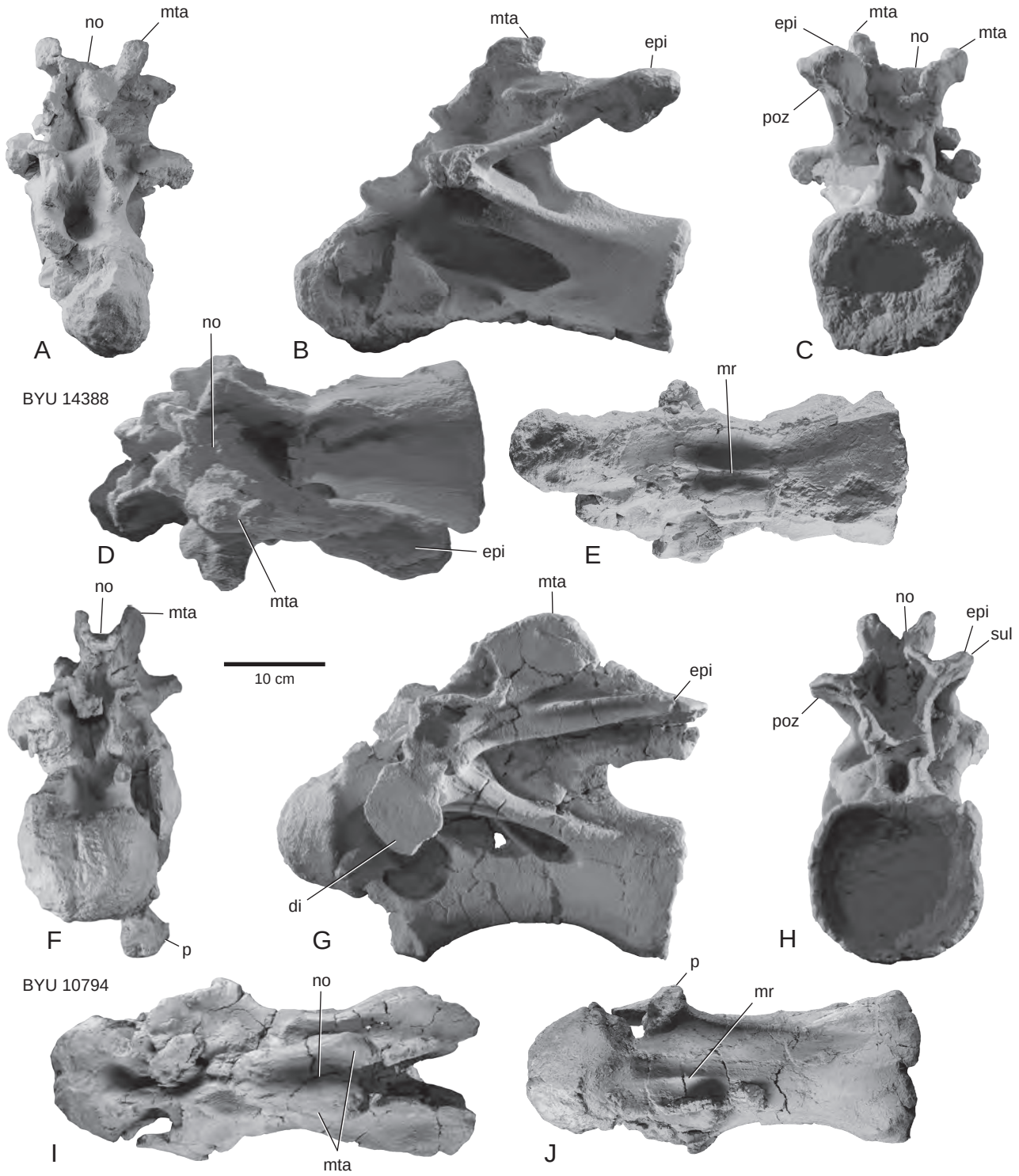

FIGURE 15 — *Moabosaurus utahensis*, referred mid-cervical vertebrae. **A–E**, mid-cervical vertebra, BYU 14388, in anterior, left lateral, posterior, dorsal, and ventral views. Anterodorsal portion of vertebra missing. **F–J**, mid-cervical vertebra, BYU 10794, in anterior, left lateral, posterior, dorsal, and ventral views. Abbreviations: *di*, diapophysis; *epi*, epipophysis; *mr*, median ridge; *mta*, metapophysis; *no*, notch; *p*, parapophysis; *poz*, postzygapophysis; *sul*, sulcus.

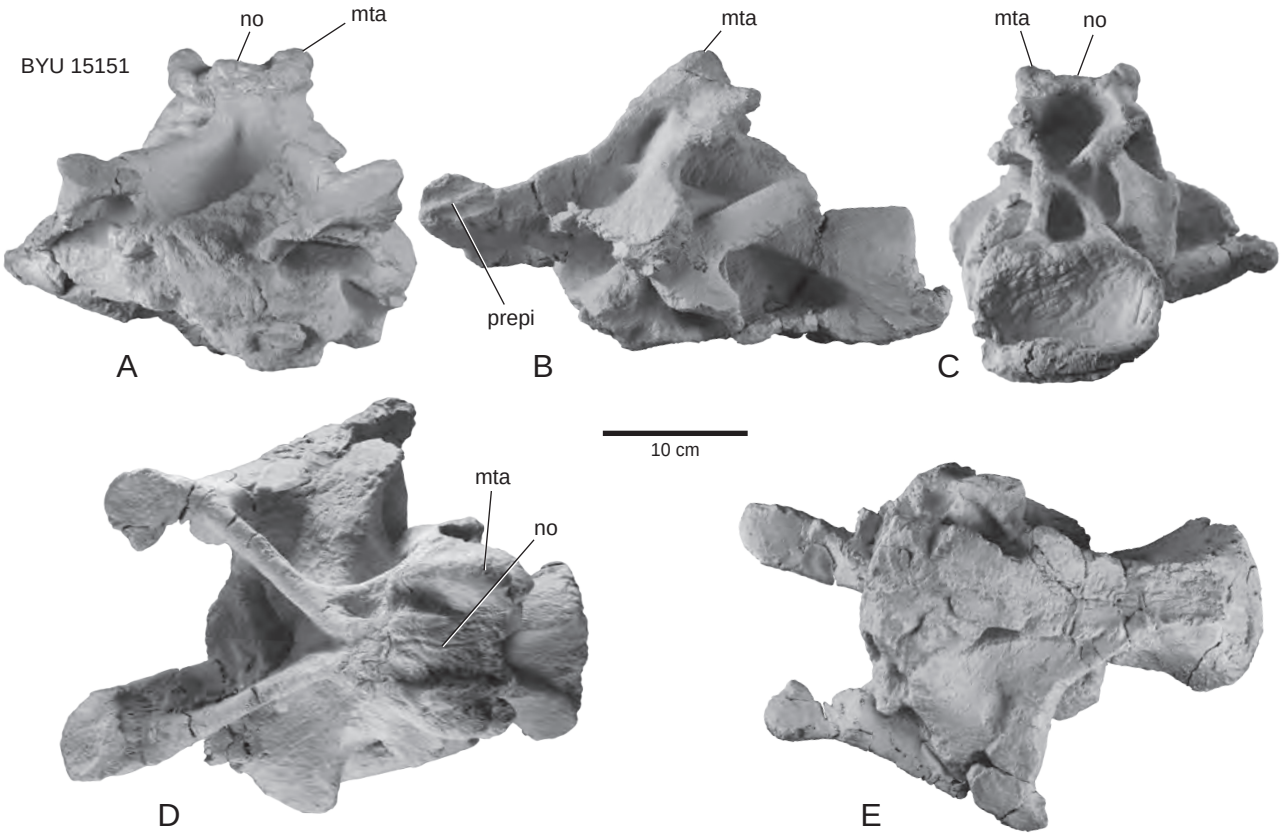

FIGURE 16 — *Moabosaurus utahensis*, referred posterior cervical vertebra BYU 15151. **A–E**, in anterior, left lateral, posterior, dorsal, and ventral views. The neural spine apex is a rectangular table bounded laterally by short but robust spinal metapophyses. The centrum condyle is damaged and largely missing. Abbreviations: *mta*, metapophysis; *no*, notch; *prepi*, pre-epipophysis.

arch with a crushed, broken, and modern root-damaged intercentrum and centrum. BYU 10815 (Fig. 12E–I) preserves little of the neural spine, but the intercentrum and centrum are complete. The axis centrum description is based on BYU 10815 (Fig. 12E–I), all portions of which are heavily built. The centrum is axially elongate. The odontoid is roughly conical but the anterior portion bears a small, anterodorsally facing concavity that is the articular facet for the occipital condyle. The posterior cotyle is slightly higher than wide (Fig. 12G). The ventral edge of the centrum is moderately concave in lateral view. In ventral view it has a narrow 'waist' and a broad V-shaped cross-section, a sharp sagittal ridge, and a moderately developed anterior hypophysial boss at the contact between the axial intercentrum and centrum (Fig. 12I). The parapophysis is large, concave posteroventrolaterally and closely appressed to the centrum. The diapophysis flange is large with a prominent, posterior tendon/muscle attachment, which is medially braced by the robust anterior centrodiapophyseal lamina. The articular face of the diapophysis is complete, robust, rectangular, and faces anteroventrally and is situated about midway along the vertebra. The floor of the neural canal, posterior to the neural arch peduncles, is a sulcus defined by thick lateral margins (Fig. 12G–H).

The centrum is camerate, with large internal pneumatic chambers and thick external walls (sensu Britt, 1993, 1997). The camera is large and expands internally anteriorly and posteriorly to fill the side of the centrum. It is separated from the opposing camera by the sagittal septum. There is a low, robust ventral ridge on the sagittal septum at midlength of the fossa. Internally, the camera extends anteriorly and posteriorly into the ends of the centrum, leaving a thin wall of bone between the camera and the articular faces of the vertebra. The external margin of the camera/pleurocoel is well-defined on the right side but on the left side the anteroventral margin lacks a rim because the fossa, median septum, and lateral margins of the centrum are confluent. Posteriorly, the pleurocoel rim ends well anterior to the posterior end of the centrum.

The neural arch of the axis is described based primarily on the juvenile specimen, BYU 9460 (Fig. 5G–J), which is moderately laterally crushed. The anterodorsal ridge of the neural spine sweeps posteriorly at about 45˚, and in transverse section the ridge is like the roof of a house. The apex of the spine is an axially thick lateral ridge of moderate

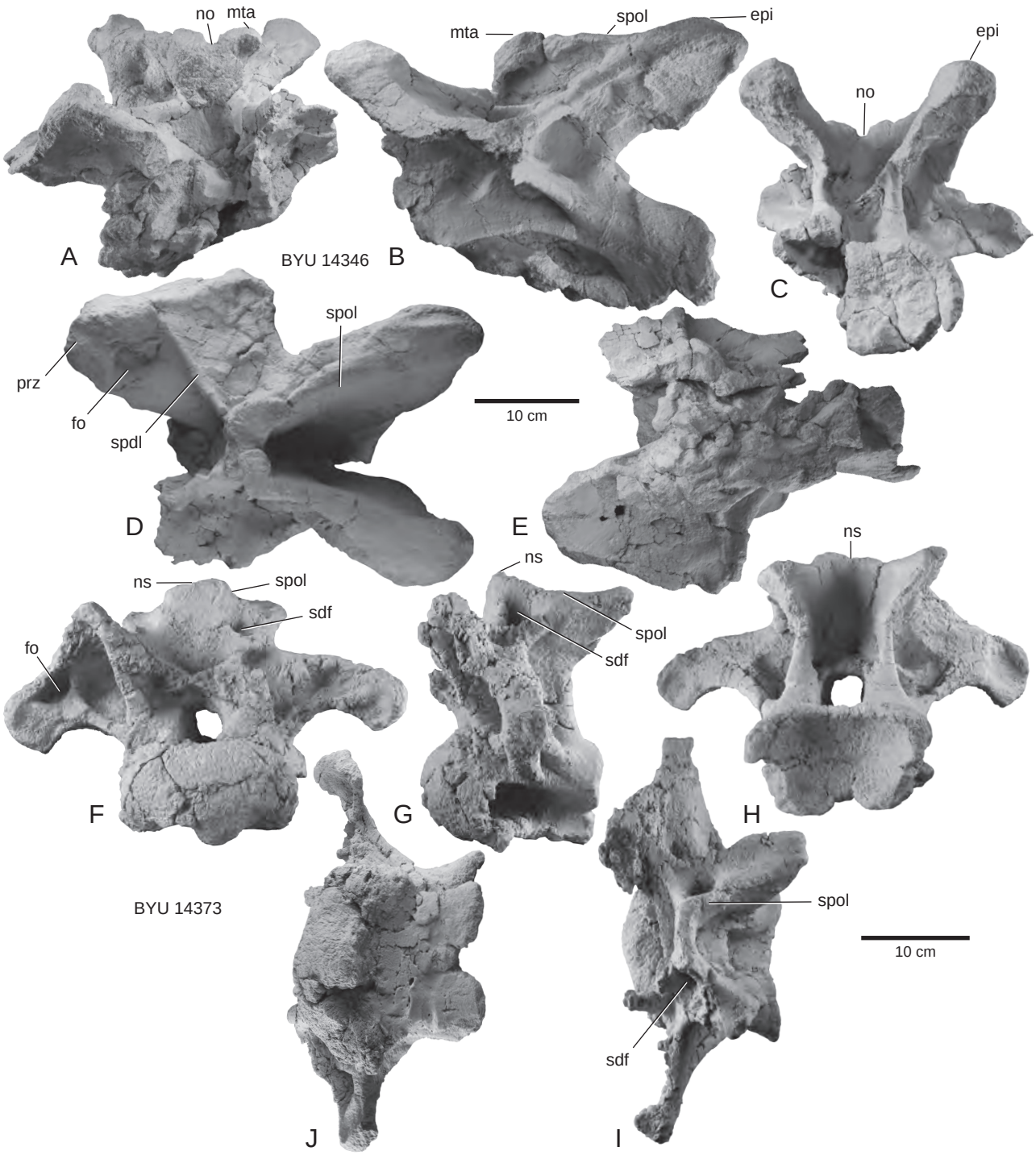

FIGURE 17 — *Moabosaurus utahensis*, referred posterior cervical vertebrae. **A–E**, posterior cervical vertebra, BYU 14346, in anterior, right lateral (reversed), posterior, dorsal, and ventral views. Relative to mid-cervical vertebrae, the spine notch is narrow and the spine is axially short. Much of the ventral surface of the centrum is crushed. **F–J**, posterior cervical vertebra, BYU 14373, in anterior, right lateral reversed, posterior, dorsal, and ventral views. This is likely the last cervical. Its small size indicates it pertains to a juvenile. Abbreviations: *epi*, epipophysis; *fo*, fossa; *mta*, metapophysis; *no*, notch; *ns*, neural spine; *prz*, prezygapophysis; *sdf*, spinodiapophyseal fossa; *spdl*, spinodiapophyseal lamina; *spol*, spinopostzygapophyseal lamina.

width, with small parasagittal apophyses anterior to the apex. The epipophysis projects laterally, and to a lesser degree posteriorly. The spinopostzygapophyseal lamina is short and robust. The postzygapophyseal facet continues ventromedially to the neural arch peduncle. The prezygapophyseal facets are minute, even on the large specimen (BYU 10815, Fig. 12E, F). The prezygodiapophyseal lamina forms a wide lateral shelf, defining, along with the anterior centrodiapophyseal lamina, a large, anterioposteriorly elongated fossa, as a function of the elongate centrum and a posterior sweeping of the diapophysis. These features are best seen on the right side, which is not illustrated. The fossa and laminae are visible but incomplete in left lateral views (Figs. 5G, 12F).

The postaxial cervical vertebrae are well represented, especially the anterior and middle portions of the series. The posterior portion of the series is poorly represented because they have thinner, broader laminae that were susceptible to transport and trample breakage and post-depositional compression. The most complete string of cervical vertebrae is in BYU 9460 (Fig. 5) which preserves the atlas through cervical 4 (partially described above). A set of two articulated vertebrae (BYU 14063A and BYU 14063B), likely cervical vertebrae 5 and 6, was closely associated with a bifid cervical rib, described below.

The postaxial cervical vertebrae are strongly opisthocoelous. The condyle and cotyle of cervical vertebrae 5 and 6 are slightly wider than tall (Fig. 14A, C, F, H), a condition that continues through the balance of the preserved cervical vertebrae (e.g., Figs. 15C, 17F, H).

All the postaxial cervical centra are camerate and relatively short, axially. The longest, BYU 14388 (Fig. 15A–E), which we interpret to be from the middle third of the cervical series, is three times longer than tall. On most cervical vertebrae, there is a deep sulcus for the spinal cord that extends posterior to the neural canal on the dorsal surface of the centrum. The ventral surface of each centrum is concave along its long axis, as best seen in lateral view on specimens lacking the parapophyses (e.g., Figs. 13G, 15B). A well-defined, median ridge marks the ventral surface of most cervical centra, being the most developed on the anterior cervical vertebrae. This ridge ranges from a long, thin, tall ridge on cervical vertebra 3 (BYU 9460; Fig. 5K–N), to ridges that extend the length of the basal centrum plate of the cervical vertebrae (BYU 18143; Fig. 13J). In middle and posterior cervical vertebrae, the ridge is approximately restricted to the middle or anterior half of the centrum, occasionally associated with paramedian fossae (Figs. 14E, J, 15E, J). As on the axis, a small hypapophysis is present on some centra, near the posterior end of the median ridge on BYU 14790 (Fig. 13E) and on the posterior one-third of the centrum on BYU 14063B (Fig. 14J).

A large pneumatic fossa/foramen, or ‘pleurocoel’ (sensu Wilson et al., 2011), is present on all post-atlantal cervical centra (Figs. 4, 12–16). The posterior end of the fossa is usually slightly pointed (Figs. 13B, G, 15G, 16B). On some cervical vertebrae, the external margins of the pleurocoel form a well-defined foramen, as on the atlas BYU 10815 (Fig. 12F) and cervical 3, BYU 14790 (Fig. 13B), whereas in others the main primary vacuity is slightly inset within a larger external fossa, as on BYU 14063A (Fig. 14B) and BYU 14388 (Fig. 15B). The parapophysis is usually incomplete or missing entirely on most of the cervical vertebrae, but those that are preserved show they were robust (Fig. 14F) and invaginated by a pneumatic chamber along the posteromedial margin (Figs. 5O, 15G).

In the anterior few postaxial cervical vertebrae there is a weakly-developed, vertical-to-angled bulge/ridge roughly in the middle of the pleurocoel (Figs. 13B, 14B). On successive vertebrae, the development of ridges dividing the fossa is variable between vertebrae and on opposing sides of a vertebra. For example, on BYU 14063B, which we interpret to be approximately cervical vertebra 6, there is a single oblique ridge on the right side and multiple ridges/bulges on the left (Fig. 14G). The prominence of these ridges generally increases posteriorly in the series. On middle cervical vertebra BYU 10794, the ridges are prominent (Fig. 15G), but on BYU 14388, which we interpret to be from a similar position, the ridges are present but not as well developed on the left side (Fig. 15B) and they strike at various angles on the right side. The presence of subdivisions of the pneumatic centrum fossa (‘pleurocoel’) in the posterior cervical vertebrae is unknown because the centra are crushed and/or incomplete (Figs. 16, 17).

With the exception of cervical vertebrae 3 and 4 (Figs. 5K–R, 13), where the neural arch is up to 25% taller than the centrum, most neural arches are only slightly taller than centrum height. On these short neural arches, the neural spine is short and usually laterally broad (Figs. 15A, D, F, and I, 16A, and D). With the exception of the posteriormost cervical vertebra, BYU 14373 (Fig. 17F, and I), the postaxial cervical spines are bifid, with a shallow notch between the two spine apices (Figs. 5P–Q, 13–17). In cervical 3 (BYU 14790), the spine bears only a small notch (Fig. 13A, C, D). The small metapophyseal ridges lateral to the notch are laterally thicker than the width of the notch (Fig. 13D). On suceeding vertebrae, the notch increases in width noticeably. The metapophyses become swollen and prominent on cervical vertebra 4, and both the notch and metapophyses are anteroposteriorly elongate (Figs. 5P–Q, 13F–I). This trend of widening and lengthening of the notch continues posteriorly until the middle cervical vertebrae, such as BYU 10794, in which the sulcus is 6 cm wide and the metapophyses are 3 cm tall (Fig. 15F–I). Thereafter, the width and length of the cleft remains relatively constant to near the base of the neck, as on BYU 15151 (Fig. 16A–D). The floor of these wide notches (up to 55 mm) is relatively flat, sometimes with a median tubercle (Fig. 16A, D). On the posterior cervical vertebrae, the length of the neural spine top shortens anterioposteriorly, and the metapophyses become flanges and the notch narrows to a slit (Fig. 17A–D). On the posteriormost one or two cervical vertebrae, the spine is a laterally broad and axially thin with a minute cleft, and protrudes only slightly above the zygapophyses (Fig. 17F–H).

Few diapophyses are intact on the cervical vertebrae, and those that are present were often deformed post-deposition. The most complete postaxial anterior cervical diapophyses are

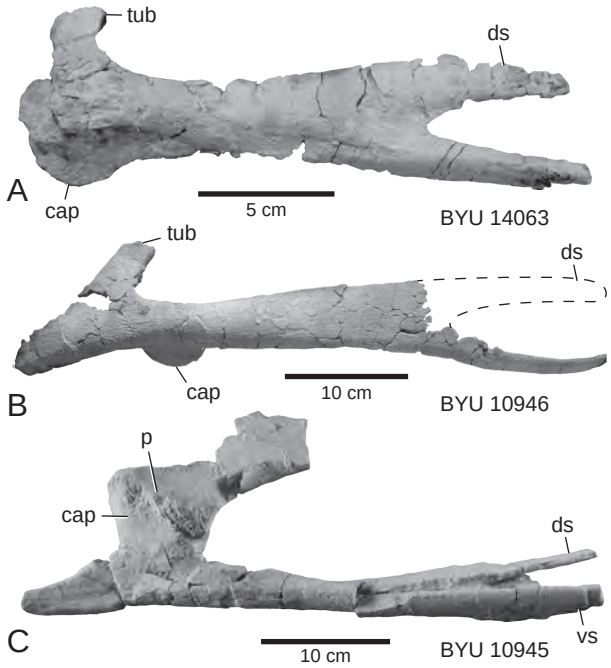

FIGURE 18 — *Moabosaurus utahensis*, referred cervical ribs. **A**, cervical rib, left, BYU 14063, in lateral view. Found in near articulation with cervical 5, BYU 14063A. **B**, cervical rib, left, BYU 10946, in lateral view. Upper shaft restored. **C**, cervical rib, right, BYU 10945, in ventral view, articulated with its parapophysis. Both rami are straps about equal in size. The dorsal blade is displaced ventrally to overlie the ventral shaft. B and C were found in field jacket 704 with two mid to posterior cervical vertebrae. Abbreviations: *cap*, capitulum; *ds*, dorsal shaft; *p*, parapophysis; *tub*, tuberculum; *vs*, ventral shaft.

on BYU 9460 (Fig. 5K–R), 14790 (Fig. 13A–D), BYU 14063 (Fig. 14), and 10794 (Fig. 15F–J). All of these are pendant and extend posteroventrally. On a single posterior cervical vertebra, BYU 14373 (Fig. 17A–E), the diapophysis extends laterally and subhorizontally, with a robust postzygodiapophyseal and posterior centrodiapophyseal lamina and a thin anterior centrodiapophyseal lamina.

Epipophyses are present on all cervical vertebrae where the postzygapophyses are preserved, but they are variably developed. They are maximally developed on anterior cervical vertebrae, such as cervical vertebrae 2 and 3 (Fig. 5H–I, M–N), where the epipophysis extends posterior to the postzygapophyseal facet. On these and other anterior vertebrae, the epipophysis extends laterally almost even with the edge of the postzygapophyseal articular facet, and the two are separated by a sulcus (Fig. 14B). They are also well developed on posterior cervical vertebrae, as on BYU 14346 (Fig. 17A–E). They are small on middle cervical vertebrae. On BYU 14388 (Fig. 15A–E), the epipophysis is small boss at the terminus of the spinopostzygapophyseal lamina. On BYU 10794 (Fig. 15F–J) it is positioned at the posterior end of an accessory dorsolaterally expressed lamina that merges anteriorly with the postzygodiapophyseal lamina. In sum, epipophyses are moderately to weakly developed in this taxon.

A small projection, termed the "pre-epipophysis" by Wilson and Upchurch (2009), is present on the anterolateral surface of the prezygapophysis of several cervical vertebrae, including middle cervical vertebra BYU 18143 (Fig. 13F, indicated by line). Cervical vertebra BYU 15151 (Fig. 16B) has a rudimentary pre-epipophysis in the form of subparallel ridges. Similar, linear ridges are present on a *Turiasaurus* middle cervical vertebra CPT 1220. On *Camarasaurus lewisi* (BYU 9047) the pre-epipophysis is sometimes part of the prezygodiapophyseal lamina and protrudes anterior to the zygapophysis. The presence/absence or degree of development is mentioned because this muscle/tendon attachment point may prove to be of use in biomechanical and/or phylogenetic studies.

In summary, in absence of an articulated series, the number of cervical vertebrae is unknown. With the exception of the atlas, axis, and proximal-most cervical vertebrae, all have low, notched neural spines. The width of the notch increases posteriorly in the series to near the base of the neck where it narrows rapidly to a groove and is lost entirely on the last vertebrae in the series, where the spine is a low, laterally wide blade just above the zygapophyses. With the exception of the cervical vertebrae of juveniles and the posteriormost cervical vertebrae, the cervical centra walls and laminae of the neural arches are exceptionally robust in *Moabosaurus*.

Cervical Ribs.— Both a single shafted cervical rib (e.g., BYU 9460; Fig. 5S) and bifurcated cervical rib shafts (BYU 10945, 10946, 14063; Fig. 18) were found in close association with cervical vertebrae referred to *Moabosaurus utahensis*. The single-shafted rib was found closely associated with cervical vertebra 4 of BYU 9460, a juvenile, as shown on the field map (Fig. 2D).

A left cervical rib (BYU 14063; Fig. 18A) was closely associated with two articulated cervical vertebrae, interpreted as cervical vertebrae 4 and 5. All were collected in the same jacket under a single field number. The blade of the rib bifurcates distally in two tapering blades, both of which are in the same vertical plane.

A left cervical rib (BYU 10496; Fig. 18B) and a right cervical rib (BYU 10945; Fig. 18C) are both from field jacket 704, which contained two middle to posterior cervical vertebrae that were badly broken. Rib BYU 10945 is fused to its parapophysis/centrum fragment. The shaft divides into two blades about 10 cm behind the capitulum. The blades overlap due to crushing, but they were once in the same vertical plane like those of BYU 14063. The blades are strap-like, with the ventral blade dorsoventrally thinner than the larger dorsal blade. The posterior shaft of BYU 10946 is a single blade for 20 cm behind the capitulum, and thereafter divides into a lower laterally thin blade, and a larger upper blade, which is incomplete.

The posterior shafts of sauropod cervical ribs are ossified tendons (Cerda, 2008; Klein et al., 2012), representing tendons of the *M. longus colli ventralis* and *M. flexor colli lateralis* (Wedel and Sanders, 2002; Taylor and Wedel, 2013).

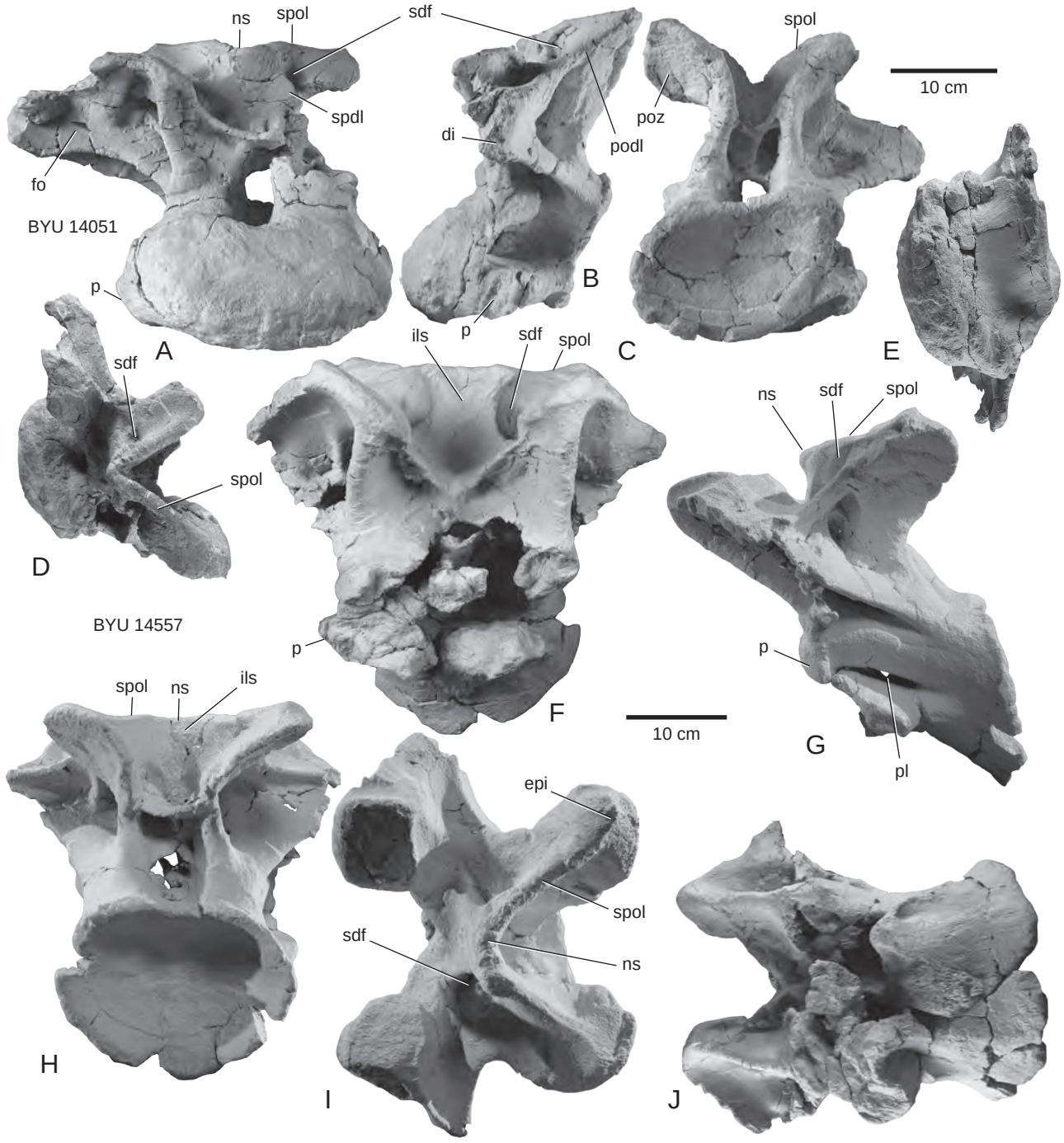

FIGURE 19 — *Moabosaurus utahensis*, referred dorsal vertebra 1, BYU 14051, and 2, BYU 14557. **A–E**, dorsal vertebra 1, BYU 14051, in anterior, right lateral reversed, posterior, dorsal, and ventral views. **F–J**, dorsal vertebra 2, BYU 14557, in anterior, right lateral (reversed), posterior, dorsal, and ventral views. Abbreviations: *di*, diapophysis; *epi*, epipophysis; *fo*, fossa; *ils*, intervertebral ligament scar; *ns*, neural spine; *p*, parapophysis; *pl*, pleurocoel; *podl*, postzygodiapophyseal lamina; *poz*, postzygapophysis; *sdf*, spinodiapophyseal fossa; *spdl*, spinodiapophyseal lamina; *spol*, spinopostzygapophyseal lamina.

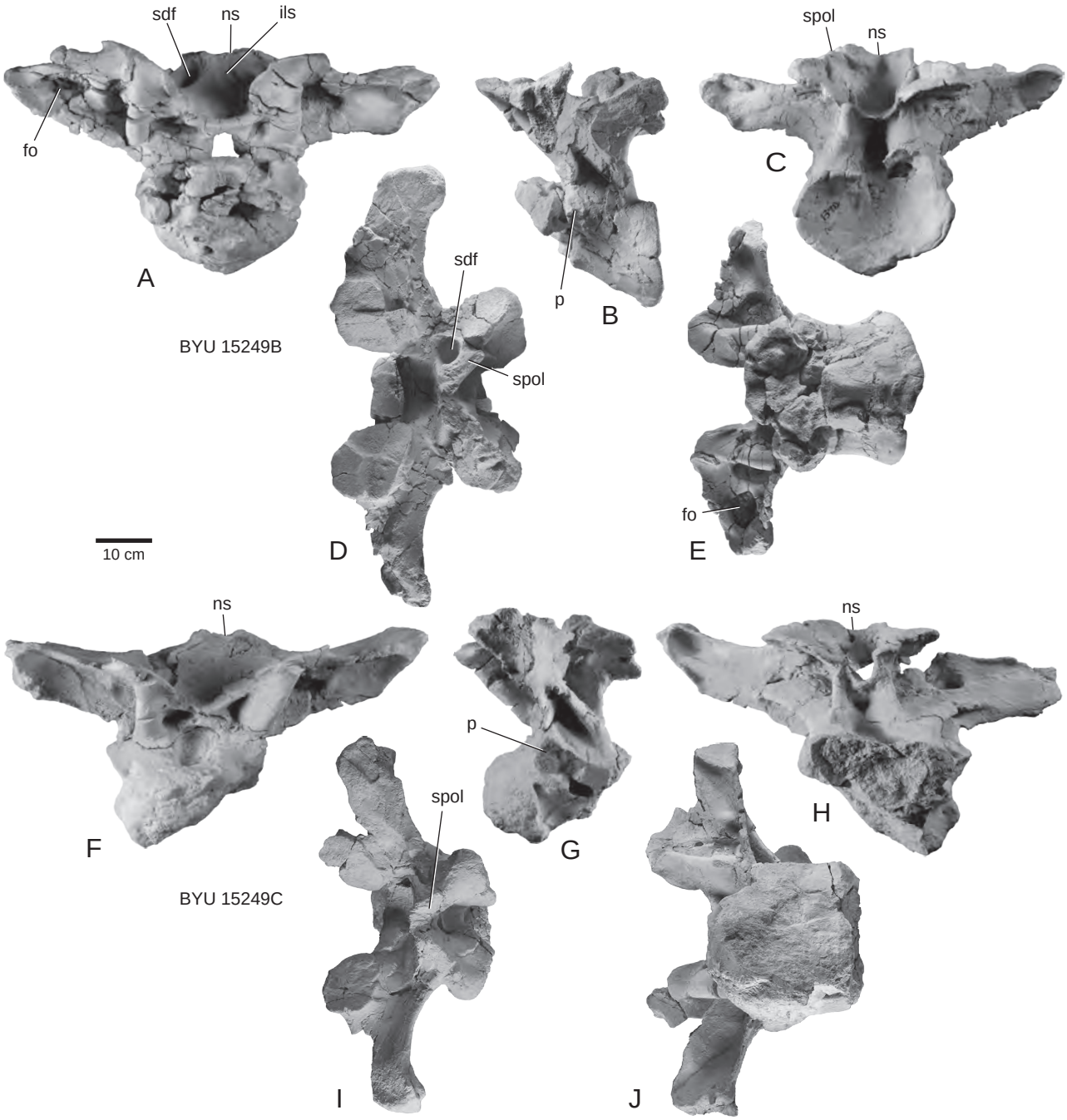

FIGURE 20 — *Moabosaurus utahensis*, referred dorsal vertebrae 2–3, BYU 15249B and C. **A–E**, dorsal 2, BYU 15249B, and dorsal vertebra 3, BYU 15249C, in anterior, left lateral, posterior, dorsal, and ventral views. **F–J**, dorsal vertebra 3, BYU 15249C, in anterior, right lateral reversed, posterior, dorsal, and ventral views. These two vertebrae were found in partial articulation in the field. Note the changing position of the parapophysis, which is level with the pleurocoel in dorsal vertebra 2 (B) and straddles the centrum and neural arch in dorsal vertebra 3 (G). Abbreviations: *fo*, fossa; *ils*, intervertebral ligament scar; *ns*, neural spine; *p*, parapophysis; *sdf*, spinodiapophyseal fossa; *spol*, spinopostzygapophyseal lamina.

The posterior rami of *Moabosaurus utahensis* ribs likely represent ossified tendons of those muscles, with the flat rami representing blade-shaped ossified tendons. The presence of single and bifid ribs in the same taxon has several possible explanations. The simplest is that rib form (single vs. bifid shafts) varies along the column for biomechanical reasons, such as differing angles of tendon attachment and varying degrees of tendon tension, with single-shafted ribs localized

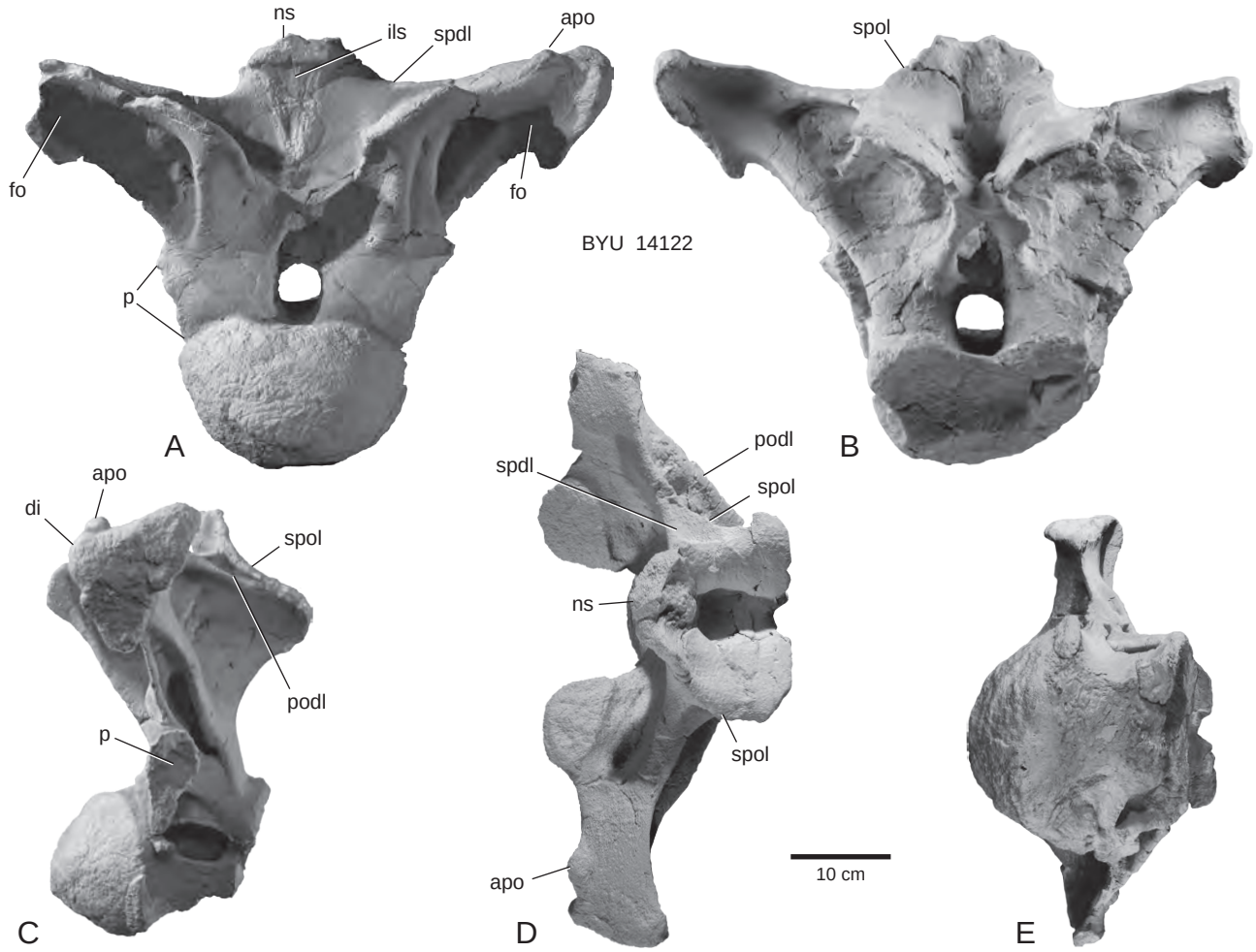

FIGURE 21 — *Moabosaurus utahensis*, referred dorsal 3, BYU 14122. **A–E**, dorsal vertebra 3, in anterior, posterior, left lateral, dorsal, and ventral views. Dorsal 3 is the first in the series with a spine extending above the supporting laminae. Accessory lateral fossae are well-developed on the anterior face of the transverse process, (A). Hyposphene development is asymmetrical, with the right side better developed than the left, (B). Posteroventral portion of centrum missing. Abbreviations: *apo*, apophysis; *di*, diapophysis; *fo*, fossa; *ils*, intervertebral ligament scar; *ns*, neural spine; *p*, parapophysis; *podl*, postzygadiapophyseal lamina; *spdl*, spinodiapophyseal lamina; *spol*, spinopostzygapophyseal lamina.

to the anterior portion of the neck. Alternatively, this feature could be a function of ontogeny, with an accessory blade developing later in life, as the tendon ossifies. The presence of a single-shafted rib on the anterior cervical vertebra of a juvenile does not help choose between these hypotheses. Other explanations include sexual dimorphism, or simply individual variation. Resolution will require additional specimens.

Dorsal Vertebrae.— Most the recovered dorsal elements are centra, because trampling is inferred to have destroyed the more delicate neural arches (see above, "Taphonomy"). Even on the best specimens, however, osteophagous insects commonly consume articular surfaces, such as condyles (Fig. 4A) and especially vertebral processes (Fig. 3B, I). Nevertheless, a number of nearly complete dorsal vertebrae are well-represented and preserved. These come from the anterior half of the dorsal series, where the neural arches are robust and the spines short.

The cervical and dorsal series are confidently linked by the derived neural spines, which are extremely short, axially thin, and transversely wide in the pectoral region, as described in the Diagnosis (see also Figs. 3, 17, 19). In the transitional zone between the cervical and the dorsal series, the neural spines are so short that in the early stages of collecting it was thought that the spines were broken and the broken edges rounded. With the accumulation of numerous, often well preserved representatives of many vertebral positions, it was confirmed that the spines were complete. Further evidence linking the cervical and dorsal series consists of logical, serial changes

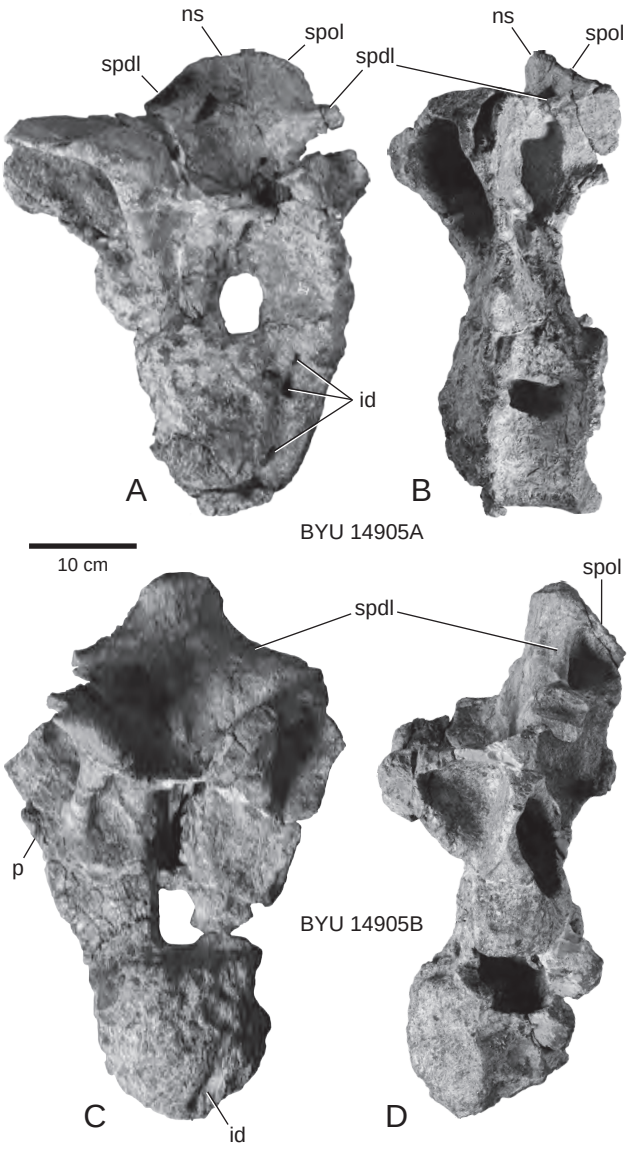

FIGURE 22 — *Moabosaurus utahensis*, referred dorsal vertebrae 3 and 4, BYU 14905A and BYU 14905B. **A–B**, dorsal vertebra 4, BYU 14905A, in anterior and right lateral reversed views. **C–D**, dorsal vertebra 5, BYU 14905B, in anterior and left lateral views. These were articulated in the field. Abbreviations: *id*, insect damage; *ns*, neural spine; *p*, parapophysis; *spdl*, spinodiapophyseal lamina; *spol*, spinopostzygapophyseal lamina.

in the neural spine shape and serial changes in laminae and fossae of the neural arch.

The posteriormost cervical vertebra (BYU 14373; Fig. 17F–J) has a neural spine that is three times broader than it is anteroposteriorly long and is only slightly elevated above the zygapophyses. Ventrolateral to the spine is a small, deep, conical spinodiapophyseal fossa. The diapophyses are less pendant than on more anterior, adjacent cervical vertebrae. Using serial homology, we identify BYU 14051 (Fig. 19A– E) and BYU 10492 as dorsal vertebra 1 because they are similar in form to the posteriormost cervical vertebra except that (1) the parapophysis is higher, occluding part of the pleurocoel; (2) the neural spine is shorter; (3) the spinodiapophyseal fossa is shallower; (4) the spinoprezygapophyseal lamina ends near the base of the neural spine; and (5) the diapophysis is wider and extends laterally, without a pendant terminus. Likewise, BYU 14557 (Fig. 19F–J) and BYU 15249B (Fig. 20A–E) are identified as dorsal vertebra 2 based on increasing neural arch height, the angle of the diapophyses, and the broadening and shallowing of the spinodiapophyseal fossa. In addition to serial homology, we used three sets of vertebrae, with overlaps between each set, to identify dorsal vertebrae 1–6. From anterior to posterior, these sets are: BYU 15249A–C, dorsal vertebrae 1–3; BYU 14905 (Fig. 22), dorsal vertebrae 3–4; and the holotype of *Moabosaurus utahensis*, BYU 14387A–C (Figs. 3, 4A–E), dorsal vertebrae 4–6. Until the balance of the dorsal series can be deciphered, we describe the first six dorsal vertebrae plus two dorsal vertebrae posterior to position 6.

All known *Moabosaurus* dorsal vertebrae are opisthocoelous and camerate (Figs 3, 4, 19–23). The degree of opisthocoely is greatest on the anterior dorsal vertebrae and decreases posteriorly in the series. But this pattern is very difficult to quantify owing to the large amount of insect damage (e.g., Figs. 4F–G, J, 22A–B, 23F–J). The condyles are wider than tall through at least the sixth dorsal centrum (Fig. 4A, C); in more posterior dorsal vertebrae the condylare outline is approximately circular (Fig. 23F–J).

The dorsal centra are thick-walled (ca. 3 cm thick) with large camerae of a grade comparable to *Camarasaurus*. Pleurocoels, opening laterally, are present on all known dorsal vertebra centra. They are oblate in outline on dorsal vertebrae 1–3, and on the balance of the dorsal vertebrae, they are shaped like rounded triangles with the apex pointing dorsally. On dorsal vertebrae 4–5, the pleurocoels span the centrum and neural arch contact, with the apex half the way up the neural arch peduncle. The margins of the pleurocoels are medially deeper posteriorly in the series until they are a foramen inset within a larger fossa (BYU 10976, Fig. 4F–J). The median septum separating the left and right pneumatic chambers of the centra bear reinforcing ridges. These ridges are variably developed but are typically low with no diagnostic pattern. The ventral surfaces of the dorsal centra are usually gently convex and most are smooth (Fig. 23J) but some bear longitudinal ridges (Fig. 23E).

The parapophysis rises rapidly on the anterior dorsal vertebrae from the position below the centrum of the cervical vertebrae. On dorsal vertebra 1 (Fig. 19B) the parapophysis partly occludes the pleurocoel, on dorsal vertebra 2 (Figs. 19G, 20B) it is at mid-height of the pleurocoel, and on dorsal vertebra 3 (Figs. 20G, 21C) it spans the neurocentral junction but is almost entirely on the neural arch. On dorsal vertebra 4 (Fig. 3), the parapophysis is high on the neural arch peduncle, and by dorsal vertebra 5 it is level with the zygapophyses. In more posterior dorsal vertebrae, it is higher than the zygapophyses and close to the diapophysis.

The neural arches, like the centra, are robust, with relatively thick laminae.

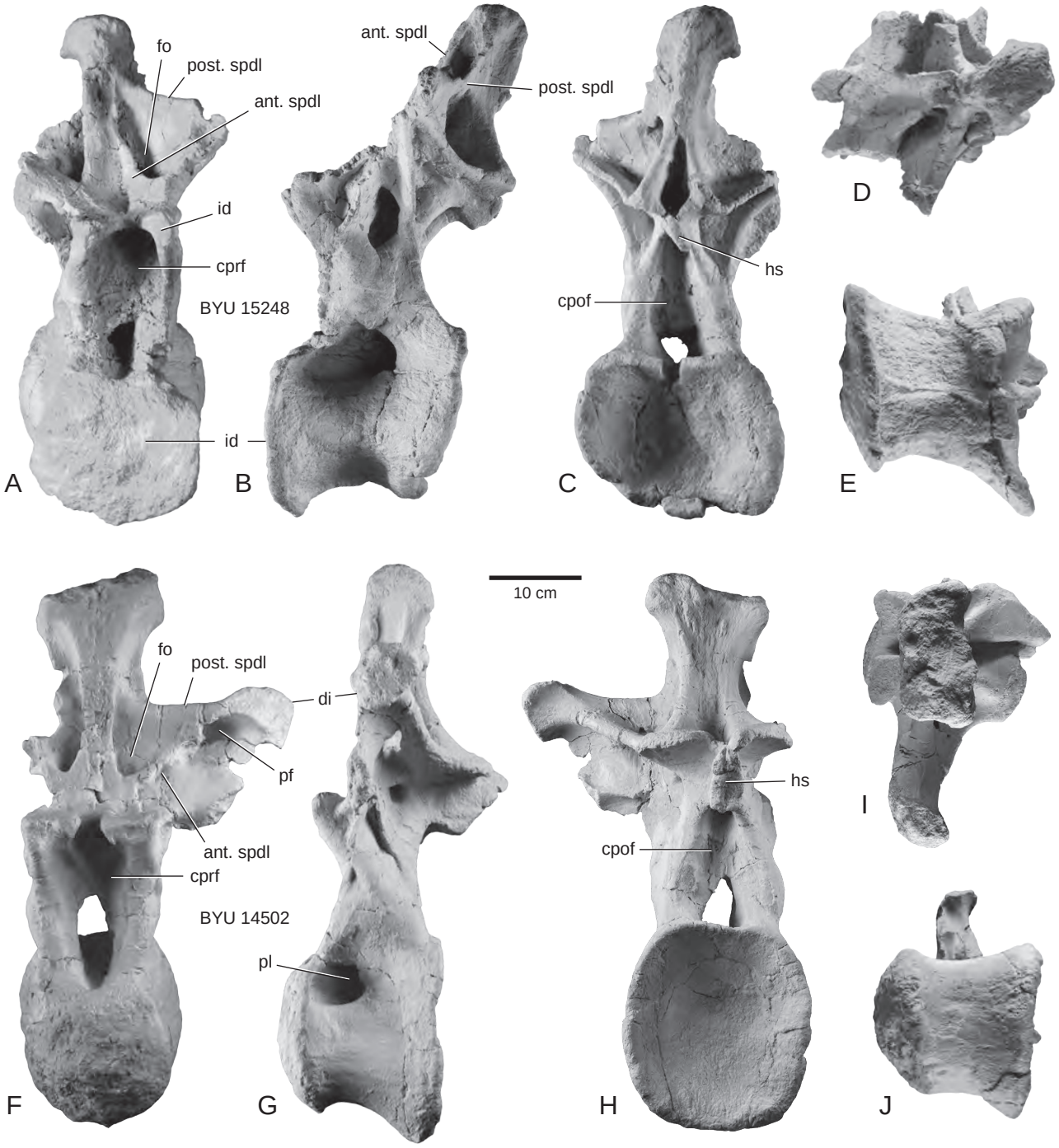

FIGURE 23 — *Moabosaurus utahensis*, referred mid-series dorsal vertebra BYU 15248, and referred posterior dorsal vertebra 14502. **A–E**, mid or posterior dorsal vertebra, BYU 15248, in anterior, right lateral reversed, posterior, dorsal, and ventral views. Most of the centrum's condyle was destroyed by insects. **F–J**, posterior dorsal vertebra, BYU 14502, in anterior, left lateral, posterior, dorsal, and ventral views. Changes in the architecture of the spinodiapopyhseal lamina suggests that both of these vertebrae are positioned posterior to dorsal vertebra 6, BYU 14387C (Fig. 4). BYU 14502, is one of the posteriormost dorsal vertebrae as the pleurocoel is small, the transverse processes are nearly horizontal, and the spine top is laterally wide. In both vertebrae, the spinodiapophyseal lamina splits into anterior and posterior spinodiapophyseal lamina, which define an arc separated by a fossa. Spine tops are incomplete, especially that of BYU 15248. Abbreviations: *ant. spdl*, anterior spinodiapophyseal lamina; *cpof*, centropostzygapophyseal fossa; *cprf*, centroprezygapophyseal fossa; *di*, diapophysis; *fo*, fossa; *hs*, hyposphene; *id*, insect damage; *pf*, pneumatic foramen; *pl*, pleurocoel; *post. spdl*, posterior spinodiapophyseal lamina.

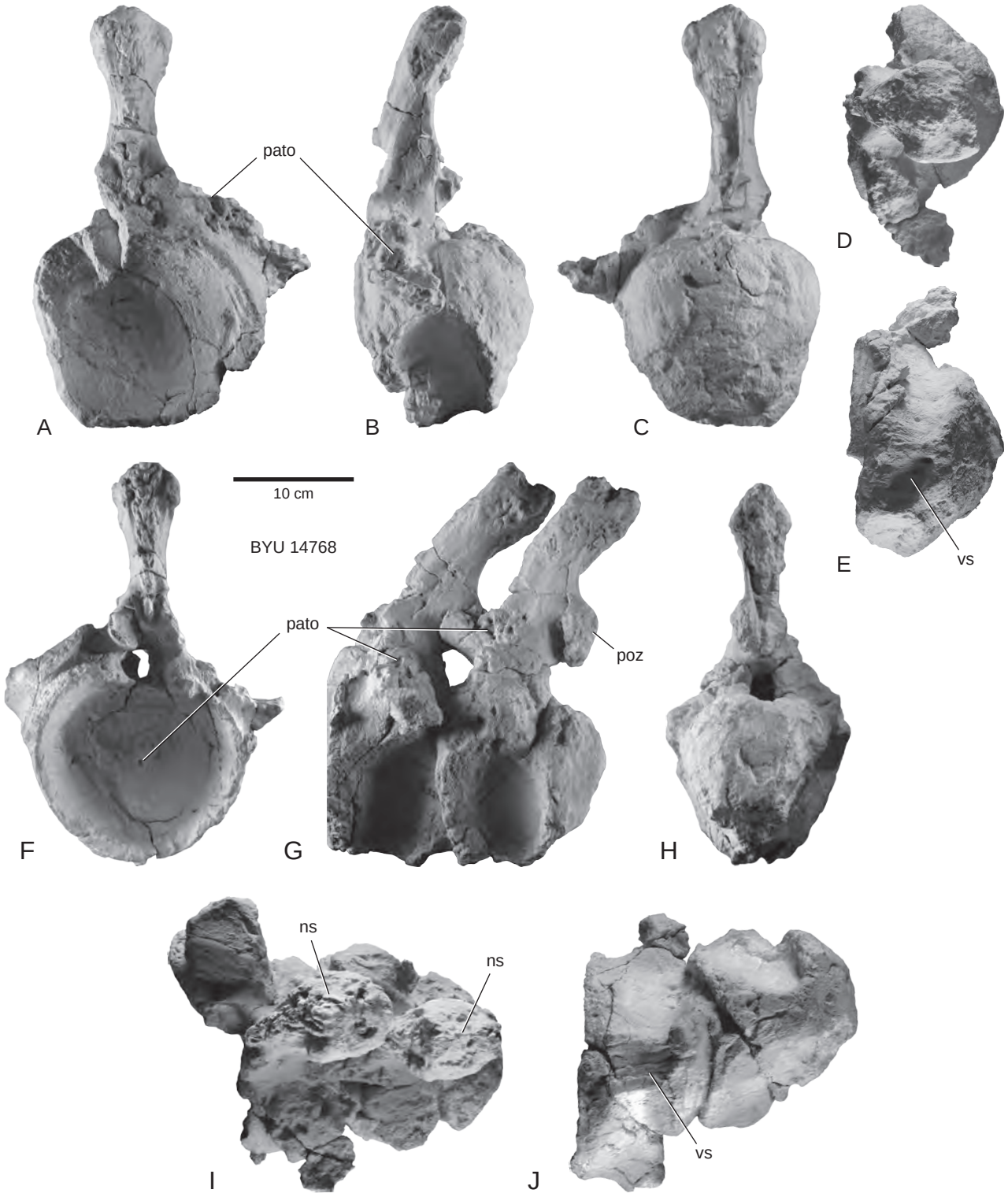

FIGURE 24 — *Moabosaurus utahensis*, referred caudal vertebrae 3–5, 14768. **A–E**, caudal vertebra 3 in anterior, left lateral, posterior, dorsal, and ventral views. **F**, caudal vertebra 4 in anterior view. **G**, caudal vertebrae 4 and 5 in left lateral view. **H**, caudal vertebra 5 in posterior view. Caudal vertebrae 4 and 5 in dorsal (**I**), and ventral (**J**) views. Abbreviations: *ns*, neural spine; *pato*, pathology; *poz*, postzygapophysis; *vs*, ventral sulcus.

Neural spine morphology changes substantially in the series, from a low, thin lateral ridge on the anterior dorsal vertebrae to a moderately high spine with triangular lateral processes of the spine top typical of neosauropods (Wilson, 2002) on middle and posterior dorsal vertebrae. On dorsal vertebrae 1 and 2, the neural spine is exceptionally low, such that there is no dorsal protrusion above the zygapophyses. At the midline, there is a flat intervertebral ligament scar with the top of the scar terminating in a rugose, rounded margin that extends posteriorly a few centimeters along the top of the spinopostzygapophyseal lamina. Unlike the relatively wide neural spines of the last cervical vertebra and dorsal vertebra 2, the first dorsal neural spine is transversely narrow and V-shaped in dorsal view, with the base of the "V" slightly truncated and pointing anteriorly. The neural spine extends only a short distance above the zygapophyses and diapophyes. The spinoprezygapophyseal lamina is thick but only extends about half the way down to the prezygapophysis.

Dorsal neural spine 2 is the lowest of the dorsal series, with its apex almost level with the zygapophyses. The anterior face is wider than it is in dorsal neural spine 1 and defined by prominent spinoprezygapophyseal laminae that extend along the entire lateral border of the intervertebral ligament scar.

Dorsal neural spine 3 (Figs. 20F–I, 21A–D) protrudes dorsally above the zygapophyses, and the laminae drape from the spine. The neural spine is laterally wider than that of other anterior vertebrae. There is a slight notch on the midline of the neural spine in BYU 15249C (Fig. 20F) and a tubercle in the same area of BYU 14122 (Fig. 21A). The dorsal edge of the neural spine is rounded and 'rolls' onto the anterior face of the spine. Dorsal neural spine 3 inclines forward or is vertical, contrary to the condition in dorsal vertebrae 4–7, where the spine is slightly reclined posteriorly. On the balance of the dorsal vertebrae, the spine is approximately vertical.

Dorsal neural spine 4 (Figs. 3A–E, 22C–D) is intermediate between the laterally broad, ridge-like spine of dorsal vertebrae 2 (Fig. 20A–D) and 3 (Fig. 20F–I) and a narrow spine of dorsal vertebra 5 (Fig. 3F–H). Dorsal neural spine 4 is more prominent than that of dorsal neural spine 3. In BYU 14905B (Fig. 22C–D) and BYU 14387A (Fig. 3A–C, E), it forms a short pillar that extends above the spinodiapophyseal lamina, which is robust and extends laterally at a low angle from the neural spine. A complete apex of dorsal neural spine 4 is not preserved on any specimen. Dorsal neural spine 5 (Fig. 3F–G) is a distinct process extending well above the shoulder of the spinodiapophyseal lamina. On the remaining dorsal vertebrae, the neural spine has a cruciate cross-section.

The anterior intervertebral ligament scar on dorsal neural spines 1–4 is rugose but flat, with minimal relief (Figs. 19A, F, 20A, F, 21A 22A). For example, the anterior intervertebral ligament scar on dorsal neural spine 3 (Fig. 21A) is in the form of a "V," with the top of the "V" as wide as the spine. On dorsal neural spine 4, there is a small spinal lamina (low ridge) on this scar (Fig. 3A). On dorsal vertebrae 5 through 6, the intervertebral ligament scar is borne on the anterior edge of a thin spinal lamina (Figs. 3G, 4A). On some of the vertebrae posterior to dorsal vertebra 6, the intervertebral ligament scar is buttressed asymmetrically by the spinoprezygapophyseal lamina (e.g., Fig. 23A).

The bulk of the neural spine shaft is cruciate in transverse section by at least dorsal vertebra 5. From dorsal vertebra 5 and beyond, the apex of the neural spine widens laterally, as does the intervertebral ligament scar. On dorsal vertebra BYU 10976 (Fig. 4F–J) the neural spine top is equally wide and axially long, approaching the form of spine tops in sacral and anterior caudal vertebrae.

The neural spine tops in the middle to posterior dorsal vertebrae are tranversely wide, with lateral triangles. There is a small, shallow median notch at midline on well preserved posterior dorsal neural spines (not figured).

The 'floor' of the anterodorsal area of the dorsal neural arch, delimited by the neural spine posteriorly and the plane of the prezygapophyses ventrally, becomes substantially larger between dorsal vertebrae 4 and 6. On dorsal vertebra 4, the neural spine is positioned anterior to mid-centrum, whereas in dorsal vertebrae 5 and 6 the neural spine is above the posterior face of the centrum.

True hyposphenes are present on all dorsal vertebrae posterior to dorsal vertebra 3. There is a weakly developed hypantrum on dorsal vertebra 2 (Fig. 19F–J) in the form of a ventral deflection of the medial postzygapophyseal facets, which are widely separated. The anteriormost occurrence of a fully formed hyposphene-hypantrum articulation is on dorsal vertebra 3 (Figs. 20F–J, 21A–E), where the prezygapophyseal facets have a near vertical median surface to form a hypantrum, and the hyposphene is defined by thin, articular surfaces, lacking a robust wedge. The hyposphene of dorsal vertebra 4 (Fig. 3C) is large and well developed, with the two sides of the wedge separated by a deep vertical notch. The hyposphene is maximally developed on dorsal vertebra 6 (Fig. 4C), where the hyposphene is a laterally wide, solid wedge lacking a medial notch. The hyposphene facets on dorsal vertebra 6 (Fig. 4C) are nearly equal in size to the upper postzygapophyseal facets, and the planar portions of the hyposphene and zygapophyseal facets meet at about 45°, with those facets joined by a curved articular surface. The hyposphene of dorsal vertebra 4 (Fig. 3C) is supported ventrally by short, robust, centropostzygapophyseal lamina above the neural canal. On more posterior dorsal vertebrae, the hyposphene is ventrally buttressed by normal intrapostzygapophyseal laminae that extend onto the neural arch peduncles (Fig. 23C). Somewhere posterior to dorsal vertebra 6 the hyposphene narrows to a thin, near vertical element that varies in morphology (Fig. 23B–C).

The transverse processes are often incomplete, but some are well enough preserved to provide useful information. Those of the first dorsal vertebra extend roughly horizontally. The tips of the diapophysis moves upward in subsequent vertebrae, with the dihedral angle gradually increasing posteriorly in the series. Of the preserved diapophyses, the most highly developed and largest are on dorsal vertebra 3 (Fig. 21). In that vertebra, the transverse process extends somewhat anteriorly placing the diapophysis anterior to the parapophysis (Fig. 21). Dorsal 3 has a well developed

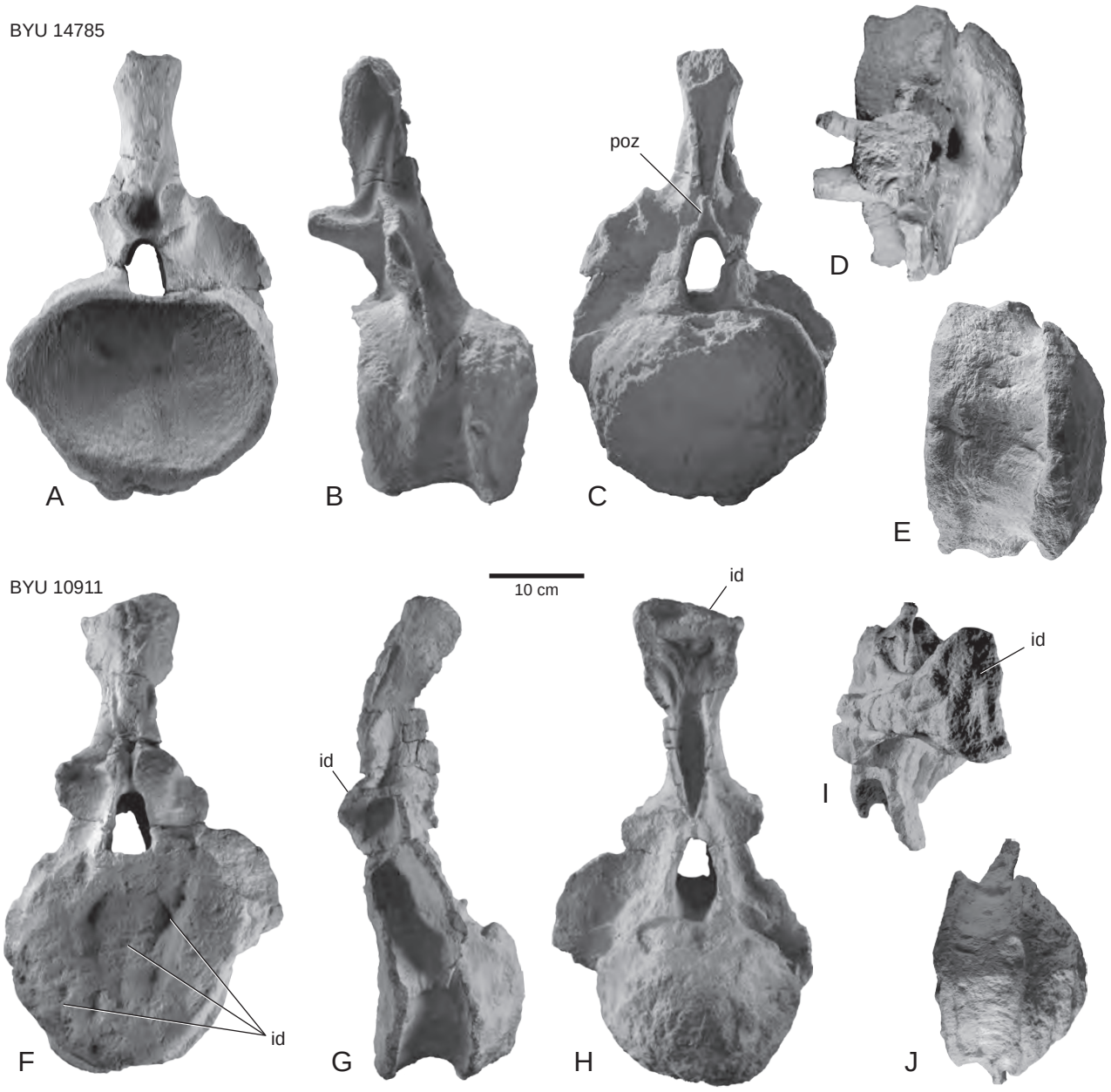

Figure 25 — *Moabosaurus utahensis*, referred proximalmost caudal vertebrae. **A–E**, caudal vertebra 1, BYU 14785, in anterior, left lateral, posterior, dorsal, and ventral views. Most of the spine top is missing. **F–J**, probably caudal vertebra 2, BYU 10911, in anterior, left lateral, posterior, dorsal, and ventral views. The rim of the anterior cotyle and the prezygapophyses were lost to osteophagous insects. Abbreviations: *id*, insect damage; *poz*, postzygapophysis.

apophysis on the anterodorsal surface of the diapophysis. On more posterior dorsal vertebrae, such as BYU 10976 (Fig. 4F–J) and BYU 14502, the transverse process likewise extends anterodorsally.

The posterior centrodiapophyseal lamina is thin and spans the centrum to the diapophysis on dorsal vertebrae 1–3. On more posterior dorsal vertebrae, the base of the lamina is located entirely on the neural arch peduncle and the lamina becomes less prominent until on BYU 10976, where it is a low but robust ridge (Fig. 4F–H). By the posteriormost dorsal vertebra (BYU 14502; Fig. 23F–H) the lamina is absent.

The neural arch peduncles are one of the most diagnostic components of the dorsal vertebrae of *Moabosaurus utahensis*. Beginning on dorsal vertebra 2 the peduncles increase in height such that the distance from the top of the centrum to the level of the upper prezygapophyseal facet is ~130% the

height of the centrum condyle. Also, along the same dorsal series, the peduncle complex becomes laterally thinner as the parapophysis moves dorsally and then laterally onto the transverse process. These high and slender penduncular complexes are exemplified by BYU 10976 (Fig. 4F–J). Accompanying this height increase, the ventrolateral laminae of the diapophysis no longer contact the centrum, with the exception of the anterior centroparapophyseal laminae on dorsal vertebra 4 (Fig. 3A–E). The the ventralmost extensions of the laminae are high on the peduncles. Laterally, the neural arch peduncle appears robust and swollen or inflated. The greatest swelling is located about mid-height of the peduncle and increases posteriorly in the series, being the most swollen in BYU 14502 (Fig. 23F–J). The peduncles are hollow and conjoin above the neural arch. These are the most highly internally pneumatized structures of the *Moabosaurus utahensis* dorsal vertebrae, and the only internally pneumatized structures of the neural arch. The medial walls are thin, only millimeters thick. The lateral walls vary in thickness from a couple of centimeters to few millimeters. A short distance below the zygapophyses and neural arch peduncles are conjoined and the pneumatic chamber of each side is separated by a thin, median septum. The lower portions of the peduncle chambers are reinforced by internal struts. The internal chamber is pneumatized via the dorsal aspect of the pneumatic centrum cavity (camera) and, at least in BYU 10976 (Fig. 4G) and BYU 14502 (Fig. 23G), via a lateral foramen at the top of the neural arch.

Beginning on dorsal vertebra 3 or 4, depending on the individual, there is a large pneumatic fossa on the anterior and posterior surfaces of the neural arch peduncles, with the anterior fossa being larger than the posterior fossa. Dorsal vertebrae 3 and 4, which the first vertebrae with the fossa, bear a sagittal septum that is lacking on subsequent vertebrae. On dorsal vertebrae 5 and 6, the fossa deepens to centrum mid-length and remains deep on the known, more posterior portion of the dorsal series. The fossa is generally smooth-walled but supporting buttresses randomly occur as on BYU 14387 (Figs. 3F–H, 4A–E) and BYU 14502 (Fig. 23F–J). The posterior peduncular fossa is equally deep and tall, but narrower. The transverse walls of the peduncles separating the anterior and posterior fossae vary in thickness, with the minimum separation being about 2 cm. A horizontal cross-section though the mid-section of the peduncle shows the bone walls form a figure-eight. This cross-sectional shape and thin walls made the neural arches especially susceptible to trample and collecting damage (see above, “Taphonomy”).

The neural canal of the anterior dorsal vertebrae is round to prolate in outline. Prolateness increases with the increasing height of the neural arch peduncles posteriorly in the series. On posterior dorsal BYU 14502 (Fig. 23F–J), the neural canal is more than twice as high as wide. This prolate character is shared with the anterior caudal vertebrae. The increased height of the neural canal may be related to an increasingly large pneumatic diverticulum that surrounded the spinal cord, as is present in extant birds (Britt, 1993).

In general, the dorsal vertebrae are characterized by robust, camerate centra, high neural arch peduncles, and, most diagnostically, by the absence of a true neural spine on dorsal vertebrae 1 and 2, very short, laterally wide neural spines on dorsal vertebrae 3–4 and short neural spines on the balance of the dorsal vertebra. The shortness of the neural spines on mid- and posterior dorsal vertebrae appears to related to the height of the neural arch peduncles, which ‘displaces’ the articular facets and their related laminae high up on the arch.

Sacral Vertebrae, Ribs, Ilium. — The most complete set of articulated/associated bones of *Moabosaurus utahensis* is BYU 14771 (Fig. 6). It consists of an articulated series of vertebrae from the last dorsal vertebra (including the penultimate dorsal postzygapophyses) through the sacrum to caudal vertebra 2. The upper portion of a right ilium was articulated with the sacrum. In addition, BYU 14771 was closely associated with a set of of vertebrae (BYU 14768) that we interpret to be caudal vertebrae 3–5 of the same individual. The small size of BYU 14771 and BYU 14768 relative to most *Moabosaurus* vertebrae indicates the individual they represent was a juvenile.

The sacrum was buried upside-down, and most of the neural spines have been bent posteriorly relative to their respective vertebrae and/or telescoped into the neural arches. Additionally, the centra on this skeleton have been dorsoventrally compressed, and sacral neural spines 4 and 5 have been displaced laterally from its original position.

The sacrum is delicate and kept in a supporting jacket such that sacral centra 4 and 5 are the only centra visible. There is sufficient offset between the last sacral and first caudal vertebrae to ascertain that the posterior face of the posteriormost sacral centrum is strongly convex.

Only the upper portion of the last dorsal neural arch was preserved, from the postzygapophyses to the spine top. The spine top is laterally wide, with a median notch that shallows posteriorly (Fig. 6B).

All five sacral vertebrae are present. The neural spines of the anterior three sacral vertebrae coalesced along the entire length of the spine tops. The spine top of sacral 1 is transversely broader than that that of the dorsal or any of the subsequent sacral vertebrae. The apices of the neural spines are expanded laterally to form a spinal table. In dorsal view, the spine tops are roughly tripartite, with a moderate, central bulbous expansion and lateral expansions, some of which are also bulbous. In anterior and posterior view, the neural spines are triangular, and the lateral expansions are pendant (Fig. 6C). The median dorsal expansion correlates with the apex of the neural spine and the lateral expansions are ossified ligament or tendon attachments. On the spines of sacral vertebrae 2–4, the spinodiapophyseal laminae are well developed and thin. On sacral vertebra 5, these laminae are thick ridges. On sacral vertebrae 2 and 3, the spinodiapophyseal laminae contribute to the delineation of pneumatic fossae below both the anterior and posterior dorsolateral expansions of the spines. The fourth sacral spine lacks a pneumatic fossa on the anterolateral side, but there is a deep fossa on the posterolateral side of the spine. The fifth sacral neural spine bears a spinodiapohysial lamina developed as a robust ridge, and there are no related pneumatic fossae.

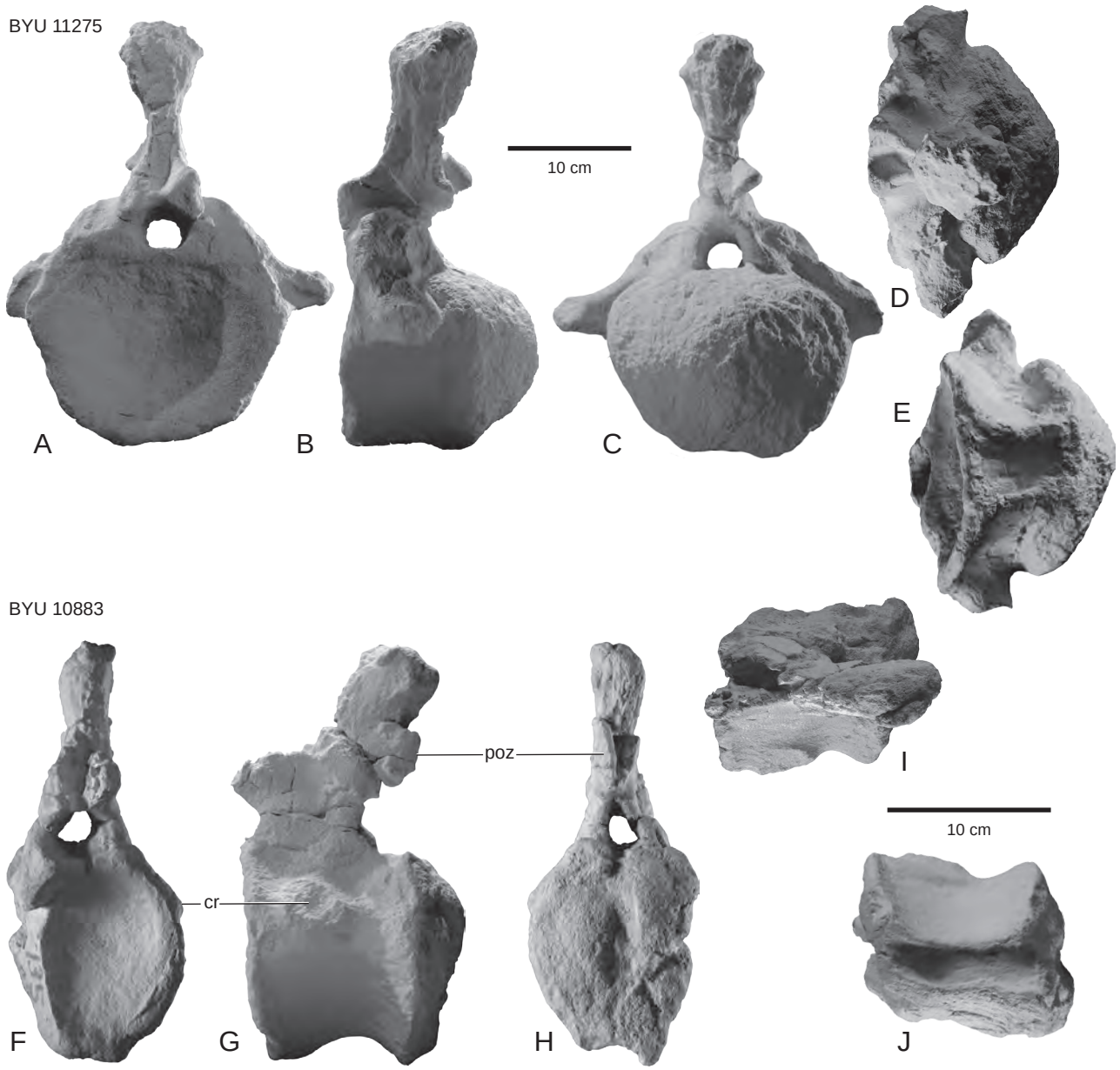

Figure 26 — *Moabosaurus utahensis*, referred proximal caudal vertebrae. **A–E**, anterior caudal vertebra (about caudal vertebra 4), BYU 11275, in anterior, left lateral, posterior, dorsal, and ventral views. **F–J**, caudal vertebra from somewhere between positions 8 to 10, BYU 10883, in anterior, left lateral, posterior, dorsal, and ventral views. Note the moderately developed condyle on centrum. Right side of centrum crushed. Abbreviations: *cr*, caudal rib; *poz*, postzygapophysis.

Spinopostzygapophyseal laminae are well-developed on sacral vertebrae 4 and 5, and they begin circa three-quarters of the way down the spine. The laminae cannot be seen on sacral vertebrae 2 and 3. Spinoprezyapophyseal laminae are present only on sacral vertebra 3, where they are weakly developed, barely protruding beyond the intervertebral ligament scar. The intervertebral ligament scars, where visible on the sacral vertebrae, protrude anteriorly and posteriorly only moderately but they are triangular and laterally broad, covering a large portion of the spine faces.

Some of the sacral ribs are not fully preserved, but those that are indicate they include a thin vertical blade, a dorsal bar over this blade, and expansions where the ribs articulate with the ilia. Distally, the preserved ribs expand to abut the ilium. The presence or absence of a sacricostal yoke cannot be determined in dorsal view. Only a fragment of the ilium is preserved, which is on the right side (Fig. 6A).

The five caudal vertebrae (described below) articulated and associated with this skeleton (BYU 14771) provide a crucial link between presacral, sacral, and caudal vertebrae.

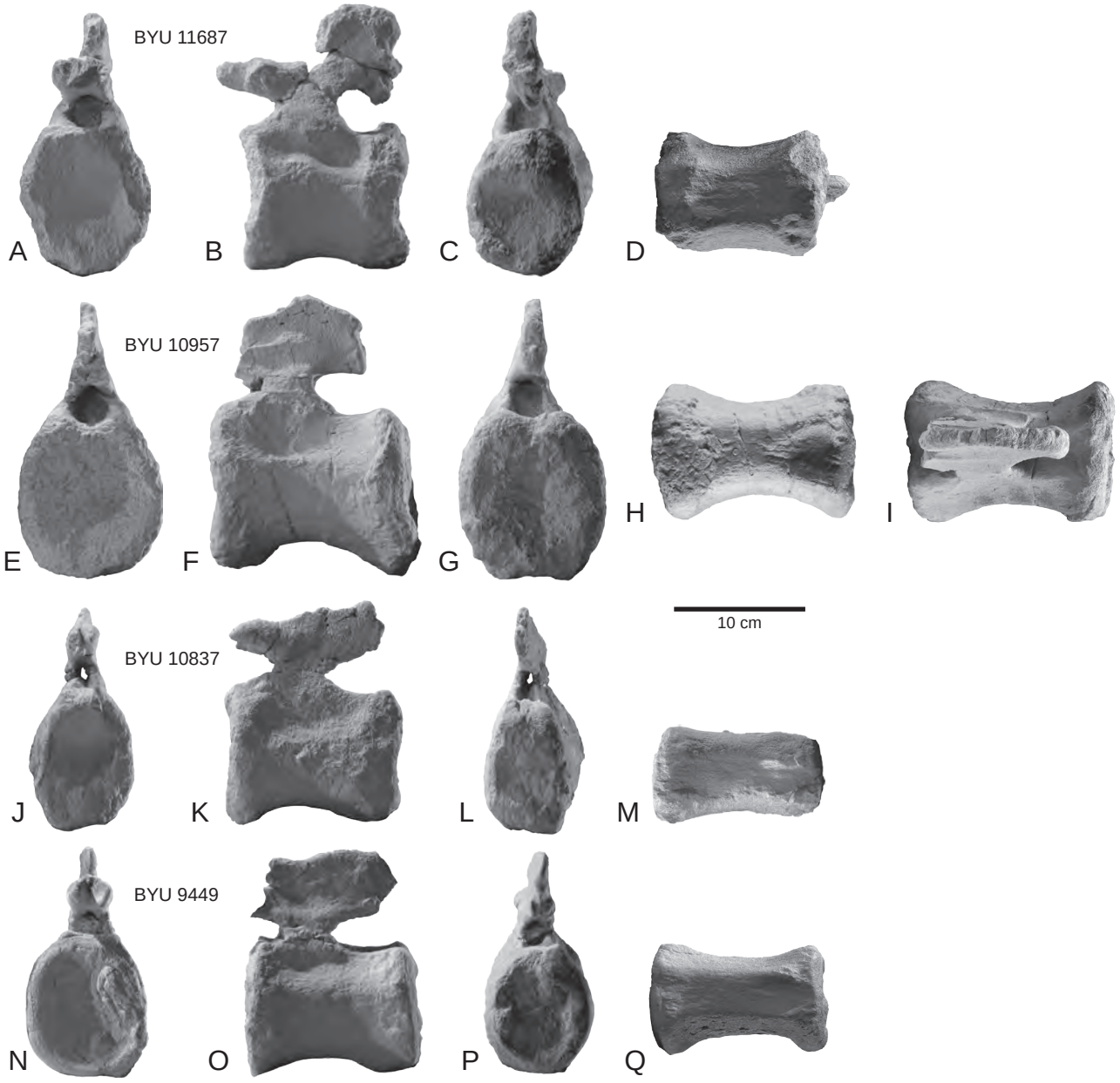

Figure 27 — *Moabosaurus utahensis*, referred mid-caudal vertebrae. **A–D**, proximal mid-caudal vertebra, BYU 11687, in anterior, left lateral, posterior, and ventral views. **E–I**, proximal mid-caudal vertebra, BYU 10957, in anterior, left lateral, posterior, ventral, and dorsal views. **J–M**, distal mid-caudal vertebra, BYU 10837, in anterior, left lateral, posterior, and ventral views. **N–Q**, distal mid-caudal vertebrae, BYU 9449, in anterior, left lateral, posterior, and ventral views.

Caudal Vertebrae.— The caudal vertebrae are the best represented portion of the vertebral column because the centra are larger relative to the neural arch, are solid, block-like, and resist trample breakage better than other vertebrae. The neural arches of all but the anteriormost caudal vertebrae, however, are delicate and often missing or incomplete. For the purposes of this description, we divide the tail into proximal, middle, and distal segments based on centrum height (H)-to-length (L) ratios, excluding the condyle if present: proximal (H/L > 1.0), middle (H/L 1.0–0.75); and distal (H/L < 0.75). The most complete caudal series consists of the first five caudal vertebrae. Caudal vertebrae 1 and 2 were found in articulation with the sacrum described above (BYU 14771, Fig. 6A–D) and caudal vertebrae 3–5 form an articulated series found close to the sacrum (BYU 14768, Fig. 24A–J). All pertain to a juvenile individual.

The first five caudal vertebrae (BYU 14771 and BYU 14768) are strongly procoelous. This allows us to confidently

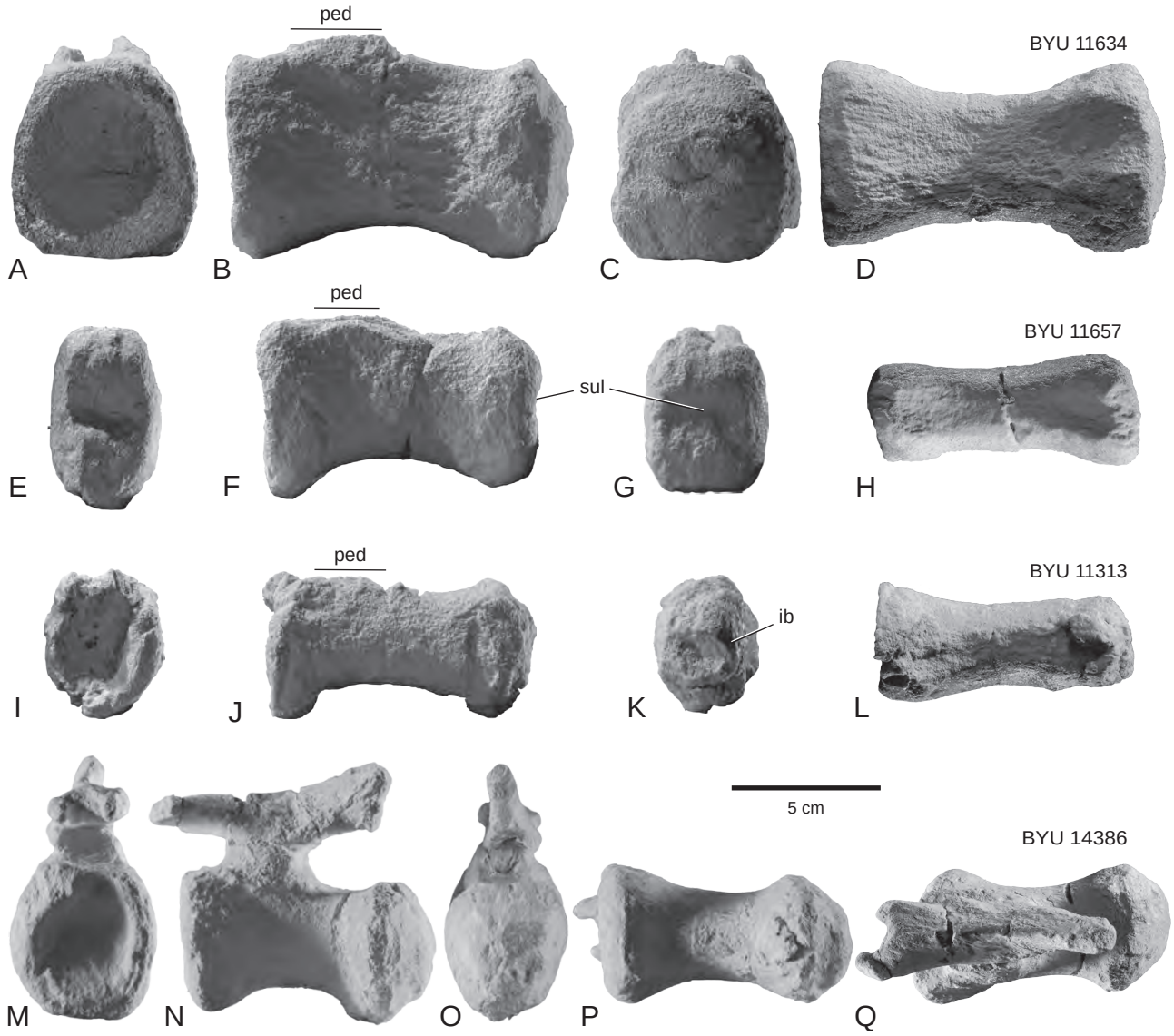

Figure 28 — *Moabosaurus utahensis*, referred distal caudal vertebrae. **A–D**, anterior distal caudal vertebra, BYU 11634, in anterior, left lateral, posterior, and ventral views. Centrum is nearly flat-sided with moderately developed condyle. **E–H**, anterior distal caudal vertebra, BYU 11657, in anterior, left lateral, posterior, and ventral views. Centrum is nearly flat-sided with partially developed condyle above and above and below horizontal sulcus. **I–L**, distal caudal vertebra, BYU 11313, in anterior, left lateral, posterior, and ventral views. The spindle-shaped centrum bears a hemispherical condyle with insect burrows. **M–Q**, near-end-of-tail caudal vertebra, BYU 14386, in anterior, left lateral, posterior, ventral, and dorsal views. Centrum is short with large, hemispherical condyle. The neural arch is nearly complete. Abbreviations: *ib*, insect burrow; *ped*, neural arch peduncle; *sul*, sulcus.

refer similarly procoelous caudal vertebrae and their serial variants to *Moabosaurus*. The proximal and most distal caudal vertebrae referred to *Moabosaurus utahensis* are procoelous, whereas the nature of the articular surfaces of the middle caudal vertebrae is variable. Those from the proximal portion of the tail are strongly procoelous, with the anterior cotyle being deeper than the posterior condyle (Figs. 6, 24–26). The condyle constitutes almost half of the length of the centrum on the first few caudal vertebrae. The more distal of the proximal caudal vertebrae can have a small condyle, but in those cases the cotyle on the same vertebra is deep, much deeper that the condyle is long, suggesting perhaps intervening cartilage is missing, as on BYU 10883 (Fig. 26F–J). The size of the posterior condyle is greatly reduced, or only poorly developed, in the middle caudal region (Fig. 27). The caudal vertebrae from the distal portion of the tail usually have a larger distal condyle than the middle caudal vertebrae (Fig. 28), with one of the posteriormost recovered

caudal vertebrae being strongly procoelous (BYU 14386, Fig. 28M–Q). On middle and posterior caudal vertebrae, there is substantial variability in the development of the distal condyle, with the condyle in some cases bifurcated by a horizontal, mid-condyle sulcus of varying dorsoventral width (Fig. 28E–G). In some caudal vertebrae, the posterior face of the centrum has a central concavity with the periphery consisting of a swollen rim (Fig. 27C, G), suggesting only the periphery of the cartilaginous condyle was ossified. In others, the posterior face bears irregularly spaced concavities and bosses (Fig. 27L, P). In some, especially on the more distal caudal vertebrae (e.g., BYU 11657, Fig. 28E–H), the anterior face similarly has bulbous partial condyles above and below a median sulcus or only at the top or bottom of the face. In more mature individuals with increased ossification, we speculate some of these vertebrae may have become biconvex.

The centra are all relatively short, with the longest (BYU 11313, Fig. 28I–L) having a centrum height-to-length ratio of 0.5. In cross-section, the proximal two caudal vertebrae (Fig. 25) are approximately round, whereas the balance of the proximal caudal vertebrae are polygonal, roughly in the shape of a heart, with the sides below the caudal ribs converging ventrally to the ventral sulcus, which narrows rapidly along the first five vertebrae (Figs. 24, 26). Centra of the middle part of the caudal series are blocky cylinders, with gently convex sides converging on the ventral sulcus. This sulcus becomes less pronounced and essentially flat at mid-centrum length, with the concave shape preserved anteriorly and posteriorly by ridges buttressing the chevron facets (Fig. 27). On the distal one-third of the tail, the more anterior centra are distinctly slab sided, grading posteriorly to become slightly convex and with the mid-centrum ventral surface being only slightly concave to more rounded and the chevron buttresses lower and less pronounced (Fig. 28A–H). Toward the end of the tail, the centrum becomes a rod (Fig. 28I–L) before shortening substantially (e.g., BYU 14386, Fig. 28M–Q). Centra from the proximal third of the tail (Figs. 24–26) are characterized by a neural canal sulcus that extends anteriorly and posteriorly beyond the neural arch. On the balance of the centra, the sulcus does not extend beyond the neural arch peduncles.

On caudal vertebra 1 (Figs. 6, 25), the rib forms an ala (wing) that extends ventrally from the level of the zygapophyses to halfway down the centra. Caudal vertebra 2 (Figs. 6C–D, 24F–J) has a similar, but smaller ala. The ribs/alae are incomplete on caudal vertebra 1 but they are nearly complete on caudal vertebra 2 and they extend laterally and terminate with a cranial extension and a flattened lateral surface. There is no ala on caudal vertebra 3 (Fig. 24A–E) but the rib has a flattened region on its upper surface, which sweeps posteriorly and extends laterally beyond the centrum. On caudal vertebrae 4 and 5 (Fig. 24F–J), the rib develops in a similar form, but they become shorter laterally and their dorsoventral dimension decreases.

The chevron facets are small throughout the caudal series. In the proximal caudal vertebrae, the anterior and posterior chevron facets are buttressed by a ridge spanning the length of the centrum (Figs. 24–26). In in the middle portion of the series, the buttresses are limited to the proximal and distal portions of the centrum (Fig. 27). The buttresses are reduced in height distally in the caudal series until they are low, broad swellings adjacent to the facets (Fig. 28D, H, L).

The neural arches of all caudal vertebrae are resticted to the anterior half of the centrum. The neural arches of the caudal vertebrae are relatively short vertically. The first caudal neural arch is only 1.25 times taller than its centrum (Fig. 25), and the height of the spine relative to the centrum decreases rapidly posteriorly. By caudal vertebra 4 (Fig. 24F–J) the neural arch is equal in height to the centrum, and this ratio gradually diminishes along the balance of the tail.

Neural spine orientation, shape, and height changes along the tail as follows. On caudal vertebra 1 the neural spine is raked forward, whereas those of succeeding caudal vertebrae are near vertical and then gradually recline posteriorly. The proximal caudal neural spines transition from being transversely thicker than axially elongate in caudal vertebrae 1–3, to being anteroposteriorly thicker. On caudal vertebra 4 and successive vertebrae in this series, the spine is still wide but becomes more blade-like, with the anteroposterior dimension slightly greater than the transverse dimension. By the end of the proximal one-third of the caudal series, the neural spines are short, with the height and anteroposterior dimension subequal, but remain transversely thick (BYU 11687). In the middle third of the tail the neural spines are low, laterally thin, and axially elongate (Fig. 27). The exact shape of most spines in the middle of the tail is unknown because they are incomplete. Likewise, the neural spines in nearly all posterior caudal vertebrae are incomplete or missing, with the exception of a caudal vertebra from near the end of the tail that shows the distal caudal vertebrae had a typical low, posteriorly oriented, rod-like spine (Fig. 28M–Q).

The apex of the neural spines changes rapidly in the proximal third of the tail. That of the first caudal vertebra is like those of the sacral vertebrae, with a laterally expanded apex that is relatively flat from side to side across the spine table, with a transverse width twice that of the axial length (Figs. 6, 25F–I). The spine is triangular in axial views with a laterally broad, triangular intervertebral ligament scar. Laminae are numerous only on the first two or three caudal vertebrae. Caudal neural spine 1, in posterior view, is convex, bounded laterally by the conjoined spinopostzygapophyseal and spinodiapophyseal laminae (Fig. 6C–D). The spinoprezygapophyseal laminae extend only slightly from the spine, but the postzygapophyseal laminae are well developed and converge ventrally at the top of the postzygapophyseal facets, below which is a rudimentary hyposphene. The robust spinodiapophyseal laminae originate at spine mid-height and extend anteroventrally to converge with the top of the caudal rib ala (Fig. 25). The first caudal vertebra is the only one with sizeable fossae and sulci between laminae. These excavations suggest that pneumatic diverticulae (Britt, 1993) extended posteriorly from the sacrum onto the first caudal vertebra but no further along the tail. The caudal neural spine 2 is preserved in its entirety (Fig. 6C–D). It is markedly narrower laterally than that of caudal vertebra 1, and the spine top is strongly convex. On

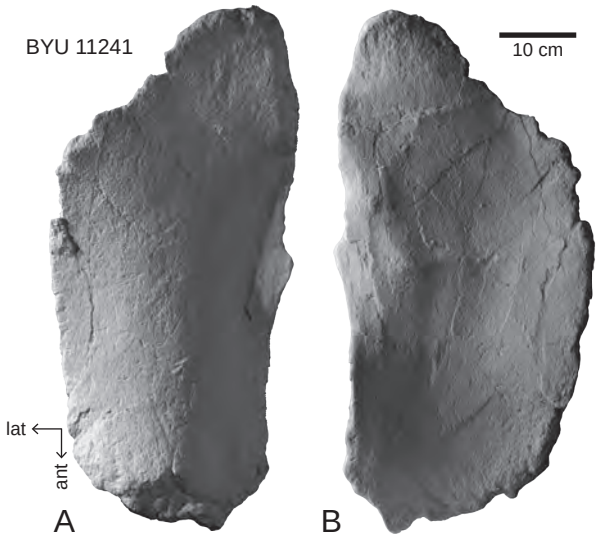

FIGURE 29 — *Moabosaurus utahensis*, referred left sternal plate, BYU 11241. In ventral **(A)** and dorsal **(B)** views. The thick end is at the bottom of the figure. The upper left margin of (A) preserves large tubercles. Abbreviations: *ant*, anterior; *lat*, lateral.

caudal vertebrae 3–5 (Fig. 24), the neural spine tops become laterally thinner and the spine apex transitions from laterally convex to laterally sloped, like the peaked roof of a house, as on spine apices of *Camarasaurus* anterior caudal vertebrae. Laterally, a rugose surface extends down one half the height of the neural spine, marking attachments for muscles/tendons. The spinoprezygapophyseal laminae are present on the lower portions of the spines. The spinopostzygapophyseal laminae are thinner and more prominent than the spinoprezyapopysial laminae, and they extend well up onto the spine.

Few zygapophyses are preserved. On the first caudal vertebra, the prezygapophyses are asymmetrical, with the right prezygapophysis being a stout rod, and the left a laterally thin blade (Fig. 25A–D). The remaining anterior caudal prezygapophyses are stout, half-round in cross-section, and the facet occupies most of the medial surface. In the middle caudal vertebrae, the few preserved prezygapophyses are conical and slender. The distal caudal vertebrae preserve only one partial set, from near the tail terminus, and the prezygapophyses are simple rods that originate anterior to the centrum (Fig. 28M–Q).

Preserved postzygapophyses are few, small, and unremarkable.

In caudal vertebrae 1 and 2 (Fig. 25), the prolate neural canal is much larger than on more posterior caudal vertebrae, being about twice as high as wide. The neural canal is 'inflated' within the neural arch, sometimes extending up to 2 cm in one direction, into the peduncles, base of the spine, or into the centrum. The neural canal of the first two caudal vertebrae of *Camarasaurus* are likewise expanded, but to a lesser degree (personal observation). The large size of the neural canal, along with is moderate, chamber like expansion of the neural canal is a caudal extension of the greatly enlarged sacral neural canals that are typical of most sauropods (Upchurch et al., 2004).

In summary, the large number of recovered caudal vertebrae provide a moderate understanding of the tail of *Moabosaurus utahensis*. The centra are axially short throughout the series. They are also strongly procoelous proximally, moderately-to-weakly procoelous in the middle portion of the tail, and the posterior condyle is variably developed in distal caudal vertebrae, ranging from moderately to strongly procoelous. The greater depth of the centrum cotyle relative to the condyle length in the middle of the series suggests a cartilaginous component is missing. Centra of the middle and distal tail are flat sided. The neural arches are relatively low throughout the tail, and the neural arch peduncles are centered on the anterior half of the centrum. Based on the relatively stocky nature of all the caudal vertebrae, including the more distal ones, we speculate the tail was short, and the number of vertebrae relatively few, for a sauropod.

Appendicular Skeleton

Sternal Plate.— The well-preserved sternal plate (Fig. 29) has all margins essentially intact except for the slightly damaged thicker end. For the purposes of this description, we follow the orientational convention proposed by Upchurch et al. (2004), which places the thickest end anterior and the convex side ventral. Following that orientation, BYU 11241 is a right sternal plate, and the shorter, thicker side would be the median contact. The sternal plate is anteroposteriorly elongate and shaped like an orange slice. The posteromedial margin is undulating, and the protrusions may represent tubercles for sternal rib articulations (Upchurch et al., 2004). The ventral surface is strongly convex along the anterior one-fourth of the bone, but the convexity decreases gradually posteriorly to the distolateral blade, which is flat and thickened terminally. Anteriorly, the convexity is a broad ridge that flares externally over the last one-fourth of the element's length to form a robust anterior margin. The dorsal surface is gently concave mediolaterally, with the exception of the distal one-third, which is flat with a dorsally oriented terminal extension. The medial margin is slightly curved and thick relative to the lateral margin. The lateral margin is thin with a small, posterolateral, triangular flange, which is also present in *Giraffatitan brancai* (Janensch, 1947). The overall shape bears similarities to the elongate, rectangular sternal plates of *Haplocanthosaurus delfsi* (McIntosh and Williams, 1988), and to a lesser degree those of *Giraffatitan brancai* (Janensch, 1947). In outline, the sternal plate is like that of *Tornieria africana* (Janensch, 1947), save that in the latter the distal end is laterally expanded. The sternal plate most closely resembles that of *Turiasaurus* (Royo-Torres et al., 2006) in that both are narrower than those of other sauropods.

Humerus.— Humeri are among the most common elements of *Moabosaurus* preserved at Dalton Wells (39 specimens recovered), most likely due their robust construction. A virtually complete left humerus (BYU 10798; Fig. 30) is

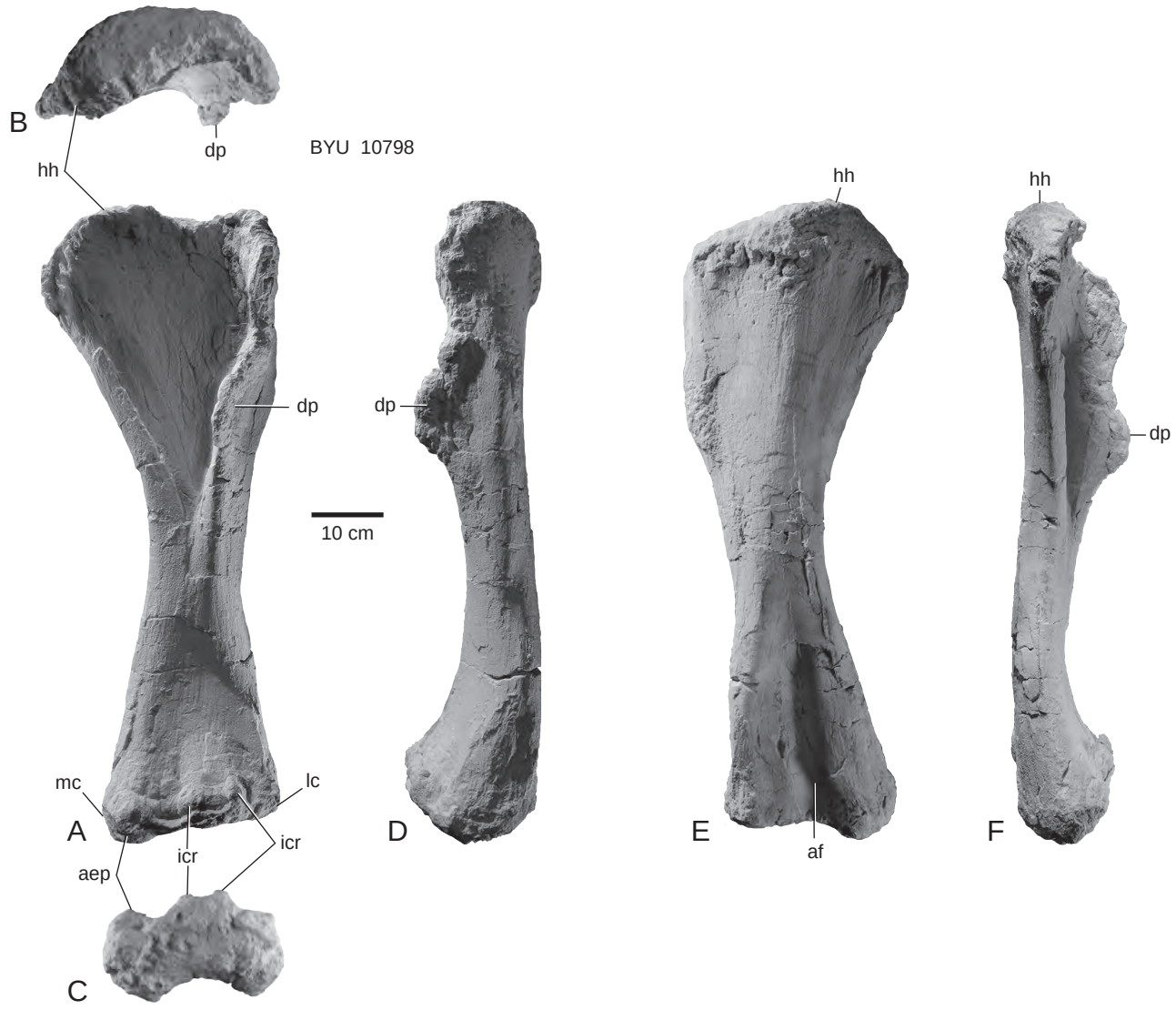

FIGURE 30 — *Moabosaurus utahensis*, referred left humerus, BYU 10798. In anterior (**A**), proximal (**B**), distal (**C**), lateral (**D**), posterior (**E**), and medial (**F**) views. Abbreviations: *aep*, anterior entepicondylar process; *af*, aconeal fossa; *dp*, deltopectoral crest; *hh*, humeral head; *icr*, intercondylar ridges; *lc*, lateral condyle; *mc*, medial condyle.

similar in both morphology and proportions to *Camarasaurus* (Wilhite, 2005)—so similar that if this bone were present in Morrison strata it would have been assigned to that genus. The proximal end of the humerus has a well-defined head that is offset medially and a well-defined deltopectoral crest. The humeral shaft is asymmetrical in cross-section, being much more convex medially than laterally. The distal end of the humerus shows the typical rugose, flat surface found in sauropods. There are intracondylar ridges positioned slightly lateral to the midline of the distal humerus. A noteworthy feature of the distal condyles is that the medial condyle extends distally significantly farther than the lateral condyle, resulting in a 10˚ proximomedial angle between the two condyles with respect to the humeral axis. The slope of the distal condyles, together with the offset of the humeral head, provide insight into the stance of *Moabosaurus*. The medially offset head clearly indicates a relatively 'wide-gauge' stance like that proposed for *Camarsaurus* by Wilhite (2005). The angled distal condyles indicate either a unique articular surface with the radius and ulna or a somewhat narrower stance than *Camarasaurus*. Besides the morphological resemblance to *Camarasaurus*, the humerus has a minimum breadth-to-length ratio of 0.17, which is virtually identical to most *Camarasaurus* specimens (Wilhite and Curtice, 1998).

Ulna.— BYU 14777 (Fig. 31) is a virtually complete left ulna missing only a portion of the distal end. The ulna is triradiate in proximal view, with a thick proximolateral process and a thin proximomedial process. A well developed olecranon

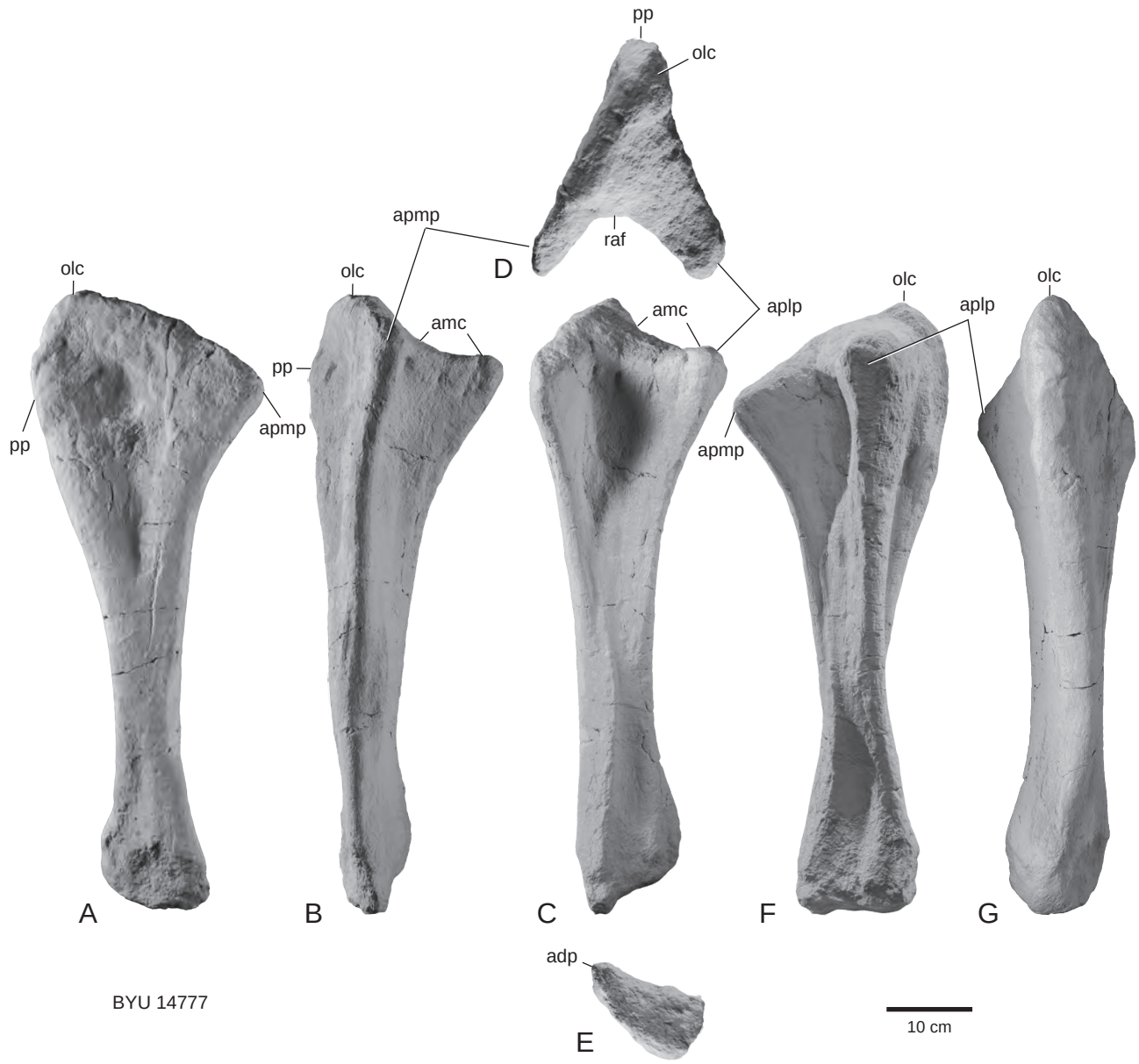

FIGURE 31 — *Moabosaurus utahensis*, referred left ulna, BYU 14777. In posterior (**A**), anterolateral (**B**), anterior (**C**), proximal (**D**), distal (**E**), medial (**F**), and posterior (**G**) views. Abbreviations: *adp*, anteriodistal process; *amc*, anteromedial process concavity; *aplp*, anterior proximolateral process; *apmp*, anterior proximomedial process; *olc*, olecranon process; *pp*, posterior process; *raf*, radial fossa.

forms the posterior projection of the proximal end of the bone as in many titanosaurs (Wilson and Carrano, 1999). The proximal radius would have articulated in the fossa formed by the medial and lateral processes of the proximal ulna (Wilhite, 2003). Although the distal end of the ulna is incomplete, it appears to have been triangular and is complete enough to estimate its total length for dimensional comparisons with other well-known North American sauropods. In contrast to the humerus, which both dimensionally and morphologically resembles *Camarsaurus*, the ulna is gracile with a minimum breadth-to-length ratio of 0.12. By comparison, the same ratio for *Camarasaurus* ulnae ranges from 0.16 to 0.18 (Wilhite and Curtice, 1998). In North America, only the sauropods *Diplodocus* and *Amphiceolias* have ulnae that are this gracile (Wilhite, 2003). With regard to stance and gait, the prominent olecranon suggests well-developed triceps musculature that would be consistent with a 'wide-gauge' stance (Wilson and Carrano, 1999; Wilhite, 2005).

Femur.— BYU 14783 is a left femur (Fig. 32) that has some damage to the proximal and distal ends as well as anteroposterior

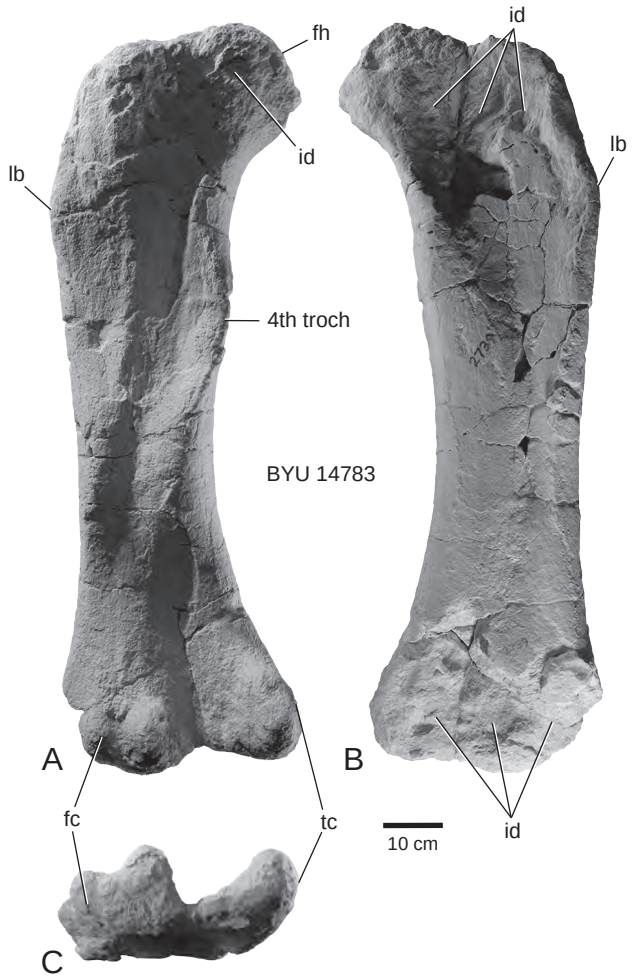

FIGURE 32 — *Moabosaurus utahensis*, referred left femur, BYU 14783. In posterior (**A**), anterior (**B**), and ventral (**C**) views. Abbreviations: *fc*, fibular condyle; *fh*, femoral head; *id*, insect damage; *lb*, lateral bulge; *tc*, tibial condyle; *troc*, trochanter.

crushing. A distinct femoral head is identifiable, as well as a slightly medially offset neck. A moderately developed lateral bulge is present. A prominent fourth trochanter is present on the lower portion of the proximal one-third of the femoral shaft. The distal end of the femur is complete posteriorly, but badly worn on the anterior surface. Therefore, little can be said about the extent of the femoral condyles. However, it is apparent that the fibular condyle is either equal in distal extent to the tibial condyle or perhaps slightly longer. The minimum breadth-to-length ratio of the femur is 0.17, which falls within the range of the robust femora of *Camarasaurus* and *Apatosaurus* (Wilhite, 2003). With the exception of the lateral bulge, the overall morphology of the femur closely resembles that of *Camarasaurus*. The flat femoral condyles and slightly offset head are both consistent with a 'wide-gauge' stance (Wilson and Carrano, 1999; Wilhite, 2007).

PHYLOGENETIC ANALYSIS

To determine the phylogenetic position of *Moabosaurus utahensis*, we performed cladistic analyses utilizing the matrices of Wilson (2002), Upchurch et al. (2004), and Carballido and Sander (2014). We followed each authors' choices for coding multistate characters where possible. Our specific analyses are described below. Phylogenetic analyses were conducted using data matrices compiled and edited in Mesquite version 3.2 (Maddison and Maddison, 2017). Trees were computed in TNT version 1.5 (Goloboff and Catalano, 2016) using 1,000 multiple replicate addition sequences (hold 1000; mult = replic 1000; hold 10).

The Wilson (2002) matrix consists of 234 characters (216 binary and 18 multistate) for 27 taxa. To this matrix, we added scores for a single additional taxon, *Moabosaurus*, but no additional characters (Appendix I). Addition of a taxon to an analysis without addition of characters can be expected to dilute overall pool of synapomorphy support (Whitlock et al., 2011). In his original analysis, Wilson treated 5 multistate characters as ordered (8, 37, 64, 66, 198) and the remaining 13 characters as unordered (36, 65, 68, 70, 72, 80, 91, 108, 116, 118, 134, 152, 181). We treated these characters the same way. Additionally, the author used two asymmetric step matrices for two characters (64 and 198), saved suboptimal trees (up to 5 steps longer), and computed majority rule consensus trees from the set of optimal and suboptimal trees. We did not employ step matrices nor compute suboptimal trees, as these methods require unnecessary *ad hoc* assumptions about character evolution. Our goal was to present a more conservative estimate of the placement of *Moabosaurus* among the taxa. Our parsimony analysis found 12 most parsimonious trees with length = 386 (CI= 0.623; RI = 0.720). The strict consensus of these trees is presented in Figure. 33. The resultant strict consensus tree differs only in minor ways from that obtained by Wilson. In Wilson (2002), *Jobaria* is placed as sister-group to Neosauropoda, whereas in our tree this node forms a polytomy including Macronaria, Diplodocoidea, and *Haplocanthosaurus*. In our analysis, *Isisaurus* is placed within Saltasauridae, whereas in Wilson (2002) it was resolved as the outgroup to Saltasauridae. *Moabosaurus* is recovered as a basal somphospodylan, sharing with that clade large cotyles on the proximal and some middle caudal vertebrae. *Moabosaurus* lacks other characters associated with somphospondylans, such as camellate sacral vertebrae and a square anteriolateral corner of the humerus (Mannion et al., 2013).

The Upchurch et al. (2004) matrix consists of 309 characters for 47 taxa. Upchurch et al. (2004) stated in the supporting documentation to their dataset that all characters, including the multistate characters, were treated as unordered (Upchurch, et al., 2004, supporting documents). This contradicts Carballido and Sander (2014), who stated that they ordered their characters following Upchurch et al. (2004; discussed below). Upchurch et al. (2004) found 1,056 most parsimonious trees in their analysis and subsequently deleted 5 taxa that appeared unstable in their set of trees,

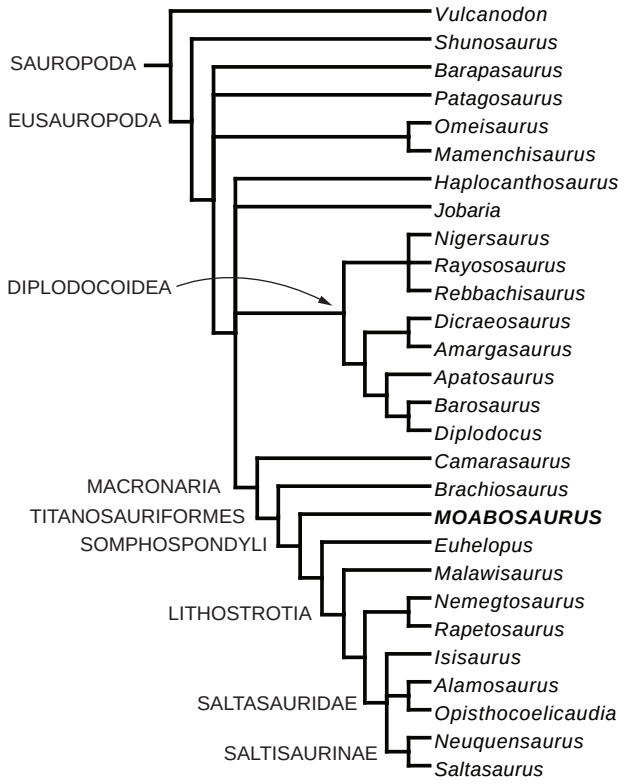

FIGURE 33 — Strict consensus tree of the MPTs obtained using the Wilson (2002) dataset with *Moabosaurus utahensis* data (Appendix I) included. Our analysis found 12 most parsimonious trees (MPTs) with length = 386 (CI= 0.623; RI = 0.72).

later computing a 'reduced consensus' cladogram from the pruned trees (Upchurch et al., 2004: fig. 13.18). The pruned taxa were *Andesaurus*, *Argentinosaurus*, *Lapparentosaurus*, *Nigersaurus*, and *Pleurocoelus*. Note that these authors did not remove these taxa and then recompute trees (as is standard practice); they simply pruned the taxa after the set of trees was computed, and then computed a new consensus from the pruned set of trees. We find this unconventional approach problematic, because the reduced set of pruned trees is not likely to be equivalent to the set of most parsimonious trees for the reduced taxa in the analysis.

We scored and added *Moabosaurus* to the Upchurch et al. (2004) matrix (see Appendix II). Because we have not been able to find any statement identifying those characters that were treated as ordered, and because the posted matrices did not have the specific commands embedded within specifying character ordering, we treated all characters as unordered. We performed two analyses: the first analysis consisted of all 48 taxa (Fig. 34A), and the second analysis used a reduced, 43-taxon dataset after removal of the 5 taxa listed above (Fig. 34B). Parsimony analysis of the full 48-taxon data set resulted in 150 most parsimonious trees (L = 687, CI = 0.473, RI = 0.767), the strict consensus of which is largely unresolved (Fig. 34A). Monophyly of Neosauropoda is supported (Fig. 34A), but within this clade only Brachiosauridae, Dicraeosauridae, and Diplodocidae are retained. *Moabosaurus* is placed within a large polytomy of genera and clades within Neosauropoda (Fig. 34A). Much more resolution was recovered in the reduced 43-taxon analysis, which resulted in 26 most parsimonious trees (L = 662, CI = 0.488, RI = 0.772), the strict consensus of which is given in Figure. 34B. Neosauropoda is recovered as monophyletic, as is Diplodocoidea with *Nemegtosaurus* + *Quaesitosaurus* as its sister-group, Titanosauriformes, Somphospondyli, and Lithostrotia. *Moabosaurus* is placed as sister group to (((*Nemegtosaurus* + *Quaesitosaurus*) + *Rayososaurus*) + Diplodocoidea).

The most comprehensive dataset we utilized is that of Carballido and Sander (2014), which consists of 341 characters and 71 taxa. Of the 49 multistate characters, 24 were treated as ordered (12, 58, 95, 96, 102, 106, 108, 115, 116, 119, 120, 154, 164, 213, 216, 232, 233, 234, 235, 256, 267, 298, 299, 301), and the remainder were treated as unordered. The authors found 4 most parsimonious trees, and their topology was highly resolved. We scored and added *Moabosaurus* (Appendix III) to the Carballido and Sander (2014) matrix and assigned the coding choices to the multistate characters. Parsimony analysis resulted in 12 most parsimonious trees (L = 1055; CI = 0.404, RI = 0.713). Our topology (Fig. 35) is entirely congruent with the topology presented by Carballido and Sander (2014), although in our analysis, relationships are somewhat less resolved within Macronaria. *Moabosaurus* is recovered as a lineage within Titanosauriformes and is placed in a polytomy with six other lineages: *Euhelopus*, *Erketu*, *Chubutisaurus*, *Galvesaurus* + *Tastavinsaurus*, Brachiosauridae, and Somphospondyli.

In sum, all four analyses agree in placing *Moabosaurus* within the Neosauropoda. Analyses using the Upchurch et al. (2004) matrix (Fig. 34) recover *Moabosaurus* as a neosauropod that is sister-group to (((*Nemegtosaurus* + *Quaesitosaurus*) + *Rayososaurus*) + Diplodocoidea). The Wilson (2002) data matrix resolves *Moabosaurus* as a basal somphospondylan (Fig. 33) and the Carballido and Sander (2014) datamatrix resolves *Moabosaurus* within Titanosauriformes (Fig. 35). Taken together, these analyses agree that *Moabosaurus* is a neosauropod. The more resolved trees indicate further that it is a macronarian, specifically a basal titanosauriform. Certain characters in *Moabosaurus*, such as its thick-walled, camerate presacral vertebrae, are inconsistent with its placement as a titanosauriform. These and other characters should be incorporated into analyses further exploring its place within Macronaria.

DISCUSSION

Size and Ontogenetic Age of *Moabosaurus*

Recovered specimens of *Moabosaurus utahensis* are relatively small for a sauropod, approximately equal in size to *Camarasaurus*. A composite mounted skeleton with a 130 cm femur measures 9.75 m long (Fig. 36). The dorsal centra in the mount average 22 cm long. The smallest known *Moabosaurus*

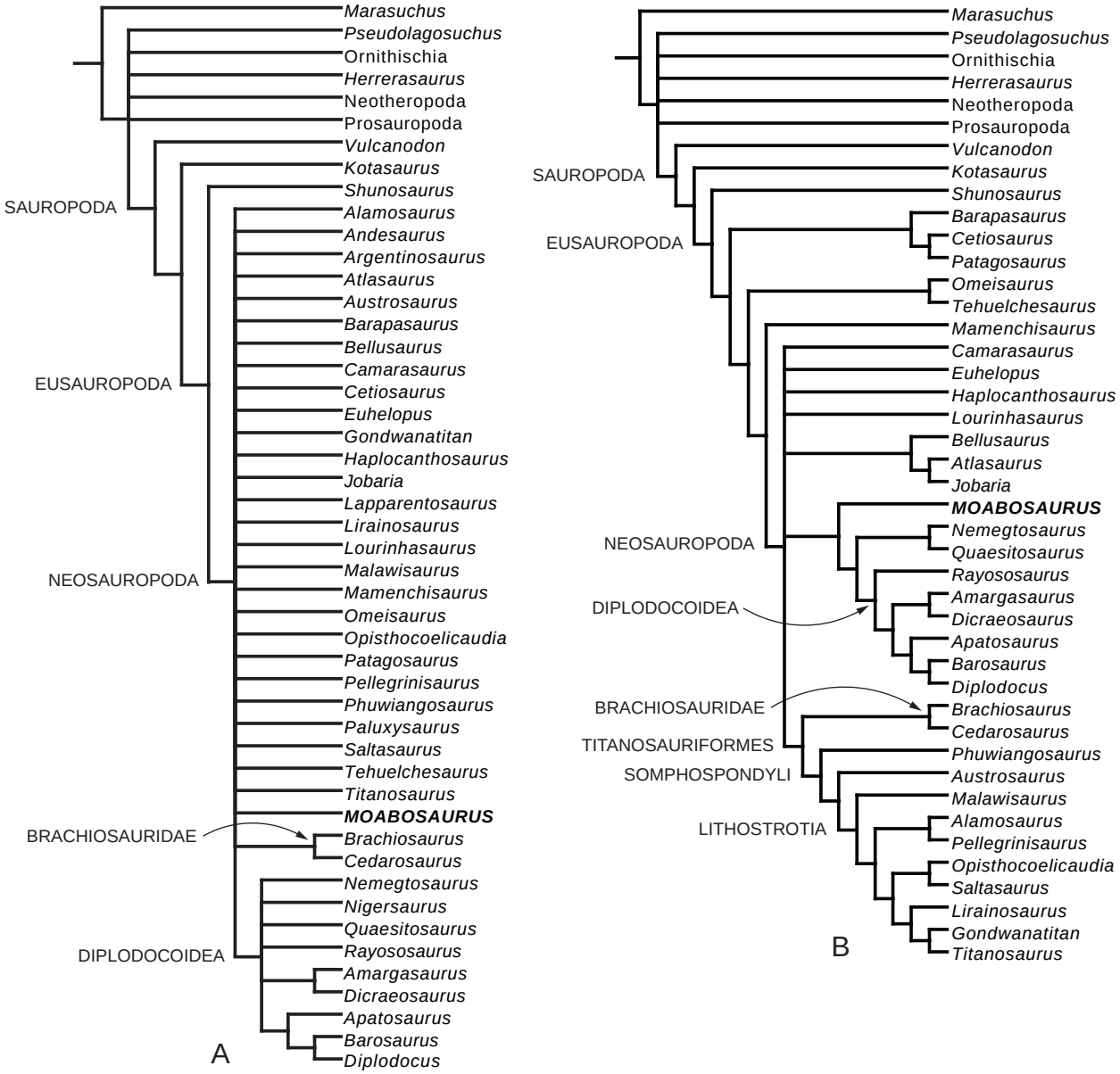

FIGURE 34 — Strict consensus trees of the MPTs obtained using the Upchurch et al. (2004) dataset incorporating *Moabosaurus utahensis* (Appendix II). (**A**), Analysis of the entire taxon data set resulted in 150 MPTs (L = 687, CI = 0.473, RI = 0.767). (**B**), Analysis of the reduced data set, from which *Andesaurus*, *Argentinosaurus*, *Lapparentosaurus*, *Nigersaurus*, and *Pleurocoelus* were removed. The analysis resulted in 26 MPTs (L = 662, CI = 0.488, RI = 0.772).

individual is represented by a mid-to-posterior dorsal neural arch that has an estimated centrum length of 7 cm (BYU 20250). The degree of fusion of neurocentral sutures does not help in determining ontogenetic stages, because the sutures are fused regardless of vertebral size. The largest femur is 150 cm long, and the largest humerus is 120 cm long. Most non-theropod dinosaurs preserved at Dalton Wells, regardless of taxon, were judged to be juveniles or subadults by Britt et al. (2009). The maturity of the largest individuals of *Moabosaurus utahensis* remains to be determined.

The large number of elements of *Moabosaurus* (e.g., 18 braincases and 38 humeri) revealed a surprisingly wide range of variation in a single element. With our present state of knowledge of the taxon, the variation appears to be a continuum, which could be a function simply of individual, ontogenetic, or sexual dimorphism, a problem that may be resolved by future study. The variation is such that end members could easily be mistaken for different taxa. As noted in description of skull elements, this degree of variation is also present in *Camarasaurus*. This problem points to the

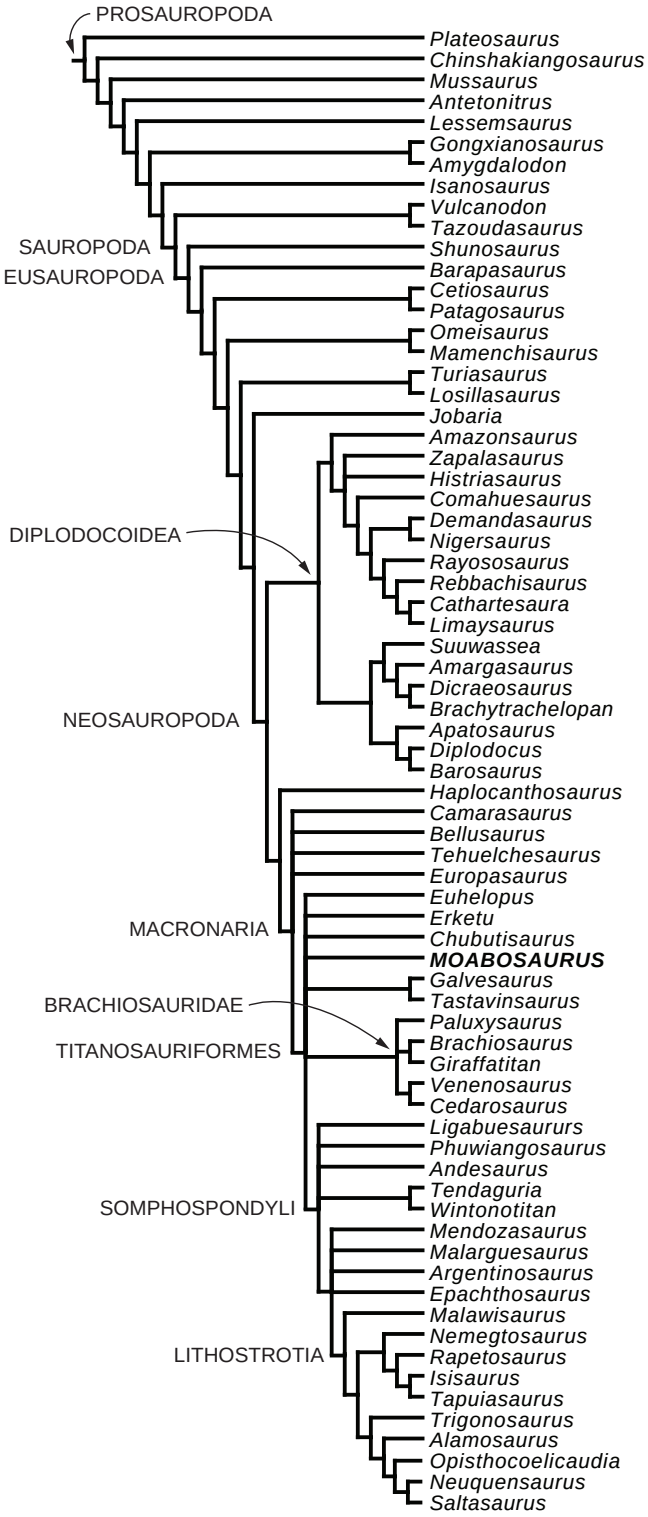

FIGURE 35 — Strict consensus tree of the MPTs obtained using the Carballido and Sander (2014) dataset incorporating *Moabosaurus utahensis* (Appendix III). Parsimony analysis resulted in 12 trees (L = 1055, CI = 0.404, RI = 0.713).

care that should be taken when erecting new taxa based on minor variance which could be interpreted as being more substantial in the absence of a large sample size. This problem is evident in previous work on the Dalton Wells fauna that recognized a camarasaurid (e.g., Britt et al., 1997; Britt, et al., 2009) in addition to what is now known as *Moabosaurus*. The camarasaurid braincase and associated cervical vertebrae (BYU 9460) pertain to a juvenile specimen of *Moabosaurus*.

Comparison with North American Early Cretaceous Sauropods

Here, we compare *Moabosaurus* to Early Cretaceous sauropods from North America. The oldest reported Cretaceous sauropod from the continent consists of two bones of a neosauropod, similar to *Camarasaurus*, from Berriasian-Valanginian-aged strata from South Dakota (D'Emic and Foster, 2016). Except for that *Camarasaurus*-like specimen, the balance of the Early Cretaceous North American sauropods are titanosauriforms, several of which occur in the Albian-to-Cenomanian Mussentuchit or Ruby Ranch members of the Cedar Mountain Formation. The most complete, *Abydosaurus*, is a brachiosaurid that occurs in the Mussentuchit Member (Chure, et al., 2010). It differs partly from *Moabosaurus* in having small, parallel-sided teeth, elongate, camellate cervical centra, and elongate arm elements. The Price River II quarry (Burge et al., 2000) and the Long Walk Quarry (DeCourten, 1991), both in the Ruby Ranch Member, have produced brachiosaurids that remain to be described. *Brontomerus mcintoshi* (Taylor et al., 2011) was also named on the basis of several bones, all from a single quarry in the Aptian to Albian Ruby Ranch Member of the Cedar Mountain Formation (Taylor et al., 2011), but it is considered a *nomen dubium* (D'Emic, 2012). Preserved elements suggest "*Brontomerus*" is a titanosauriform (Taylor et al., 2011; D'Emic, 2012). It differs from *Moabosaurus* in that the scapula has a large expansion of the distal blade, the dorsal ribs are pneumatic, and presacral vertebrae are camellate.

There are two titanosauriform sauropods in the basal (Aptian) sequence of the Cedar Mountain Formation: *Cedarosaurus* and *Venenosaurus*. Both are consistently recovered as brachiosaurid titanosauriforms (D'Emic, 2012; Carballido and Sander, 2014) and both occur in the same stratigraphic horizon as *Moabosaurus*. *Cedarosaurus* and *Venenosaurus* differ from *Moabosaurus* in the following features: there are numerous moderate-sized pneumatic chambers in the cotyles of the dorsal centra; dorsal ribs are pneumatic; caudal vertebrae have concavo-plano to amphiplatyan articular surfaces and fossae ventral to the caudal ribs; caudal ribs are strongly backswept; the posterior articular faces of caudal vertebrae 7–10 are lower than the anterior faces; most caudal neural spines are anteriorly inclined; humeri and ulnae are elongate; the proximal ulna has anteriorly projecting lateral and medial processes that differ substantially in length; ulna lacks an olecranon process (Tidwell et al., 1999). *Cedarosaurus* and *Venenosaurus* share

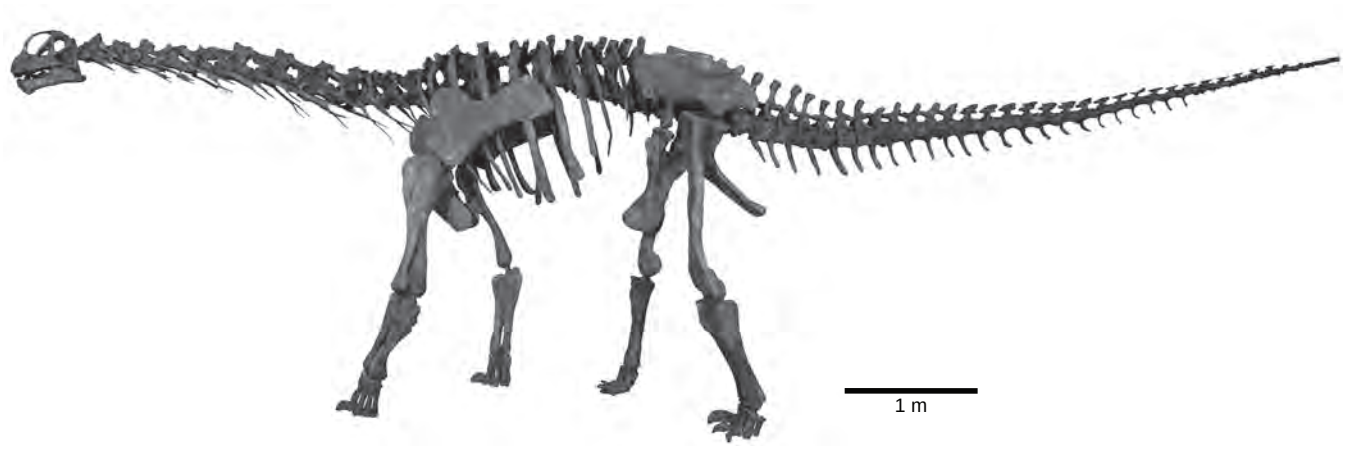

FIGURE 36 — *Moabosaurus utahensis* skeletal mount. A composite of the holotypic dorsal vertebrae (BYU 14387) and referred elements plus a skull of *Camarasaurus*. The skeleton is 9.75 m long.

with *Moabosaurus* neural arches set anteriorly on the centra, and femur with a high, medially positioned head and a lateral bulge (Tidwell et al., 1999).

Venenosaurus was reported from the Dalton Wells Quarry (Britt et al., 2009), in part based on a slender ischium (BYU 14072). This taxon differs from *Moabosaurus* in having pneumatic dorsal ribs; the middle caudal vertebrae bear a lateral fossa on the centra of middle caudal vertebra and their neural spine is inclined anteriorly; the lateral and medial processes of the ulna differ substantially in length in proximal view.

Astrodon and *Pleurocoelus* are poorly known genera based on isolated elements from the Albian of Maryland (Johnston, 1859; Leidy, 1865; Marsh, 1888). Both taxa are now considered *nomina dubia* (D'Emic, 2013). "*Astrodon*" teeth are narrow and parallel-sided relative to those of *Moabosaurus*. The caudal vertebrae of "*Pleurocoelus*" differ from *Moabosaurus* in that the anterior caudal centrum (USNM 8488) is amphiplatyan. As in *Moabosaurus*, the neural arches of the caudal vertebrae are positioned anteriorly on the centrum.

Sauroposeidon proteles is known from Early Cretaceous sites in Texas, Oklahoma, and Wyoming (Wedel et al., 2000a, b). It was originally considered to be a brachiosaurid, but it is now considered a somphospondylan that is the senior synonym of *Paluxysaurus jonesi* (D'Emic and Foreman, 2012; D'Emic, 2013). *Sauroposeidon* is differentiated from *Moabosaurus* by the following features: greatly elongated cervical vertebrae; coarsely camellate presacral vertebrae; internally pneumatized neural arches; undivided cervical neural spines; pneumatic fossa on anterior caudal centra; gracile humerus; and weakly developed olecranon process of the ulna.

Astrophocaudia slaughteri, from the lower Albian Paluxy Formation of the Trinity Group of Texas, has been recovered as a member of the Somphospondyli (D'Emic, 2013). It differs from *Moabosaurus* in having parallel sided teeth; cervical vertebrae are thin-walled and possibly camellate; pneumatic dorsal ribs; and plani-concave caudal vertebral centra (*sensu* Tidwell et al., 2001).

Sonorasaurus is a brachiosaurid from the Albian-to-Cenomanian Turney Ranch Formation of Arizona (Ratkevich, 1998). The specimen is fragmentary, but it differs from *Moabosaurus* in having only weakly procoelous caudal centra, caudal ribs that are strongly posteriorly directed, and unequally developed lateral and medial processes on the ulna.

Rugocaudia is based primarily on fragmentary caudal vertebrae and fragments of other referred elements, including a tooth from the Cloverly Formation of Montana. (Woodruff, 2012). It was originally considered to be a novel titanosauriform, but D'Emic and Foreman (2012) consider it to be a *nomen dubium*. We judge the highly vascularized centra to be pathologic in origin. The anterior caudal vertebrae of *Moabosaurus* have much larger cotyles than those of "*Rugocaudia*." The slightly procoelous middle centra of "*Rugocaudia*" are similar to those of *Moabosaurus*, but the distal caudal vertebrae lack the posterior cotyles of *Moabosaurus*. A referred tooth is parallel-sided, which is distinct from the spatulate teeth of *Moabosaurus*.

Comparison with *Turiasaurus* and *Tendaguria*

From the preceding, it is clear that *Moabosaurus* can be readily differentiated from other North American Early Cretaceous sauropods, as well as from the Late Jurassic *Camarasaurus*. We now compare *Moabosaurus* to two roughly contemporaneous taxa that share a number of similarities, *Turiasaurus* of Spain and *Tendaguria* of Tanzania.

Turiasaurus riodevensis, from the latest Jurassic or earliest Cretaceous of Spain (Royo-Torres et al., 2006) shares a number of characters with *Moabosaurus* including: an axially thin ventral basioccipital region with delicate vertical pillars supporting the basitubera; camerate presacral vertebrae; shallowly notched neural spine tops bounded laterally by stout metapophyses, cervical vertebrae with prominent ala on postzygodiapophyseal lamina; low neural spines and pre-epipophyses on cervical vertebrae; bifid cervical ribs; and narrow, elongate sternal plates.

Turiasaurus is typically recovered in positions outside of Neosauropoda (Royo-Torres et al., 2006; Royo-Torres and Upchurch, 2012; Upchurch et al., 2015; Carballido and Sander, 2014). Using Wilson's (2002) matrix, Royo-Torres and Upchurch (2012) recovered *Turiasaurus* as a macronarian close to *Camarasaurus* when *Losillasaurus* and *Galveosaurus* were excluded from the matrix. Royo-Torres and Upchurch (2012), however, rejected the macronarian hypothesis based on the results obtained using the Upchurch et al. (2004) matrix, which recovered Turiasauria as the sister clade to Neosauropoda. Royo-Torres and Upchurch (2012) concluded that the *Turiasaurus* skull is similar to that of several sauropods, including *Camarasaurus*. *Moabosaurus* differs from *Turiasaurus* in that: tooth crowns are linguiform, not heart-shaped; pre-and postspinal laminae present in dorsal vertebrae; upper half of the humerus is not bent medially; posterior dorsal neural spines have a narrow, shallow median cleft, not a wide, deep cleft; the ulna lacks a posterior ridge on its distal half; and distal caudal vertebrae are procoelous, not opisthocoelous. This comparison is necessarily limited, because *Turiasaurus* is known from a limited number of bones. Based on what is available for comparison (Royo-Torres et al., 2006), *Moabosaurus* appears to be most closely allied with *Turiasaurus*. The hypothesis that *Turiasaurus* is a non-neosauropod (Royo-Torres et al., 2006; Royo-Torres and Upchurch, 2012; Upchurch et al., 2015; Carballido and Sander, 2014) does not match our hypothesized position for *Moabosaurus* within Macronaria or Titanosauriformes, but in light of the noted similarities we speculate that *Turiasaurus* may be later shown to be a neosauropod, possibly a macronarian.

A number of *Moabosaurus* characters are shared with specimens from Tanzania that come from the Upper Dinosaur Member of the Tendaguru Formation and are likely Late Jurassic or possibly Early Cretaceous in age (Bussert et al., 2009). Bones relevant to our discussion are:

1. Two articulated, anterior dorsal vertebrae (Nb4, MB.R.2092.1; Nb5, MB.R.2092.2) assigned to *Tendaguria* by Bonaparte et al. (2000). These share low neural spines consisting primarily of an intervertebral ligament scar on a laterally wide, axially thin ridge, not much higher than the zyagapophyses, and camerate construction with unusually thick vertebral walls with *Moabosaurus*.

2. Two ulnae (Ulna P9, MB.R.2095.8; Ulna P12, MB.R.2095.11) assigned to *Janenschia* (Bonaparte et al., 2000). These ulnae share with *Moabosaurus* a prominent olecranon process and nearly equally developed medial and lateral process that project anteriorly.

3. A robust cervical vertebra (G45, MB.R.2091.31) that was tentatively assigned to *Tendaguria* (Bonaparte et al., 2000). This vertebra shares with *Moabosaurus* a laterally broad, axially thin neural spine, and a large pneumatic fossa on the dorsolateral surface of the prezygodiapophyseal lamina.

4. A string of 30 caudal vertebrae (MB.R.2091.1–30, G1–G30) that Bonaparte et al. (2000) indicated likely did not pertain to *Janenschia*. Royo-Torres and Cobos (2009) proposed they represent a turiasaur, and Mannion et al. (2013) determined they pertain to a mamenchisaurid. These caudal vertebrae share with *Moabosaurus* strongly procoelous proximal centra with the degree of procoely decreasing posteriorly in the series.

All these elements were originally referred to *Janenschia robusta*, but Bonaparte et al. (2000) made the two dorsal vertebrae the holotype of a new genus and species, *Tendaguria tanzaniensis*, and he referred the cervical vertebra to the same taxon. Bonaparte et al. (2000) determined that the caudal series did not pertain to *Janenschia* or *Tendaguria*. The taxonomic history of *Janenschia* is complex and the reader is referred to Bonaparte et al. (2000) for details.

Certain elements from Tendaguru have been suggested to demonstrate affinities with turiasaurs (Royo-Torres and Cobos, 2009), whereas others have suggested affinities with mamenchisaurids (Mannion et al., 2013). We propose an alternate hypothesis, that suggests a single affinity for these seemingly disparate elements based in part on the combination of characters presented by *Moabosaurus*, which demonstrates that ulnae with a large olecranon and large lateral process, robust, camerate presacral vertebrae, and procoelous caudal vertebrae can coexist in a single taxon. That character association supports the referral by Bonaparte el al. (2000) of the cervical vertebra (G45, MB.R.2091.31) to *Tendaguria tanzaniensis*, the holotype of which consists of two dorsal vertebrae. We speculate that the pair of ulnae (Ulna P9, MB.R.2095.8; Ulna P12, MB.R.2095.11) and the caudal vertebral series (MB.R.2091.1-30, G1-G30) also pertain to *Tendaguria*. We further suggest that *Tendaguria* shares a close relationship with *Moabosaurus* and *Turiasaurus*.

Moabosaurus and Related Genera

Phylogenetic analyses indicate *Moabosaurus* is a macronarian neosauropod, perhaps a basal titanosauriform. Its braincase, presacral vertebrae, and humerus are generally similar to those of *Camarasaurus*. But *Moabosaurus* also shares derived characters with *Turiasaurus*, including an axially thin basioccipital region, bifid cervical rib shafts, and elongate sternal plates. *Moabosaurus* also shares an unusual suite of characters with *Tendaguria*, supporting the proposal of Royo-Torres and Cobos (2009) that turiasaurs were present in Africa. Coding and scoring additional characters from these genera will help resolve the position of *Turiasaurus*, which is generally considered to be a non-neosauropod (Royo-Torres et al., 2006; Royo-Torres and Upchurch, 2012; Carbadilldo and Sander, 2014). We suspect that *Tendaguria* and *Turiasaurus*, like *Moabosaurus*, are macronarian neosauropods. If they are closely related, this Late Jurassic to Early Cretaceous macronarian clade occurs in Europe, Africa, and North America. This distribution would indicate a faunal interchange made possible by continued or intermittent tectonic connections between what is now North America, Laurasia (Europe), and West Gondwana (Africa) during the Late Jurassic and Early Cretaceous.

SUMMARY

We provide a detailed description of the skull and postcranial axial skeleton of *Moabosaurus utahensis*, from early Aptian strata of the Cedar Mountain Formation of western North America. *M. utahensis* is diagnosed in part by axially thin ventral basioccipital with posteriorly sweeping basal tubera, shallowly notched, low-cervical neural spines, extremely low-spined pectoral vertebrae, and strongly procoelous anterior caudal vertebrae and variably procoelous middle and distal caudal vertebrae. Phylogenetic analyses indicate it is a macronarian neosauropod, possibly a basal titanosauriform. Certain characters ally *Moabosaurus* with *Turiasaurus* of Spain, which is usually considered a non-neosauropod. The combination of an ulna with a large olecranon and well-developed lateral and medial processes, camerate presacral vertebrae with extremely low neural spines in pectoral vertebrae in *Moabosaurus* provides evidence that corroborates the referral to the African taxon *Tendaguria* of a number of postcranial elements (Bonaparte et al., 2000). We suspect that *Tendaguria* is closely allied with *Moabosaurus.*

Finally, the large number of individuals at Dalton Wells provides a rare opportunity to study individual variation within a species. In some elements, the range is striking when looking at end members but as a whole, the variation is a morphological continuum, indicating care should be taken when diagnosing closely related taxa from a small sample.

ACKNOWLEDGEMENTS

This paper was improved by insights from two anonymous reviewers, whose help is greatly appreciated. This research was funded by Brigham Young University, the Museum of Western Colorado, and a grant from the Dinosaur Society. The Dalton Wells Quarry is on land owned by the State of Utah administered by the State of Utah School and Institutional Trust Lands Administration, and we thank the state for protecting the site and granting us excavating access. We especially thank James Kirkland and Martha Hayden for issuing State of Utah collecting permits and Jeff Scott of the Orem Community Hospital and Kent Sanders for CT imaging. Ken Stadtman and quarry volunteer Jeff Higgerson toiled many years in the quarry. We thank volunteers at the Museum of Western Colorado, especially, B. Carter, L. Farber, K. Fredette, G. Anderson, D. Bowden and R. Nash for specimen preparation. We thank Melissa Gonzales and Alan J. Matthews for illustration and photographic assistance, respectively. Jeffrey Wilson kindly shared sauropod photographs to aid comparisons. We acknowledge and thank Lin Ottinger for finding and reporting the locality. We especially thank the late James A. Jensen for initiating this project.

LITERATURE CITED

BAKKER, R. T. 1978. Dinosaur feeding behaviour and the origin of flowering plants. Nature, 274: 661–663.

BARRETT, P. M. and P. UPCHURCH. 2005. Sauropod diversity through time: possible macroevolutionary and paleoecological implications. In: K. A. Curry- Rogers and J. A. Wilson (eds.), Sauropod Evolution and Paleobiology, Berkeley: University of California Press, 125–156.

BONAPARTE, J. F., W. D. HEINRICH, and R. WILD. 2000. Review of *Janenschia* WILD, with the description of a new sauropod from the Tendaguru beds of Tanzania and a discussion on the systematic value of procoelous caudal vertebrae in the Sauropoda. Palaeontographica Abteilung A, 256(1–3): 25–76.

BRITT, B. B. 1993. Pneumatic postcranial bones in dinosaurs and other archosaurs. Geology and Geophysics, University of Calgary, 383 pp.

———. 1997. Postcranial pneumaticity. In: P. J. Currie and K. Padian (eds.), The Encyclopedia of Dinosaurs. Academic Press, San Diego. 590–593.

——— D. A. EBERTH, R. D. SCHEETZ, B. W. GREENHALGH, and K. L. STADTMAN. 2009. Taphonomy of debris-flow hosted dinosaur bonebeds at Dalton Wells, Utah (Lower Cretaceous, Cedar Mountain Formation, USA). Palaeogeography, Palaeoclimatology, Palaeoecology, 280(1): 1–22.

———, ———, D. B. BRINKMAN, R. D. SCHEETZ, K. L. STADTMAN, and J. S. McINTOSH. 1997a. The Dalton Wells fauna (Cedar Mountain Formation): a rare window into the little-known world of Early Cretaceous Dinosaurs in North America. Geological Society of America Annual Meeting, Abstracts with Programs, A–104.

——— R. D. SCHEETZ, D. B. BRINKMAN, and D. A. EBERTH. 2006. A Barremian neochoristodere from the Cedar Mountain Formation, Utah, USA. Journal of Vertebrate Paleontology, 26(4): 1005–1008.

———, ———, J. S. McINTOSH, and K. L. STADTMAN. 1998. Osteological characters of an Early Cretaceous titanosaurid sauropod dinosaur from the Cedar Mountain Formation of Utah. Journal of Vertebrate Paleontology, Abstracts, 18(3): 29A.

——— K. L. STADTMAN, and R. SCHEETZ. 1996. The Early Cretaceous Dalton Wells dinosaur fauna and the earliest North American titanosaurid sauropod. Journal of Vertebrate Paleontology, Abstracts, 16(3): 24A.

———, ———, ———, and J. S. McINTOSH. 1997b. Camarasaurid and titanosaurid sauropods from the Early Cretaceous Dalton Wells Quarry (Cedar Mountain Formation) Utah. Journal of Vertebrate Paleontology, Abstracts, 17(3): 34A.

BURGE, D. L., J. H. BIRD, B. B. BRITT, D. J. CHURE, and R. D. SCHEETZ. 2000. A brachiosaurid from the Ruby Ranch Member (Cedar Mountain Formation) near Price, Utah, and sauropod faunal change across the Jurassic-Cretaceous boundary of North America. Journal of Vertebrate Paleontology, Abstracts, 20(3): 32A.

BUSSERT, R., W. D. HEINRICH, and M. ABERHAN. 2009. The Tendaguru Formation (Late Jurassic to Early Cretaceous, southern Tanzania): definition, palaeoenvironments, and sequence stratigraphy. Fossil Record, 12(2): 141–174.

CARBALLIDO, J. L. and P. M. SANDER. 2014. Postcranial axial skeleton of *Europasaurus holgeri* (Dinosauria, Sauropoda) from the Upper Jurassic of Germany: implications for sauropod ontogeny and phylogenetic relationships of basal Macronaria. Journal of Systematic Palaeontology, 12(3): 335–387.

CAREY, M. A. and J. H. MADSEN JR. 1972. Some observations on the growth, function and differentiation of sauropod teeth from the Cleveland-Lloyd Quarry. Proceedings of the Utah Academy of Sciences, Arts, and Letters, 49(1): 40–43.

CARPENTER, K. and V. TIDWELL. 1998. Preliminary description of a *Brachiosaurus* skull from Felch Quarry 1. Garden Park, Colorado. Modern Geology, 23(14): 69–84.

CERDA, I. 2008. Consideraciones sobre la histogénesis de las costillas cervicales en los dinosaurios saurópodos. Ameghiniana, 46: 193–198.

CHURE, D., B. B. BRITT, J. A. WHITLOCK, and J. M. WILSON. 2010. First complete sauropod dinosaur skull from the Cretaceous of the Americas and the evolution of sauropod dentition. Naturwissenschaften, 97: 379–391.

D'EMIC, M. D. 2012. Early evolution of titanosauriform sauropod dinosaurs. Zoological Journal of the Linnean Society, 166 (3): 624–671.

———. 2013. Revision of the sauropod dinosaurs of the Lower Cretaceous Trinity Group, southern USA, with the description of a new genus. Journal of Systematic Palaeontology, 11(6): 707–726.

——— and B. Z. FOREMAN. 2012. The beginning of the sauropod dinosaur hiatus in North America: insights from the Lower Cretaceous Cloverly Formation of Wyoming. Journal of Vertebrate Paleontology, 32(4): 883–902.

——— and J. R. FOSTER. 2016. The oldest Cretaceous North American sauropod dinosaur. Historical Biology, 28(4): 470–478.

DECOURTEN, F. L. 1991. New data on Early Cretaceous dinosaurs from the Long Walk Quarry and tracksite, Emery County, Utah. In: T. C. Chidsey Jr (ed.), Geology of East-Central Utah. Utah Geological Association Publication, 19: 311–324.

EBERTH, D. A., B. B. BRITT, R. SCHEETZ, K. L. STADTMAN, and D. B. BRINKMAN. 2006. Dalton Wells: Geology and significance of debris-flow-hosted dinosaur bonebeds in the Cedar Mountain Formation (Lower Cretaceous) of eastern Utah, USA. Palaeogeography, Palaeoclimatology, Palaeoecology, 236(3): 217–245.

GALTON, P. M. and J. A. JENSEN. 1979. Remains of ornithopod dinosaurs from the Lower Cretaceous of North America. Brigham Young University Geology Studies, 25(3): 1–10.

GOLOBOFF, P. A. and S. A. CATALANO. 2016. TNT vers. 1.5, including a full implementation of phylogenetic morphometrics. Cladistics, 32(3): 221–238.

GREENHALGH, B. and B. BRITT. 2007. Stratigraphy and sedimentology of the Morrison/Cedar Mountain formational boundary, east-central Utah. In: G. C. Willis, M. D. Hylland, D. L. Clark, T. C. Chidsey Jr. (eds.), Central Utah — Diverse Geology of a Dynamic Landscape, Utah Geological Association Publication, 36 (2007): 81–100.

HUNT, A. P., M. G. LOCKLEY, S. G. LUCAS, and C. A. MEYER. 1994. The global sauropod fossil record. GAIA, 10: 261–279.

JANENSCH, W. 1935–1936. Die Schädel der Sauropoden *Brachiosaurus*, *Barosaurus* und *Dicraeosaurus* aus den Tendaguruschichten Deutsch-Ostafrikas. Palaeontographica, (Supplement 7) 2: 147– 298.

———. 1947. Pneumatizitat bei Wirbeln von Sauropoden und anderen Saurischiern. Palaeontographica-Supplementbande, 1–25.

KLEIN, N., A. CHRISTIAN, and P. M. SANDER. 2012. Histology shows that elongated neck ribs in sauropod dinosaurs are ossified tendons. Biology Letters, 8: 1032–1035.

LONGRICH, N. 2008. A new, large ornithomimid from the Cretaceous Dinosaur Park Formation of Alberta, Canada: implications for the study of dissociated dinosaur remains. Palaeontology, 51(4): 983–997.

MADDISON, W. P. and D. R. MADDISON. 2017. Mesquite: a modular system for evolutionary analysis. Version 3.2 http://mesquiteproject.org

MADSEN, J. H., J. S. McINTOSH, and D. S. BERMAN. 1995. Skull and atlas-axis complex of the Upper Jurassic sauropod *Camarasaurus* sp. Cope (Reptilia: Saurischia). Bulletin of the Carnegie Museum of Natural History, 31: 1–115.

MANNION, D., P. UPCHURCH, R. N. BARNES, and O. MATEUS. 2013. Osteology of the Late Jurassic Portuguese sauropod dinosaur *Lusotitan atalaiensis* (Macronaria) and the evolutionary history of basal titanosauriforms. Zoological Journal of the Linnean Society, 168: 98–206.

McINTOSH, J. A. 1990. Sauropoda. In: D. B. Weishampel, P. Dodson, and H. Osmólska (eds.), The Dinosauria. University of California Press, Berkeley, 345–401.

——— and M. E. WILLIAMS. 1988. A new species of sauropod dinosaur, *Haplocanthosaurus delfsi* sp. nov., from the Upper Jurassic Morrison Formation of Colorado. Kirtlandia, 43: 3–26.

McCREA, R. T., L. G. BUCKLEY, A. G. PLINT, P. J. CURRIE, J. W. HAGGART, C. W. HELM, and S. G. PEMBERTON. 2014. A review of vertebrate track-bearing formations from the Mesozoic and earliest Cenozoic of western Canada with a description of a new theropod ichnospecies and reassignment of an avian ichnogenus. New Mexico Museum of Natural History and Science, Bulletin, 62: 5–93.

RATKEVICH, R. 1998. New Cretaceous brachiosaurid dinosaur, *Sonorasaurus thompsoni* gen et sp. nov, from Arizona. Arizona-Nevada Academy of Science, 31: 71–82.

RÉGENT, V. 2011. Die Bezahnung des Zwerg-Sauropoden *Europasaurus holgeri* aus dem Oberjura Norddeutschlands—ontogenetische und funktionelle Muster. Bonn: unpublished Diploma Thesis, Universität Bonn.

ROYO-TORRES, R., A. COBOS, and L. ALCALÁ. 2006. A giant European dinosaur and a new sauropod clade. Science, 314(5807): 1925–1927.

——— and ———, 2009. Turiasaur sauropods in the Tendaguru beds of Tanzania. Journal of Vertebrate Paleontology, Abstracts, 29(3): 173A.

——— and P. UPCHURCH. 2012. The cranial anatomy of the sauropod *Turiasaurus riodevensis* and implications for its phylogenetic relationships. Journal of Systematic Palaeontology, 10(3): 1–31.

SCHEETZ, R., B. BRITT, and J. HIGGERSON. 2010. A large, tall-spined iguanodontid dinosaur from the Early Cretaceous (Early Albian) basal Cedar Mountain Formation of Utah. Journal of Vertebrate Paleontology. Society of Vertebrate Paleontology, Abstracts, 28(3): 158A.

TAYLOR, M. P. and M. J. WEDEL. 2013. Why sauropods had long necks; and why giraffes have short necks. PeerJ, 1:e36: 1–41. doi:10.7717/peerj.36

———, ———, and R. L. CIFELLI. 2011. *Brontomerus mcintoshi*, a new sauropod dinosaur from the Lower Cretaceous Cedar Mountain Formation, Utah, USA. Acta Palaeontologica Polonica, 56(1): 75–98.

TEICHERT, C. 1948. A simple device for coating fossils with ammonium chloride. Journal of Paleontology, 22(1): 102–104.

TIDWELL, V. and K. CARPENTER. 2003. Braincase of an Early Cretaceous titanosauriform sauropod from Texas. Journal of Vertebrate Paleontology, 23(1): 176–180.

——— and ———. 2007. First description of cervical vertebrae for an Early Cretaceous titanosaur from North America. Journal of Vertebrate Paleontology, Abstracts, 27(3): 158A.

———, ———, and W. BROOKS. 1999. New sauropod from the Lower Cretaceous of Utah, USA. Oryctos, 2: 21–37.

———, ———, and S. MEYER. 2001. New titanosauriform (Sauropoda) from the Poison Strip Member of the Cedar Mountain Formation (Lower Cretaceous), Utah. In: Mesozoic Vertebrate Life. D. H. Tanke and K. Carpenter (eds.), Indiana University Press, 139–165.

UPCHURCH, P., P. M. BARRETT, and P. DODSON. 2004. Sauropoda. In*:* D. B. Weishampel, P. Dodson, and H. Osmólska (eds.), The Dinosauria, 2nd edition, University of California Press, Berkeley, California, 259–324.

———, P. D. MANNION, and M. P. TAYLOR. 2015. The anatomy and phylogenetic relationships of "*Pelorosaurus*" *becklesii* (Neosauropoda, Macronaria) from the Early Cretaceous of England. PLoS ONE, 10(6): e0125819. doi:10.1371/journal.pone.0125819

WEDEL, M. J., R. L. CIFELLI, and R. K. SANDERS. 2000a. *Sauroposeidon proteles*, a new sauropod from the Early Cretaceous of Oklahoma. Journal of Vertebrate Paleontology, 20(1): 109–114.

———, ———, and ———. 2000b. Osteology, paleobiology, and relationships of the sauropod dinosaur *Sauroposeidon*. Acta Palaeontologica Polonica, 45: 343–388.

——— and R. K. SANDERS. 2002. Osteological correlates of cervical musculature in Aves and Sauropoda (Dinosauria: Saurischia), with comments on the cervical ribs of *Apatosaurus*. PaleoBios, 22(3): 1–6.

WHITLOCK, J. A., M. D. D'EMIC, and J. A. WILSON. 2011. Cretaceous diplodocoids in Asia? Re-evaluating the phylogenetic affinities of a fragmentary specimen. Palaeontology, 54: 351–364.

WIERSMA, K. and P. M. SANDER. 2016. The dentition of a well-preserved specimen of *Camarasaurus* sp.: implications for function, tooth replacement, soft part reconstruction, and food intake. Paläontologische Zeitschrift, doi:10.1007/s12542-016-0332-6

WILHITE, D. R. 2003. Biomechanical reconstruction of the appendicular skeleton in three North American Jurassic sauropods. Dissertation, Louisiana State University, 2003.

———. 2005. Variation in the appendicular skeleton of North American sauropod dinosaurs: taxonomic implications. 2007. In: V. Tidwell and K. Carpenter (eds.), Thunder-Lizards: The Sauropodomorph Dinosaurs, 268–301 pp.

——— and B. CURTICE. 1998. Ontogenetic variation in sauropod dinosaurs, Journal of Vertebrate Paleontology, Abstracts, 18(3): 86A.

WILSON, J. A. 1999. A nomenclature for vertebral laminae in sauropods and other saurischian dinosaurs. Journal of Vertebrate Paleontology, 19(1): 639–653.

———. 2002. Sauropod dinosaur phylogeny: critique and cladistic analysis. Zoological Journal of the Linnean Society, 136(2): 215–275.

———. 2006. Anatomical nomenclature of fossil vertebrates: standardized terms of lingua franca? Journal of Vertebrate Paleontology, 26: 511–518.

——— and M. T. CARRANO. 1999. Titanosaurs and the origin of "wide-gauge'' trackways: A biomechanical and systematic perspective on sauropod locomotion, Paleobiology, 25(2): 252–267.

———, M. D. D'EMIC, T. IKEJIRI, E. M. MOACDIEH, and J. A. WHITLOCK. 2011. A nomenclature for vertebral fossae in sauropods and other saurischian dinosaurs. PLoS ONE, 6(2): e17114. doi:10.1371/journal.pone.0017114

——— and P. C. SERENO. 1998. Early evolution and higher-level phylogeny of sauropod dinosaurs. Memoirs of the Society of Vertebrate Paleontology, 5: 1–68.

——— and P. UPCHURCH. 2009. Redescription and reassessment of the phylogenetic affinities of *Euhelopus zdanskyi* (Dinosauria: Sauropoda) from the Early Cretaceous of China. Journal of Systematic Palaeontology, 7(2): 199–239.

WOODRUFF, D. C. 2012. A new titanosauriform from the Early Cretaceous Cloverly Formation of Montana. Cretaceous Research, 36: 58–66.

Museum of Paleontology, The University of Michigan
1109 Geddes Avenue, Ann Arbor, Michigan 48109-1079
Daniel C. Fisher, Director

Contributions from the Museum of Paleontology, University of Michigan is a medium for publication of reports based chiefly on museum collections and field research sponsored by the museum. When the number of issued pages is sufficient to make a volume, a title page plus table of contents will be sent to libraries on the Museum's mailing list (and to individuals on request). Separate issues may be obtained from the Publications Secretary (paleopubs@umich.edu). Jeffrey A. Wilson, Editor.

Publications of the Museum of Paleontology are accessible online at: http://deepblue.lib.umich.edu/handle/2027.42/41251

ISSN 0097-3556

APPENDIX 1 — *Moabosaurus utahensis* scored for Wilson (2002) dataset. The top numbers are the character numbers of Wilson (2002).

1	2	3	4	5	6	7	8	9	10	11	12	13	14	15	16	17	18	19	20	21	22	23	24	25	26	27	28	29	30
?	?	?	?	?	?	1	?	?	?	?	?	?	?	?	1	0	1	1	1	0	0	0	?	0	1	0	?	?	?
31	32	33	34	35	36	37	38	39	40	41	42	43	44	45	46	47	48	49	50	51	52	53	54	55	56	57	58	59	60
?	?	1	1	1	?	?	?	?	?	?	?	?	1	1	0	0	1	0	1	0	?	0	0	?	?	0	?	?	?
61	62	63	64	65	66	67	68	69	70	71	72	73	74	75	76	77	78	79	80	81	82	83	84	85	86	87	88	89	90
?	?	?	?	1	?	1	0	1	1	1	2	?	0	1	1	0	1	1	?	0	1	1	0	1	0	1	0	1	0
91	92	93	94	95	96	97	98	99	100	101	102	103	104	105	106	107	108	109	110	111	112	113	114	115	116	117	118	119	120
?	0	0	1	0	1	1	1	1	0	0	1	1	0	1	0	0	2	1	?	0	?	0	?	?	1	0	1	0	0
121	122	123	124	125	126	127	128	129	130	131	132	133	134	135	136	137	138	139	140	141	142	143	144	145	146	147	148	149	150
1	0	0	0	1	1	1	0	0	0	0	0	0	1	0	?	?	?	1	1	0	?	0	?	?	?	0	?	1	0
151	152	153	154	155	156	157	158	159	160	161	162	163	164	165	166	167	168	169	170	171	172	173	174	175	176	177	178	179	180
0	1	1	1	1	0	?	1	0	1	0	1	0	1	1	1	0	1	1	1	1	?	?	?	?	?	?	?	?	?
181	182	183	184	185	186	187	188	189	190	191	192	193	194	195	196	197	198	199	200	201	202	203	204	205	206	207	208	209	210
?	?	?	?	1	?	0	0	0	1	?	?	?	?	?	1	1	1	1	1	1	0	?	?	?	?	?	?	?	1
211	212	213	214	215	216	217	218	219	220	221	222	223	224	225	226	227	228	229	230	231	232	233	234						
1	1	1	0	?	?	?	?	?	?	?	?	?	?	?	?	?	?	?	?	?	?	?	0						

APPENDIX II— *Moabosaurus utahensis* scored for Upchurch et al. (2004) dataset. The top numbers are the character numbers of Upchurch et al. (2004).

1	2	3	4	5	6	7	8	9	10	11	12	13	14	15	16	17	18	19	20	21	22	23	24	25	26	27	28	29	30
0	?	0	0	?	?	?	?	1	?	?	0	?	?	?	?	?	?	?	?	?	?	?	?	?	?	?	1	?	?
31	32	33	34	35	36	37	38	39	40	41	42	43	44	45	46	47	48	49	50	51	52	53	54	55	56	57	58	59	60
?	?	?	1	1	1	1	?	0	1	0	0	0	?	?	1	0	0	?	0	0	0	0	0	0	0	?	?	?	?
61	62	63	64	65	66	67	68	69	70	71	72	73	74	75	76	77	78	79	80	81	82	83	84	85	86	87	88	89	90
?	?	?	?	?	1	1	?	?	?	?	?	?	?	?	?	?	1	1	1	?	1	1	1	1	1	0	9	9	0
91	92	93	94	95	96	97	98	99	100	101	102	103	104	105	106	107	108	109	110	111	112	113	114	115	116	117	118	119	120
?	0	1	?	?	?	?	?	?	?	1	0	1	1	1	1	1	0	1	2	1	1	0	1	1	1	0	1	1	1
121	122	123	124	125	126	127	128	129	130	131	132	133	134	135	136	137	138	139	140	141	142	143	144	145	146	147	148	149	150
1	?	?	?	?	0	0	1	1	1	0	1	0	0	0	1	1	0	0	1	2	0	0	1	0	0	1	2	0	0
151	152	153	154	155	156	157	158	159	160	161	162	163	164	165	166	167	168	169	170	171	172	173	174	175	176	177	178	179	180
1	1	1	1	0	1	1	0	?	0	1	1	0	1	0	0	0	1	?	?	0	0	1	1	1	0	0	0	0	0
181	182	183	184	185	186	187	188	189	190	191	192	193	194	195	196	197	198	199	200	201	202	203	204	205	206	207	208	209	210
1	0	1	0	1	0	1	1	1	1	1	0	?	?	?	?	0	?	?	0	0	9	1	1	0	0	1	1	?	2
211	212	213	214	215	216	217	218	219	220	221	222	223	224	225	226	227	228	229	230	231	232	233	234						
0	0	0	?	?	?	1	0	1	0	0	0	1	1	?	?	?	?	?	?	?	?	?	?						

APPENDIX III— *Moabosaurus utahensis* scored for Carballido and Sander (2014) dataset. The top numbers are the character numbers of Carballido and Sander (2014).

1	2	3	4	5	6	7	8	9	10	11	12	13	14	15	16	17	18	19	20	21	22	23	24	25	26	27	28	29	30
?	?	?	1	?	?	?	?	?	?	1	?	?	?	?	?	?	?	?	?	?	?	?	?	?	?	?	?	?	?
31	32	33	34	35	36	37	38	39	40	41	42	43	44	45	46	47	48	49	50	51	52	53	54	55	56	57	58	59	60
1	0	1	1	1	1	0	0	?	0	0	1	0	?	0	1	0	?	?	0	?	1	1	0	1	0	?	?	?	?
61	62	63	64	65	66	67	68	69	70	71	72	73	74	75	76	77	78	79	80	81	82	83	84	85	86	87	88	89	90
?	?	?	?	0	1	1	0	0	1	0	0	0	1	0	0	0	0	0	0	?	?	?	?	?	?	?	?	?	?
91	92	93	94	95	96	97	98	99	100	101	102	103	104	105	106	107	108	109	110	111	112	113	114	115	116	117	118	119	120
?	?	1	?	?	0	1	?	1	1	1	0	1	1	0	2	1	0	?	1	1	1	1	2	3	1	1	0	1	1
121	122	123	124	125	126	127	128	129	130	131	132	133	134	135	136	137	138	139	140	141	142	143	144	145	146	147	148	149	150
0	1	0	1	1	0	0	0	1	1	0	1	0	?	1	0	0	2	1	0	0	1	1	0	0	1	0	1	0	0
151	152	153	154	155	156	157	158	159	160	161	162	163	164	165	166	167	168	169	170	171	172	173	174	175	176	177	178	179	180
0	1	0	0	1	0	1	0	1	1	1	0	1	1	1	1	1	0	0	0	0	0	1	2	1	0	?	1	0	?
181	182	183	184	185	186	187	188	189	190	191	192	193	194	195	196	197	198	199	200	201	202	203	204	205	206	207	208	209	210
2	1	?	0	?	1	?	0	?	0	0	0	2	0	1	1	1	0	1	1	0	0	1	0	0	0	0	1	0	1
211	212	213	214	215	216	217	218	219	220	221	222	223	224	225	226	227	228	229	230	231	232	233	234	235	236	237	238	239	240
1	0	3	1	0	?	1	0	0	?	?	?	0	?	?	?	0	?	1	0	0	1	0	0	0	0	0	0	0	1
241	242	243	244	245	246	247	248	249	250	251	252	253	254	255	256	257	258	259	260	261	262	263	264	265	266	267	268	269	270
1	1	0	?	0	0	1	0	0	0	?	?	1	0	1	0	0	1	0	0	1	1	0	?	?	?	?	?	?	?
271	272	273	274	275	276	277	278	279	280	281	282	283	284	285	286	287	288	289	290	291	292	293	294	295	296	297	298	299	300
?	?	?	?	?	?	?	?	?	1	1	0	0	?	?	1	1	?	0	0	0	?	?	?	?	?	?	?	1	1
301	302	303	304	305	306	307	308	309	310	311	312	313	314	315	316	317	318	319	320	321	322	323	324	325	326	327	328	329	330
1	1	0	1	1	1	0	1	?	?	?	?	?	?	?	1	1	1	1	1	0	?	?	?	?	?	?	?	?	?
331	332	333	334	335	336	337	338	339	340	341																			
?	?	?	?	?	?	?	?	?	?	?																			